

LASER COOLING OF SOLIDS

to appear in *Advances in Atomic, Molecular, and Optical Physics*

Carl E. Mungan
Department of Physics
The University of West Florida
Pensacola, Florida 32514-5751
(850) 474-2645

and

Timothy R. Gosnell
Condensed Matter and Thermal Physics Group, Mail Stop E543
Los Alamos National Laboratory
Los Alamos, New Mexico 87545
(505) 667-2265 (voice)
(505) 665-4267 (FAX)
e-mail: gosnell@lanl.gov

LASER COOLING OF SOLIDS

CONTENTS

I. Introduction.....	3
A. Overview of Basic Concepts.....	3
B. Summary of Experimental Results.....	5
C. Comparison to Laser Doppler Cooling.....	7
II. Historical Review of the Thermodynamics of Fluorescence Cooling.....	8
A. Viability of Anti-Stokes Cooling Processes.....	8
B. Thermodynamics of Electroluminescence.....	11
C. Thermodynamics of Photoluminescence.....	15
III. Working Substances for Fluorescence Cooling.....	22
A. Gases.....	22
B. Organic Dye Solutions.....	25
C. Semiconductors.....	31
D. Ruby.....	36
E. Rare-Earth Ions in Solids.....	38
IV. Laser Cooling of Ytterbium-Doped ZBLANP Glass.....	42
A. Photothermal Deflection Spectroscopy.....	44
B. Bulk Cooling Experiments.....	49
V. Fundamental Limits.....	54
A. Thermodynamics.....	54
B. Minimum Temperature.....	67
C. Maximum Cooling Power and Optical Refrigerators.....	70
VI. Conclusions and Prospects.....	73
References.....	77
Figure Captions.....	81

I. Introduction

A. OVERVIEW OF BASIC CONCEPTS

Laser cooling of a solid may occur when the average energy of the photons emitted by the solid is larger than the energy of the ones it absorbs. More formally, the *anti-Stokes emission*, which occurs at frequencies larger than that of the pump laser, must dominate the *Stokes emission* that occurs at smaller frequencies. A crucial additional requirement is that the nonradiative decay rates of the laser-pumped states be negligible in comparison to their radiative decay rates. For the sake of specificity, these states will be taken to be those of a set of isolated ions embedded within an insulating host, although in general they could equally well be those of gas-, liquid-, or solid-phase neutral atoms or molecules, or even those of the energy bands of intrinsic semiconductors. A typical system will consist of a ground-state manifold and an excited-state manifold well separated from one another, with at least one of these manifolds split into two or more levels (cf. Fig. 1). For a host temperature of T , a cooling cycle begins by optical pumping of the thermally populated high-lying levels of the ground-state manifold to low-lying states of the excited-state manifold. Next, both the excited- and ground-state manifolds rethermalize, typically through the net absorption of host-lattice phonons by the ions. Complete *intramanifold* thermalization is often assured since this process typically occurs on a picosecond time scale (Miniscalco, 1993), at least for intramanifold energy splittings on the order of $k_B T$, while the time scales for *intermanifold* radiative decay will range from nanoseconds for strongly allowed electronic transitions to as long as milliseconds for vibrational or nominally forbidden electronic transitions (Miniscalco, 1993). To conclude the cooling cycle, the excited manifold radiatively relaxes back to the ground manifold, after which both manifolds will most likely undergo additional rethermalization.

In practice, however, nonradiative processes that de-excite the active ions across the intermanifold energy gap compete with the radiative decay. While direct multiphonon relaxation between the two manifolds will be strongly suppressed for an energy gap ~ 10 times larger than the host's maximum phonon frequency, more problematic will be nonradiative quenching of the excited active ions by low concentrations of unwanted bulk or surface impurities. The net effect of both processes is most simply quantified in terms of the fluorescence quantum efficiency, η_Q , defined as the ratio of the average number of emitted photons per pump photon absorbed.

In terms of the quantum efficiency, fluorescence cooling of the sample can be understood more quantitatively in the following way. Let E_F be the average energy of an emitted photon, with a corresponding wavelength of $\lambda_F = hc / E_F$. Similarly, let E_{abs} be the energy of a pump photon of wavelength λ . An empirical rule of thumb, one that has come to be known as Vavilov's Law,¹ states that λ_F is independent of λ , or very nearly so (Vavilov, 1945; Zander and Drexhage, 1995). In that case, the average cooling energy per cycled photon is $E_{cool} = \eta_Q(E_F - E_{abs}) - (1 - \eta_Q)E_{abs}$. Multiplying by the cycling rate to give powers rather than energies, one obtains an expression for the cooling efficiency, η , defined as the ratio of the cooling power to the absorbed laser power. (Technically, this should be called the relative cooling efficiency, in contrast to the absolute cooling efficiency, defined as the ratio of the cooling power to the *incident* laser power. These two efficiencies are, however, simply related via the absorbance of the sample.) The result is $\eta = (\lambda - \lambda'_F) / \lambda'_F$, where $\lambda'_F \equiv \lambda_F / \eta_Q$. Knowledge of the absorption and fluorescence spectra therefore suffices to determine η under the best-case scenario of $\eta_Q = 1$. The reason anti-Stokes fluorescence cooling is so difficult to obtain in practice is implicit in the last two expressions: since $\eta > 0$ implies $\eta_Q > \lambda_F / \lambda \approx 1 - k_B T / E_{abs}$ and since E_{abs} will typically

¹Erickson (1972) incorrectly claimed that Vavilov's Law states that the *quantum efficiency* is independent of pump wavelength; Vavilov clearly never believed this (cf. Sec. II.A).

be at least $20k_B T$ in order to minimize multiphonon relaxation, η_Q must be close to unity. The high emission quantum efficiencies of most solid-state laser materials therefore make them natural candidates for anti-Stokes fluorescence coolers. In this context, one can view these materials as optically pumped lasers running in reverse.

B. SUMMARY OF EXPERIMENTAL RESULTS

The first observation of net fluorescence cooling of a solid was reported in 1995 (Epstein *et al.*, 1995a). Trivalent ytterbium ions doped into a heavy-metal fluoride glass were pumped in the near-infrared at $\sim 1 \mu\text{m}$; in the initial experiments, a temperature drop of 0.3 K below room temperature was measured for a 43-mm^3 sample in the shape of a rectangular parallelepiped. In later experiments, a 16-K drop was reported for a $250\text{-}\mu\text{m}$ -diameter optical fiber (Mungan *et al.*, 1997b). Spectroscopic measurements have since indicated that relative cooling efficiencies similar to those observed in these room-temperature experiments should be obtained even at liquid-nitrogen temperatures (Mungan *et al.*, 1997a; Mungan *et al.*, 1997c).

There have been two other published accounts of attempts to laser cool solids. In both experiments, however, parasitic heating processes dominated the cooling effect and net refrigeration was not observed. In 1968, a large crystal of $\text{Nd}^{3+}:\text{YAG}$ was inserted into a $1.064\text{-}\mu\text{m}$ laser cavity containing an independent, flash-lamp-pumped crystal of $\text{Nd}^{3+}:\text{YAG}$ (Kushida and Geusic, 1968). Trace amounts of impurities such as Dy^{3+} , which are difficult to chemically separate from Nd^{3+} , were thought to be responsible for net heating of the sample. More recently, there has also been encouraging progress towards the goal of optically cooling a thin wafer of GaAs (Gauck *et al.*, 1997). Unfortunately, the large index of refraction of this material helps trap the emitted radiation within the sample, thus increasing the probability of reabsorption and subsequent heat-generating nonradiative decay. However, strong ongoing in-

interest in industrial opto-electronic applications of direct-gap semiconductors should lead to further progress in this approach to laser cooling.

Outside the realm of solid materials, anti-Stokes cooling of molecules in gases and liquids has also been observed. In 1981, low-pressure carbon dioxide was laser cooled by 1 K starting from 600 K (Djeu and Whitney, 1981). The experiment consisted in optical pumping with a 10.6- μm CO₂ laser between the $v_1=1$ symmetric-stretch vibration and the higher-frequency $v_3=1$ antisymmetric stretch. Since radiative relaxation of the antisymmetric mode to the vibrational ground state was highly favored, thermal repopulation of the depleted fundamental symmetric mode, assisted by a buffer gas of Xe, cooled the CO₂-Xe mixture.

More recently, two different European groups have optically cooled laser dyes dissolved in ethanol at room temperature. Zander and Drexhage (1995) employed a photothermal lensing technique to observe a transition from heating to cooling in a dye-laser-pumped region interior to a larger volume of rhodamine 6G solution. They did not, however, attempt to measure overall, net cooling of the entire sample. This claim has since been made for solvated rhodamine 101 by Clark and Rumbles (1996). However, there may have been less question (Mungan and Gosnell, 1996) about their results had these workers begun with photothermal measurements and more-detailed spectroscopic studies such as those of Zander and Drexhage.

Anti-Stokes laser cooling of materials is thus an active field of experimental study at present. The topic likewise continues to provide fertile ground for theorists interested in the interactions between light and matter, as shall be discussed at length in Sec. II.C below.

C. COMPARISON TO LASER DOPPLER COOLING

Anti-Stokes laser cooling of solids, liquids, and gases is closely related to the technique of laser Doppler cooling of free atoms (Chu, 1991; Cohen-Tannoudji and Phillips, 1990; Wineland and Itano, 1987), for the practical development and extensions of which the 1997 Nobel prize in physics was awarded to S. Chu, C. Cohen-Tannoudji, and W. Phillips. This process is also crucial in the cooling of dilute gases down to the Bose-Einstein condensation temperature (Anderson *et al.*, 1995). The idea behind the technique was first proposed for neutral atoms by Hänsch and Schawlow (1975) and can be understood as arising from the radiation pressure of pairs of counterpropagating laser beams directed along three mutually perpendicular axes. Translational cooling occurs when the optical frequency is slightly detuned toward the low-frequency wing of an appropriate atomic-absorption line, wherein the pump light will be Doppler shifted into resonance only for those atoms that are moving towards a particular laser source, thus slowing them down like ping-pong balls striking an oncoming bowling ball.

It is easier to understand the conceptual similarity between the anti-Stokes and Doppler cooling techniques by considering the latter from an energy rather than a momentum point of view. The atoms absorb low-energy photons and then—on average— isotropically re-radiate photons, so that the emitted light is not Doppler shifted and hence is of higher mean frequency. That is, the mean fluorescence is up shifted relative to the absorbed light, with the difference representing the amount of heat carried away from the atoms.

Thus, both Doppler and anti-Stokes cooling involve the emission of photons of higher mean energy than those absorbed. On the other hand, certain differences are also evident: the first technique involves translational cooling of noninteracting two-level atoms, while the second method works by cooling the internal degrees of

freedom, at least two of which are coupled to the surrounding medium by thermalizing collisions. Furthermore, anti-Stokes cooling is a much more efficient process: even restricting attention to gases, it has been estimated that Doppler cooling is about six orders of magnitude less efficient (Djeu and Whitney, 1981). Of course, the intended applications of the two techniques are quite different.

II. Historical Review of the Thermodynamics of Fluorescence Cooling

A. VIABILITY OF ANTI-STOKES COOLING PROCESSES

Early in this century, Raman (1928) in India discovered the spectroscopic effect named after him, namely, that if a beam of monochromatic light passes through a medium, the scattered light will contain lines having lower frequencies (called Stokes lines) and higher frequencies (called anti-Stokes lines) than the frequency of the incident beam. This nomenclature for the set of lower-frequency lines reflects an outdated principle known as Stokes' rule or law, which states that a substance cannot emit light of wavelength shorter than that of the exciting radiation (Stokes, 1852). Exceptions to this rule (Wood, 1928), however, were already well known by the time of Raman's experiments and had accordingly come to be known as anti-Stokes emission. While it was understood that the excess energy necessary for such anti-Stokes radiation arose from thermal population of low-frequency sideband levels, such as the rotational states within a vibrational manifold, a controversy nevertheless erupted regarding whether a system can emit light which *on average* is of higher frequency than the incident radiation. In this situation, the "energy yield" or "luminescence efficiency" is said to exceed unity (Chukova, 1969a, 1969b, 1971, 1976; Stepanov and Gribkovskii, 1968). The contrary view was that the second law of thermodynamics requires that any anti-Stokes fluorescence be accompanied by

enough entropy-compensating Stokes emission to insure that the luminescence efficiency would be always less than one. This question was first clearly discussed by Pringsheim (1929), who adopted the former position, arguing that a continual cooling of a gas by anti-Stokes scattering is thermodynamically allowable because the system is not closed—as for any refrigerator, an outside agency supplies work to the system.

Pringsheim's position was subsequently opposed in print by Vavilov, leading to an intriguing quartet of short papers appearing at the end of World War II. Vavilov (1945) argued that an excitation–fluorescence cycle is reversible and hence an energy yield greater than unity would be equivalent to the (unallowable) complete transformation of heat into work. Introducing the concept of the average emission frequency, he pointed out that all spectroscopic data available at that time, including measurements on dye solutions (Jablonski, 1933) and on uranium glass, indicated that the intensity of luminescence fell to zero as the excitation frequency decreased towards this average value. Pringsheim (1946) responded that the optical cycle cannot be reversible because the monochromatic and unidirectional incident beam is converted into isotropic, broad-bandwidth radiation with a corresponding increase in its entropy. Putting it another way, he argued that irradiation of a low-temperature sample by a source of high “excitation temperature” entails a thermodynamically irreversible energy flow. Pringsheim included in his response a brief discussion of the fundamental conditions necessary for cooling, namely, a “quantum efficiency” or “quantum yield” (to be distinguished from the energy yield) as near unity as possible and thermal equilibration of the excited state prior to emission. (Ironically, Pringsheim weakens his response by suggesting that the explanation for the refuting evidence of the spectroscopic data just mentioned is that the quantum yield in many systems decreases when their absorption bands are pumped in the wings. In the condensed phase, for example, this was attributed to the increased elec-

trostatic perturbation experienced by the outlying centers giving rise to these wings rather than to spurious impurity effects.) Vavilov (1946) immediately rebutted by considering a reversible cycle built around an ideal optical cavity into which the anti-Stokes cooling sample is placed along with a Stokes heating sample. In his analysis of this system, the net effect of the cycle was the (impossible) work-free transfer of heat from a cooler to a hotter reservoir. Furthermore, Vavilov criticized Pringsheim's suggestion that the loss of directionality of the scattered light is an indication of irreversibility by citing an apparatus—dating back to 1743—wherein an arrangement of convex lenses and plane mirrors surrounding the sample could be used to re-collimate the fluorescence. He also suggested, with the example of a gaseous cooling sample, that there may be a contradiction between the requirement that the density be kept low enough to prevent excited-state quenching through nonradiative collisional de-excitation while simultaneously maintaining thermal equilibrium between the pumped and the fluorescing excited states. Presciently, he ends his article by calling for experimental measurements of the luminescence efficiency of solid phosphors pumped at long wavelengths.

Finally, Vavilov's concerns prompted a paper from Landau (1946) in which he presented for the first time a sound thermodynamic argument proving that photoluminescence energy yields can in fact exceed unity. To calculate the radiation entropy, he applied Bose statistics to the photon gas, integrating over the spectral bandwidth and the solid angle. After introducing the concept of an "effective temperature" or "brightness temperature" of the source, defined as the temperature of blackbody radiation whose spectral intensity matches that of the pump radiation at its peak wavelength, the final result was that the energy yield exceeds unity by an amount proportional to the ratio of the sample temperature and the effective temperature. Both Vavilov and Landau dismissed this excess as being insignificant,

even though it clearly can be of the order of several percent or more. Nonetheless, the essential physical viability of the concept had thus been established.

B. THERMODYNAMICS OF ELECTROLUMINESCENCE

In the early 1950s, the phenomenon of electroluminescence of semiconductor diodes was discovered (Haynes and Briggs, 1952; Lehovec *et al.*, 1951; Newman, 1953). It was quickly noticed that the energies of the photons emitted at the shortest wavelengths exceeded the applied electrical energy per injected electron; Lehovec *et al.* (1953) deduced that the difference corresponds to the withdrawal of internal energy from the semiconductor lattice. The possibility of using this effect for cooling purposes was briefly discussed by Tauc (1957). He derived an expression for the cooling power that reduces to $(E_g / eV - 1)iV$ when certain transport contributions and Joule heating are neglected. Here i is the electrical current, V is the forward bias across the diode, and E_g is the energy of the bandgap, across which the luminescence is assumed to occur with unit quantum efficiency.

This concept was taken seriously enough in 1956 to merit application for a U.S. patent, which was granted three years later (Bradley, 1959). The patented device consists of a series of electrically pumped semiconductor cells (Si, Ge, CdSe, InSb, AlSb, CdTe, CdS, GaSb, and GaP with carefully controlled impurity concentrations were specifically cited as possible compositions) laid out in a flat grid over which a thin layer of a transparent, heat-exchanging liquid such as CCl_4 would circulate. The resistivity and geometry of the cells would be tailored to reduce ohmic losses and total internal reflection, respectively. Advantages of this cooler would include high efficiency and the absence of moving mechanical parts; its intended applications were gas liquefaction and cooling of infrared detectors.

This initial interest in electroluminescence cooling developed independently of the earlier work on photoluminescence cooling summarized in Sec. A above. From a theoretical point of view, however, the two processes are similar, differing only in the method of excitation, provided that secondary issues such as electrical Joule heating are ignored. Weinstein (1960), working at General Electric's lighting division, appears to have been the first to recognize this concordance and address the general thermodynamic issue of converting heat into light. He was interested in calculating the "technical efficiency" of the process, defined as the ratio of the power of the emitted luminescence to the power of the input work, and consequently equal to unity plus a cooling efficiency. A "flux temperature" (to use the term adopted by later workers), T_{F_h} , of the fluorescence was defined as the ratio of the emitted power to the net rate at which the light carries entropy away from the sample. In general, this entropy flux and hence T_{F_h} depend on the thermal radiation incident on the sample from the environment, a quantity that depends in turn on the ambient temperature T , taken to be the same as that of the sample. In this way, T_{F_h} correctly reduces to T in the limit where the rate of input work falls to zero. It follows simply from the second law of thermodynamics that the technical efficiency must be smaller than $T_{F_h} / (T_{F_h} - T)$, which is, incidentally, the same as the reciprocal of the maximum efficiency of a solar cell when T_{F_h} refers to the input light.

Weinstein's calculation of the radiation energy and entropy essentially follows the derivation of Landau (1946), with the resulting flux densities for these quantities reducing to the familiar blackbody expressions when the output radiation field is in thermodynamic equilibrium with the surroundings. However, for situations of practical interest, such as emission within a narrow band, the luminescence power is very large compared to the ambient thermal emission within the same spectral bandwidth. Assuming that the fluorescence is isotropic, T_{F_h} then becomes approximately equal to the "brightness temperature" of the fluorescence T_{B_h} , defined as

the temperature at which a blackbody would have the same intensity as at the spectral peak of the emission. Note that T_{F_h} is infinite if the emitted radiation is either monochromatic or strictly unidirectional. Since the coolest blackbody that significantly emits in the visible range has a temperature of about 800 K, the maximum theoretical cooling efficiency of a visibly fluorescing sample at room temperature is about $300 / (800 - 300) = 0.6$. But this impressive thermodynamic result is of little practical utility because it assumes that the energy levels of the sample can be arranged in any way one pleases, while at the same time preserving unit radiative quantum efficiency.

In a brief letter published in 1965, Gerthsen and Kauer (1965) applied a physical model of an electroluminescent diode to the calculation of the technical efficiency. They showed that for unit quantum efficiency Weinstein's expression, $T_{F_h} / (T_{F_h} - T)$, reduces to E_g / eV when the rate of radiative recombination is explicitly modeled as the product of the electron and hole concentrations. This result was in agreement with that of Tauc for an electroluminescent semiconductor diode; accordingly, Gerthsen and Kauer viewed the diode as a heat pump that transfers energy from a low-temperature reservoir (the lattice) to a high-temperature reservoir (the radiation field).

Moving closer to an actual experiment, Landsberg and Evans (1968) re-examined Weinstein's treatment of the thermodynamics of an electroluminescent diode and noted that one can calculate the rate of excess-entropy generation within the diode in terms of experimentally observable quantities. This entropy production depends on the sample temperature, forward-bias voltage, mean emitted-photon energy, quantum efficiency, and the brightness temperature of the fluorescence. The latter quantity, in turn, can be calculated by assuming uniform, isotropic emission of light with a known spectral profile and depends additionally on the electric current and the surface area of the diode's emitting region. For a room-temperature GaAs diode,

the experimental data at the time indicated a technical efficiency of less than 6%, far below the cooling threshold of 100%, implying a large rate of entropy generation within the diode amounting to 30–50 k_B per injected electron. More encouragingly, however, the technical efficiency for a typical set of experimental conditions would rise to 120% if all nonradiative processes could be eliminated. After re-examining previous measurements, Landsberg and Evans suggested that reduced sample temperatures and careful epitaxial growth might result in the necessary increased quantum efficiencies.

More recently, Berdahl (1985) has treated the problem of electroluminescence cooling by semiconductor diodes. He defined a coefficient of performance (COP) as the ratio of the cooling power produced to the rate of external electrical work required. In the forward-biased, light-emitting mode, the Carnot value of the COP is $T / (T_R - T)$, where T is the temperature of the diode and T_R is the temperature of the diode's radiative environment. For operation at 0 °C in room-temperature surroundings, the COP is therefore about 10. Assuming values of unity for the emissivity, refractive index, and quantum efficiency of a diode in vacuum, a cooling rate of 650 W per square meter of junction area was deduced for an (unrealistic) energy gap of 3–5 $k_B T$ and an actual COP of 1.25. Cooling would still be obtained for significantly lower quantum efficiencies (due, e.g., to Auger recombination), albeit with a reduced COP, but this may be of little practical consequence given that Joule heating and other parasitic effects had not been taken into account.

In his paper, Berdahl offered some explicit advice for the experimentalist. In order to defeat the limitations of refractive indices greater than one, he suggested frustrating the total internal reflection occurring at the semiconductor surface by bringing an external absorber within a couple of microns of the diode. In practice, however, avoiding accidental thermal conduct between the two optical elements would probably prove difficult. Berdahl's most innovative suggestion, however, was to run

the diode in its reverse-biased mode, in which case it cools a neighboring object by absorbing its thermal emission, a phenomenon he termed “negative luminescence.” The effect of parasitic losses in the diode can then be reduced by mounting it on a separate heat sink. To our knowledge, however, no one appears to have followed up on this idea.

C. THERMODYNAMICS OF PHOTOLUMINESCENCE

The concept of anti-Stokes photoluminescence cooling did not begin to arouse serious practical interest until the advent of the laser, which could serve as the requisite source of high-intensity, narrow-bandwidth radiation. The story begins in the late 1950s, when Scovil and Schulz-DuBois (1959) at Bell Laboratories realized that a maser run backwards would act like a refrigerator. They considered a system with three levels, labeled 0 through 2 (cf. Fig. 2), where states 1 and 2 are in thermal equilibrium with a cold reservoir of temperature T_c ; these two states are separated by a transition frequency of ν_{12} . In turn, the 0 and 2 states are coupled to a hot reservoir at temperature T_h and are separated by a transition frequency of ν_{02} . Scovil and Schulz-Dubois then defined the efficiency of maser action as $\eta_M = \nu_{01} / \nu_{02}$ (i.e., the maser output energy divided by the input pump energy, assuming unit quantum efficiency), where T_c is taken to be the sample temperature. For example, T_c might be the temperature of a crystalline lattice to which is coupled spin levels of maser-active rare-earth ions, while T_h would be the temperature of a microwave gas discharge used to pump the system. From knowledge of the Boltzmann population factors, one then obtains inversion on the 0–1 transition provided $\eta_M \leq \eta_C$, where the Carnot efficiency is $\eta_C = (T_h - T_c) / T_h$. Since the maser can be regarded as a heat engine, as depicted in Fig. 2, this result is a simple expression of the second law of thermodynamics. Reversing the cycle then cools the crystal and an analogous analy-

sis leads to $\eta \leq \text{COP}_C$. Here the cooling efficiency is simply $\eta = \nu_{12} / \nu_{01}$ —the cooling energy divided by the maser energy—while the Carnot COP of the refrigerator is $\text{COP}_C = T_c / (T_h - T_c)$.

Mazurenko (1965a, 1965b) has applied thermodynamics to the irreversible generation of stimulated radiation in a laser. He used Prigogine's (1954) "local" formulation of the second law to consider the rate of entropy change for a set of particle oscillators in contact with both a nonequilibrium radiation field and a thermal reservoir, the latter taken to be the host medium. Mazurenko then derived an inequality for the laser efficiency η_L , defined as the ratio of the laser output power to the absorbed optical pump power. Landsberg and Evans (1968) have since generalized this result to obtain $\eta_L \leq (1 - T / T_{F_p}) / (1 - T / T_{F_L})$, where T is the temperature of the thermal reservoir, and T_{F_p} and T_{F_L} are the flux temperatures of the pump and laser radiation, respectively, defined as the ratio of the corresponding energy and entropy fluxes. The limiting value is the ratio of two Carnot efficiencies because we can interpret a laser in terms of a combined forward- and reverse-running pair of heat engines, as depicted in Fig. 3, with the output work of the forward-running engine driving the operation of the reverse engine. Both share a common cold reservoir at temperature T , but the first engine's hot reservoir has a flux temperature of T_{F_p} , while the second's is of temperature T_{F_L} . Since an ideal laser carries energy but no entropy, $T_{F_L} = \infty$ in this case, and thus $\eta_L \leq (T_{F_p} - T) / T_{F_p}$. Running a laser backwards as an optical cooler, what was formerly the pump radiation will now be identified as the output fluorescence with an affiliated flux temperature of T_{F_h} ; the technical efficiency will then be given by the reciprocal of the laser efficiency η_L . Hence, the technical efficiency must be less than $T_{F_h} / (T_{F_h} - T)$, which agrees with the inequality derived by Weinstein in the case of electroluminescence cooling.

Kafri and Levine (1974) have also emphasized entropy considerations in lasing and cooling cycles, expressing the change in the entropy of the medium during

thermal relaxation as $\Delta S_c \geq \Delta S_p + \Delta S_h$, where ΔS_p and ΔS_h are the medium's entropy changes during absorption of the pump and during the subsequent optical emission, respectively. For laser cooling, $\Delta S_p \approx 0$ and $\Delta S_c < 0$, so that coherent emission (for which $\Delta S_h > 0$) is not possible. If the cooling system consists of three energy levels 0 through 2, with the pumping on transition 1–2 and the fluorescence on 2–0, then the ratio of the populations of levels 1 and 0 is $n_1 / n_0 = \exp(\Delta S_c / k_B)$ if these two levels are in thermal equilibrium with each other. Thus, the refrigeration process depletes (“cools”) the population of level 1. Kafri and Levine suggested that a possible practical application of this scheme would be to the increase of gain in a laser whose lower level is 1 (and whose upper level is presumably substantially above 2).

For work performed up to 1980, a unified review of the thermodynamics of systems that convert light into heat or work, or vice-versa, was prepared by Landsberg and Tonge (1980). In complete generality, they considered an energy converter to be a box, into which energy and entropy is entering at certain rates from a pumping system and is flowing out at another pair of rates to a sink. Also contributing to energy and entropy flow to and from the box are terms for the conventional transfer of heat to a thermal reservoir and the delivery of work. Adding one final term to quantify the irreversible generation of entropy within the box (such as would arise from nonradiative relaxation of optically pumped centers or Joule heating during electrical excitation), a pair of energy- and entropy-balance equations for steady-state or cyclic operation of the converter are readily written down. Applied to a laser cooler, the two balance equations imply $\eta \leq T / (T_{F_h} - T)$ once again, where η is the “first-law” cooling efficiency (ratio of the rate of heat withdrawn from the thermal reservoir at temperature T to the input optical pump power) and where as before the fluorescence flux temperature T_{F_h} is defined as the ratio of the emitted rates of energy and entropy.

An important clarifying point that Landsberg and Tonge emphasize in their review—one not fully appreciated by previous workers—is the difference between flux temperatures, which are not “absolute thermodynamic temperatures” (i.e., derivatives of entropy with respect to energy), and brightness temperatures, which are. In any case, the right-hand side of their inequality is effectively a Carnot efficiency, whose calculation requires a determination of the entropy carried away by the *nonequilibrium* emitted radiation field. Landsberg and Tonge argue that this entropy is given by the usual *equilibrium* expression, namely, an integral of the logarithm of photon occupation numbers over all radiation modes contained within the spectral bandwidth, range of solid angles, and polarization directions of the emission. However, the fluorescence-energy flux density can also be written as an integral over these same photon occupation numbers. Hence, given a knowledge of the fluorescence spectrum, the entropy rate can be related to the energy rate, so that T_{F_h} is ultimately expressible purely in terms of the emission intensity. [This analysis implicitly assumed that T_{F_h} is much larger than the ambient temperature of the surroundings—see Weinstein (1960), whose results Landsberg and Tonge are essentially rederiving, for a discussion of this point.] As a simple example, Landsberg and Tonge considered the case where the fluorescence spectrum is constant over a narrow band of frequencies and zero elsewhere; they graphed values of the fluorescence flux temperature versus the emission center frequency for various choices of the energy flux density per unit bandwidth. They also quoted expressions applicable to the case of a Gaussian spectrum, which may be adaptable to some of the experimental results discussed in Sec. III below.

Recent experimental successes in cooling glasses, semiconductors, and liquids have led to a resurgence of theoretical interest in laser cooling of condensed matter. Oraevsky (1996) and other Russian workers (Rivlin and Zadernovsky, 1997; Zadernovskii and Rivlin, 1996) have considered the processes that limit the lowest

attainable temperature and the rate of cooling in laser-excited semiconductors. They all calculated the absorption coefficient from semi-empirical equations describing electron-hole creation, excitonic effects, and intraband absorption by free carriers. Including corrections for impurity-related and Auger recombination of the charge carriers, Oraevsky found that it should be possible to cool GaAs from 300 to 10 K by using a laser intensity near the saturation level, i.e., about 2000 W/cm^2 at room temperature and 300 W/cm^2 at the lowest temperatures. These calculations neglected the trapping of emitted photons by total internal reflection and further assumed that any surface states had been passivated by growing GaInP_2 on both sides of the GaAs layer. For simplicity, Oraevsky's model sample was taken to be optically thin, planar, and uniformly irradiated.

On the other hand, Zadernovskii and Rivlin focused on balancing the rate of cooling due to radiative recombination against the blackbody heat load from the room-temperature surroundings. They estimated a low-temperature limit of 3 K for a pump-laser intensity of 12 W/cm^2 . In their most recent article, they plotted the expected final sample temperature versus the pump-photon flux density for various values of the laser linewidth and of the ambient temperature. They explicitly checked that the phonon-relaxation time of the charge carriers remains at least two orders of magnitude shorter than the radiative-decay time at all temperatures of interest, so that the electrons and holes would be sure to thermalize with the lattice prior to recombination. Thus, these theoretical investigators continue to be optimistic about the prospects for laser cooling of semiconductors, although their calculations do not help to resolve the experimental difficulties to be discussed in Sec. III.C below.

Andrianov and Samartsev (1997a) have briefly reviewed the experimental results on laser cooling of ZBLANP glass doped with Yb^{3+} (Epstein *et al.*, 1995a) and of rhodamine 101 in liquid ethanol (Clark and Rumbles, 1996), again with an eye to-

wards estimating the theoretical limits on the cooling rates and on the coldest temperatures that can be attained. The optical Bloch equations for the populations of the relevant levels were solved, allowing in principle for both spontaneous and stimulated Stokes and anti-Stokes transitions, in addition to direct resonance fluorescence. The experimental systems were divided into two components—the set of active ions or molecules and the embedding medium—and each assigned separate heat capacities. With the help of photon-echo data previously obtained on materials similar to the laser-cooling systems analyzed in their paper, Andrianov and Samartsev deduced that under the experimental conditions of interest, the temperature difference between the ytterbium ions and the glass host is only 30 μK , while between the rhodamine 101 molecules and the ethanol solvent the temperature difference is about 3 mK. Unfortunately, too many unknown parameters exist in their resulting theoretical equations to make quantitative tests or predictions.

Finally, a few authors have begun to address the possibility of exploiting coherent effects in laser cooling. Kosloff and co-workers (Bartana *et al.*, 1997; Geva and Kosloff, 1996) have derived a generalized quantum master equation that predicts the existence of a “refrigeration window” for a three-level system coupled to hot and cold quantum heat baths. The system is optically pumped at extremely high intensities; therefore the pump is modeled as a classical electromagnetic field that performs work on the system. Operation within the refrigeration window allows heat to be extracted out of the cold bath until its temperature reaches absolute zero, thus overcoming the weak-field saturation limit on the cooling as first calculated by Scovil and Schulz-DuBois (1959). Nevertheless, the results are in compliance with the three laws of thermodynamics. In particular, the cooling rate drops to zero at 0 K, in agreement with the third law, although it is admitted that the issue of thermalization time scales probably becomes significant before this ultimate limit is reached.

In other work involving optical coherence, Andrianov and Samartsev (1996a, 1997b) have considered exploiting induced superradiance in a two-level system as a cooling technique. In one scheme, taking Frenkel excitons in a pure crystal as the two-level systems, the required population inversion would be created using an intense, nonresonant pulse. Lloyd (1997a, 1997b) has discussed the concept of a coherently pumped, quantum optical refrigerator. He showed that if the inverse Rabi frequency for the laser-driven atoms is smaller than the radiative relaxation rate of the excited state, then a cyclical process using two π -pulses of the same frequency results in cooling with significantly higher efficiency than what is achieved with incoherent pumping. In particular, the cooling rate need not approach zero as the Carnot limit is approached. Lloyd has also considered what he termed a quantum-mechanical "Maxwell's demon." In an explicit example, the idea is applied to a two-level system, conveniently visualized as a magnetic spin. First, an incident pulse acquires information about the state of the spin: if it is in the thermally excited high-energy level, a second pulse, of pulse area π , coherently extracts its energy. Such information measurement can be performed using a technique known as spin-coherence double resonance, for example. In this thought experiment, decoherence due to spin dephasing introduces thermodynamic inefficiencies in accordance with the second law.

An important advantage of coherent cooling processes is that the cycling time can be reduced, thus increasing the cooling power. However, high-power pulsed excitation is required by such schemes. So far, no experimental attempt to achieve coherent, solid-state refrigeration has been performed, but this is clearly a promising arena for future work.

III. Working Substances for Fluorescence Cooling

A. GASES

In his pioneering article, Pringsheim (1929) discussed the possibility of cooling Na vapor by anti-Stokes processes. The idea was to pump the D_1 line ($1\ ^2S_{1/2} \rightarrow 2\ ^2P_{1/2}$) at $5896\ \text{\AA}$ using suitably filtered D_1 light obtained from an independent sodium source. The gas pressure of the cooling sample would be kept low enough so that collisional de-excitations would occur only rarely and therefore the atomic relaxation would be primarily radiative. At the same time, the Na pressure would be high enough to permit at least partial thermalization among the pair of higher-lying $2\ ^2P_{1/2}$ and $2\ ^2P_{3/2}$ levels. To reduce the heat load, the gas would be kept in a transparent, thermally insulating dewar. Finally, emission on the D_2 line ($2\ ^2P_{3/2} \rightarrow 1\ ^2S_{1/2}$) at $5890\ \text{\AA}$ would cool the gas.

Twenty-one years later, the French researcher Kastler (1950) expanded upon Pringsheim's idea, which he called an *effet lumino-frigorique* ("photo-refrigerating effect"). As applied to the cooling of sodium vapor, achieving the dual requirements of minimized collisional quenching of the optically pumped level and maximized thermalization within the narrow $2\ ^2P$ manifold is accomplished by introducing an inert buffer gas, such as helium or argon, into the sample cell. Suggested pressures were $1\text{-}10\ \mu\text{torr}$ for the alkali vapor and $\sim 0.1\ \text{torr}$ for the buffer. At moderate optical intensities it would be possible to excite every Na atom about 10,000 times per second. Since the $17\ \text{cm}^{-1}$ frequency splitting between the D_1 and D_2 lines corresponds to a temperature difference of 24 K, a peak cooling rate of over 10 K/s was predicted. Kastler never attempted this experiment himself, and in fact concludes his abstract with a sentence that we translate as, "Even if one succeeds in realizing the necessary

experimental conditions for radiative cooling, this effect is likely to remain a scientific curiosity rather than a practical technique for obtaining low temperatures.”

Pringsheim (1946), in his response to Vavilov’s criticisms (cf. Sec. II.B), proposed that diatomic gases such as I_2 could be radiatively cooled via the vibrational sidebands of their electronic transitions. For example, the pump light could be filtered so as to populate an excited electronic manifold with only those molecules initially lying in the thermally populated, fifth vibrational level ($v'' = 4$) of the electronic ground state. These molecules may then relax by emitting anti-Stokes radiation corresponding to transitions to the $v'' = 3, 2, 1,$ or 0 levels of the ground state. The relative intensities of these various lines depend only on the Franck-Condon factors and can be larger than the Stokes or the Rayleigh line strengths in an appropriate system. Since cooling is no longer dependent on collision-mediated thermalization in the excited-state manifold, an advantage of this idea is that the sample pressure can now be made as low as one pleases in order to eliminate collisional quenching (at the expense of a reduced cycling rate).

A similar idea consists in pumping the rotational sidebands of the vibrational levels of a heteronuclear diatomic gas such as carbon monoxide (Djeu, 1978). By pumping the R branch of the rovibrational spectrum (e.g., $v=0, J=2'' \rightarrow v=1, J=1'$), the rate of P -branch relaxation ($v=1, J=1' \rightarrow v=0, J=0''$) can be enhanced, which cools the gas as the ground rotational manifold rethermalizes. After accounting for the branching ratio for radiative relaxation via the P and R branches, and provided that nonradiative vibrational–translational de-excitation is negligible, the average cooling energy is found to be $2BJ'$ per cycle, where B is the rotational constant of the molecule. Evidently it is an advantage in this experiment to pump the highest J' levels possible, at least as long as the intra-rotational thermalization times remain short in comparison to the cycling time.

Yet another possibility would be to excite a high vibrational overtone (say $\nu = 3$) of a gaseous CO molecule that subsequently relaxes through a sequence of $\Delta\nu = 1$ radiationless energy-transfer exchanges with neighboring, unexcited CO molecules (Treanor *et al.*, 1967; Yardley, 1971). Because of vibrational anharmonicity, the $3 \rightarrow 2$ and the $2 \rightarrow 1$ transition energies are smaller than the $0 \rightarrow 1$ energy and hence the exchanges are endothermic, again cooling the gas. In similar fashion, one might be able to achieve cooling by pumping large $\Delta\nu$ transitions of solid-state systems such as CN^- doped in alkali halides or large ΔJ transitions of rare-earth ions in crystals (Epstein *et al.*, 1995b). For that matter, one could mix two different but nearly resonant species in the sample and pump the lower-energy system. The rate of phonon-assisted energy transfer to the second species is enhanced by insisting that this latter species' concentration be much higher than that of the first. In essence, the combination of the two species yields a two-level upper manifold in which the higher-energy state is highly degenerate, thus favoring radiative relaxation out of this state and cooling of the lattice. All of these cases require a high radiative efficiency for the final $1 \rightarrow 0$ decay and the absence of trapping centers such as heavy isotopes of CO and CN^- or other contaminating impurities. Also, the efficiencies of these schemes depend on large coupling strengths for the operative radiationless transitions relative to other possible decay channels and on sufficient absorption strengths for the optically pumped transitions. As far as CO and CN^- are concerned, many of these ideas are therefore probably not viable in practice. Nevertheless, they provide helpful starting points for broader thinking on possible fluorescence-cooling mechanisms.

A final scheme for anti-Stokes cooling of gases has been actually demonstrated experimentally and was in fact the first observation of non-Doppler fluorescence cooling of any material system. In the early 1980s, Djeu and Whitney (1981) at the Naval Research Laboratory successfully cooled CO_2 gas by 1 K along the path of a 1-cm-diameter pump beam passing through a sample cylinder whose walls were

maintained at 600 K. The 10.6- μm (100) \rightarrow (001) vibrational combination transition was pumped by using a 300-W CO_2 laser running on the $P(20)$ line. Cooling resulted from 4.3- μm anti-Stokes emission of the (001) asymmetric-stretch mode to the (000) vibrational ground state, a process highly favored owing to the 99.8% radiative branching ratio for this transition. Thermal repopulation of the laser-depleted (100) symmetric-stretch mode was assisted by three factors: a near resonance of this state with the first overtone of the (010) bending mode, the 600-K ambient temperature, and mixing of the CO_2 sample at a partial pressure of 64 mtorr with Xe at a partial pressure of just under 0.2 torr. Xenon was chosen as the buffer gas because of its low thermal conductivity and because it only weakly deactivates the CO_2 (001) state; its partial pressure in the sample cell was determined by trial and error to optimize the cooling rate. In the absence of the Xe buffer, the carbon-dioxide pressure was set just at the onset of collision-induced relaxation of the (001) state. The resulting CO_2 density, in turn, determined the choice of the cell diameter, namely 12.7 cm, in order to minimize self-absorption of the 4.3- μm radiation. The inner walls of the cell were painted flat black to prevent reflections of the fluorescence back into the gas. The temperature changes were determined by measuring the axial-pressure changes with a capacitance manometer; while disagreeing in absolute magnitude with theoretical calculations, the overall shape of the measured temperature dependence on the Xe partial pressure was verified, thus supporting the cooling results.

B. ORGANIC DYE SOLUTIONS

The question of whether anti-Stokes emission from fluorescent dyes dissolved in liquid solvents could yield a cooling effect was first asked by Vavilov (1945), which reflected spectroscopists' great interest in such systems over the preceding two decades (Jablonski, 1933; Wood, 1928). As late as 1970, this question was still being answered in the negative, based on a theoretical analysis of experimental results for

a variety of molecules including rhodamine-B and fluorescein in ethanol (Ketskeméty and Farkas, 1970). Two years later, however, Erickson (1972) performed a careful set of measurements of anti-Stokes emission by rhodamine 6G in both ethanol and glycerol solvents and found that the luminescence quantum efficiencies remain independent of the wavelength of excitation, even for pump frequencies 2500 cm^{-1} smaller than the 0–0 transition frequency. Specifically, yellow emission out of the first-excited singlet S_1 manifold was observed following 632.8-nm HeNe excitation starting from high-lying rovibrational levels in the singlet-ground-state S_0 manifold. The long-wavelength absorption was exponential in $h\nu / k_B T$ and could be simply modeled by assuming a Boltzmann population distribution over a set of equally spaced levels in the ground electronic manifold. All transitions to the excited state originating in these levels were taken to occur with the same cross section. From his data, however, Erickson estimated an absolute fluorescence quantum efficiency for rhodamine 6G in ethanol of only 0.88. As a possible explanation for this low value, he noted a broad luminescence peak at $\sim 665 \text{ nm}$ that did not fit his model, nor could the peak be attributed to triplet states, dimers, or photobleaching products, and thus was ultimately attributed to fluorescent impurities that must have quenched the rhodamine emission.

Simultaneously, Chang *et al.* (1972) were making similar measurements on rhodamine-B in methanol and in polyurethane thin films. Assuming the absorption coefficient of the host to be negligible, they deduced that the ratio of the cooling power to the absorbed laser power (i.e., the cooling efficiency) is given by $\lambda \eta_Q / \lambda_F - 1$, where λ is the pump wavelength, η_Q is the fluorescence quantum efficiency, and λ_F is the mean fluorescence wavelength. For 632.8-nm excitation of rhodamine-B in methanol, this group deduced that a minimum value for the quantum efficiency of 0.94 is required to obtain cooling. Chang *et al.*'s conference abstract ended with the sentence, "This cooling effect is being investigated," yet no further

results of this research were published and the field of laser cooling of condensed materials remained dormant for the next 20 years.

It was only in the early 1990s that Drexhage's research group in Siegen, Germany succeeded in laser cooling a solvated organic dye (Zander, 1991; Zander and Drexhage, 1995). They found it necessary to modify Chang *et al.*'s expression for the cooling efficiency by subtracting the quantity A_{nf} / A_{dye} , where A_{nf} is the spurious absorbance due to both nonfluorescent impurities and the solvent itself, and A_{dye} is the absorbance of the dye molecules alone. In the wavelength region of interest, the intrinsic ethanol absorbance was independently measured and found to be significantly lower for the monodeuterated form of the solvent than for the nondeuterated form. In turn, Erickson's model for the long-wavelength dye absorption was fit to A_{dye} , thus revealing a constant residual background absorbance of 2.3×10^{-4} (for a 1-cm path length) in this wavelength region. This excess absorption was attributed to impurities present in the solute but, impressively, was fully eliminated when the starting dye was purified by column chromatography. The mean fluorescence wavelength λ_F was calculated as $\left[\int F_\lambda d\lambda \right] \left[\int F_\lambda d\lambda / \lambda \right]^{-1}$, where F_λ measures the emission spectrum, although this expression is not rigorously correct unless F_λ is the spectral intensity normalized by the photon energy—see Eq. (2) of Sec. IV.A. In any case, λ_F was thus found to be 563 nm for a 10^{-5} -M solution of rhodamine 6G at 293 K. Combining their spectroscopic results, Zander and Drexhage concluded that cooling of the dye solution would occur, at an optimal pump wavelength of 579 nm, if the fluorescence quantum efficiency exceeded a threshold value of 0.984.

A photothermal lensing technique was then used to measure the actual value of η_Q . In this experiment, the output beam from a krypton-ion-pumped dye laser was brought to a focus about one Rayleigh length in front of the sample. Within the sample itself, this pump beam's radial intensity distribution generated a temperature gradient in the solution which was associated, in turn, with a gradient in the

liquid's refractive index. Since the index decreased with increasing temperature, a weak diverging lens formed in the liquid at pump wavelengths that heated the sample. Defocusing was then observed for a weak but stable HeNe probe beam that overlapped the pump beam. After blocking the unabsorbed pump radiation with a bandpass filter, the degree of defocusing could be detected by measuring the probe beam power transmitted through a pinhole centered on the HeNe optical axis.

A key advantage of this photothermal lensing technique is that an analytic expression for the time dependence of the signal can be obtained. It is a function of just two parameters, t_c and θ , where t_c is a characteristic thermal diffusion time that depends on the diameter of the pump beam and on the density, specific heat, and thermal conductivity Λ of the solution. The quantity θ measures the rate of heat deposition and depends on the difference between the absorbed and emitted power, the laser wavelength, the gradient in the refractive index, and Λ . Thus, in principle, the data could be fit with no free parameters to yield the fluorescence quantum efficiency. In practice, the model's dependence on the inexactly known thermo-optic coefficients was eliminated by comparison with the signal obtained from a reference sample composed of a nonfluorescent compound dissolved in the same solvent. The results were $\eta_Q = 0.980$ for an air-equilibrated solution of rhodamine 6G-perchlorate in C_2H_5OD , a value which rose to 0.990 after deaeration of the sample with a nitrogen gas stream. Thus, by all indications, the sample would cool if pumped in the wavelength range of 570–585 nm. Zander and Drexhage indeed observed a switch in the sign of the thermal lens from diverging to converging as the pump wavelength was tuned beyond 570 nm, conclusively demonstrating cooling of the internal pumped volume of the sample. They measured a peak absolute cooling efficiency P_{cool} / P_{laser} of 3.2×10^{-5} at a pump wavelength of 575 nm, corresponding to a cooling power of 1 μ W and to a relative cooling efficiency P_{cool} / P_{abs} of 1.1%.

More recently, Clark and Rumbles (1996) have also observed laser cooling of a rhodamine dye dissolved in alcohol. Specifically, rhodamine 101 was chosen, as it exhibits little triplet-state crossover or two-photon absorption. Their sample consisted of a 0.3-mL volume of 10^{-4} -M rhodamine 101 in acidified ethanol, which was sealed into a cylindrical, fused-silica tube following degassing of the solution by freezing and vacuum pumping. The tube was suspended in an evacuated cryostat, the temperature of which was initially stabilized, but it is not clear whether the cryostat temperature was subsequently monitored for drifts over the multi-hour course of each cooling run. The sample was optically pumped in the 580–680-nm range with up to 350 mW from an argon-ion-pumped cw dye laser. At 15-minute intervals, the dye laser was blocked and the fluorescence intensity measured at 620 nm using a monochromator. (This fluorescence was excited by an auxiliary 1-mW HeNe laser beam focused into the pumped volume of the liquid.) The sample temperatures could then be deduced from these intensity values via a previously determined calibration curve obtained by measurement of the emission intensity for known temperatures in the range of 150–300 K. The dye solution was observed to heat when pumped at 583 and 605 nm and to cool when pumped at 620 and 634 nm, as expected since the former wavelengths correspond to photon energies larger than the average emitted photon energy while the latter wavelengths correspond to smaller energies. In particular, a maximum temperature drop of 3 K below ambient (290 K) was measured after pumping the sample at 634 nm for 4 hours with 350 mW of laser power.

Several criticisms, however, have been directed towards Clark and Rumbles' results (Mungan and Gosnell, 1996). An emissivity near unity is estimated for an ethanol–silica combination in the range of wavelengths over which radiative emission is significant for a room-temperature blackbody. This implies that the sample was subject to a blackbody thermal load that was larger than the actual laser-induced

cooling power, a problem that is not considered in the original paper. Secondly, Clark and Rumbles observed a linear change of the sample temperature even after 4 hours exposure to the pump laser, at which point no further measurements were made. But theoretically an exponential dependence of temperature on pumping time is expected; their sample's heat capacity of 3 J/K would have entailed a time constant of only 40 min. Hence, the temperature should have leveled off within 2 hours. Finally, the original experiments did not include a reference run performed with the dye laser tuned to the null wavelength where the sample should neither heat nor cool. Such a run would have provided a good measure of the overall thermal drifts of the system and a powerful test of the underlying theory.

These criticisms are partially resolved in a reply by Rumbles and Clark (1996). A 4-hour reference run of the type just described showed that no net heating or cooling occurred during the run. However, temperature fluctuations in the latter measurement spanned a range of 3 K, leaving unaddressed the issue of thermal drifts of the system. The question of the radiative heat load is not discussed in Rumbles and Clark's reply except for an unsubstantiated comment that the radiative coupling between the sample and surroundings must be "less than optimum." More positively, a new run showed the return of the sample temperature to the ambient value following laser cooling at a pump wavelength of 635 nm. This result is encouraging, but again the detailed shape of the curve at long times is unclear. One would expect the time dependence of the sample temperature during the cooling and re-equilibration periods to both follow an exponential form with the same time constant. This prediction deserves testing.

In any case, it may prove difficult to scale up the dye results to obtain larger temperature changes. Clark and Rumbles themselves note that increasing the solute concentration leads to the formation of nonfluorescent molecular aggregates such as dimers, as well as to an efficiency-reducing increase in the mean emission wave-

length due to re-absorption of the emitted radiation. Already, the peak emission wavelength of their 10^{-4} -M rhodamine 101 solution was found to be 8 nm longer than the peak wavelength that obtains in the limit of zero optical density. Reducing the sample size does not ameliorate these problems because the surface of the sample cell promotes nonradiative relaxation; an analogous issue arises in the anti-Stokes fluorescence cooling of gases. Embedding the dye molecules in a polymer host may eliminate this problem if the quantum efficiency remains high and if photodegradation of the dye does not occur. This suggestion emphasizes the greater practicality of cooling solids rather than fluids.

C. SEMICONDUCTORS

In the early 1960s, gallium arsenide was identified as a candidate for fluorescence refrigeration. Keyes and Quist (1962) fabricated diodes by diffusing Zn into single-crystal n -type GaAs to create a p -type overlayer. The forward current-voltage characteristics were measured at 298 and 77 K, and the current i was found to vary exponentially with $eV / 2k_B T$ just below saturation. The luminescence spectra of the diode was measured and consisted of two peaks at both temperatures, with the higher energy peak—centered at 1.33 eV at 77 K and 1.44 eV at 298 K—identified with emission across the bandgap. On the other hand, the relative intensity of the broad, low-energy peak was sample and temperature dependent and hence was presumably not intrinsic. An absolute calibration of the emission intensity indicated that approximately 40% of the injected electrons gave rise to externally emitted bandgap photons at 298 K, an amount which fell to about 5% at 77 K because internal reflection trapped a large fraction of the radiation. After correcting for this effect, an internal quantum efficiency for bandgap emission of between 0.48 and 0.85 was deduced. The term *internal* quantum efficiency is here defined as the ratio of the number of pho-

tons emitted anywhere inside the material to the number of injected electrons. In contrast, the *external* quantum efficiency is the corresponding quantity in terms of photons that actually escape from the medium. Keyes and Quist found that the emission intensity varied linearly with the density of the injection current, saturating at about 2.5 kA/cm². At 77 K, the luminescence spectrum exhibited a weak tail extending well into the visible range. These researchers thus concluded that electroluminescence refrigeration with a cooling power of $i(V_f - V)$, where V_f is the average emitted photon energy in volts, would be feasible if the external quantum efficiency could be made large enough.

Further measurements related to this suggestion were made at temperatures down to 27 K by Dousmanis *et al.* (1963, 1964), as has been reviewed by Pankove (1975). Beginning with a thermodynamic analysis, these workers showed that the cooling efficiency η cannot exceed T / T_{B_h} , where T is the sample temperature and T_{B_h} is the fluorescence brightness temperature. The latter quantity is related to the emitted photon occupation number n_v^h according to $n_v^h = 1 / [\exp(hv / k_B T_{B_h}) - 1]$, with hv the photon energy. (Note that the total rate of photon emission is $\int n_v^h dv = \eta_Q i / e$.) At low carrier currents i , $T_{B_h} \approx T$ and the cooling efficiency η is expected to be large, although this operating condition is not particularly useful since the cooling rate would be negligibly low. In the opposite limit of high currents, the lasing threshold of the GaAs diode is reached, corresponding to $T_{B_h} \rightarrow \infty$, and η falls to zero. But at intermediate currents, the frequency of the spectral peak of the incoherent emission favorably rises with the drive current; it likewise rises by increasing the dopant concentration. On the other hand, Joule heating limits the cooling rate obtainable at large carrier currents. It is also clear that $\eta \rightarrow 0$ as $T \rightarrow 0$. These facts imply that compromises are required in selecting the operating current, dopant concentration, and operating temperature.

Dousmanis *et al.*'s best diode was prepared by epitaxial solution growth of an n -type GaAs layer on a p -type substrate. For an applied voltage V of 1.335 V (corresponding to a vacuum wavelength of $hc / eV = 927$ nm), an injection current of 5 mA, a diode temperature of 78 K, a Zn acceptor concentration of $3 \times 10^{19} \text{ cm}^{-3}$, and a Te donor concentration of about 10^{19} cm^{-3} , the luminescence band peaked at 897 nm and about 94% of the emitted photons had energies exceeding eV . Taking this peak wavelength to correspond to the average emission energy implies a cooling efficiency of 3%, assuming unit quantum efficiency and zero Joule heating. To put it another way, 0.97 is the threshold value of the external quantum efficiency for cooling to occur. However, because of the diode's $\sim 0.5\text{-}\Omega$ resistance and the commensurate i^2R loss, the threshold value of the external quantum efficiency rises to 0.99 for an operating current of 30 mA. By reducing the current to 10 mA, 250 μW of net cooling is expected at 78 K if $\eta_Q = 0.99$. Dousmanis *et al.*, however, never reported a direct attempt at measuring the cooling effect.

The above discussion suggests that one can do better through optical rather than electrical pumping of the sample, thereby avoiding Joule heating and eliminating the need for a p - n junction. Even so, a system with a near-unit external quantum efficiency is required. For this reason, no further experimental progress on laser cooling of semiconductors was achieved until recently. In 1993, a team of researchers at Bellcore (Schnitzer *et al.*, 1993) demonstrated an internal fluorescence quantum efficiency of $99.7\% \pm 0.2\%$ for a 500-nm thick, CVD-grown AlGaAs/GaAs/AlGaAs double heterostructure etched off of an AlAs release layer. The sample was Van der Waals bonded to an SiO_2 -coated gold reflector and optically pumped at 780 nm using a cw AlGaAs laser. The active GaAs layer was p -doped and had a refractive index of 3.54, implying an emission escape cone due to total internal reflection encompassing only 2% of 4π steradians. Furthermore, even within the escape cone, the transmittance is only $\sim 30\%$. Hence, fluorescence was trapped between the sample surfaces,

and consequently absorbed and re-emitted (“reincarnated”) many times before final escape. Such trapping multiplies the effect of parasitic losses such as those due to absorption by dark impurities, nonradiative electron-hole recombination, and absorption by the gold mirror. As a result, the measured external quantum efficiency was only 72%. From this measurement, however, the above-quoted value of 99.7% was obtained for the internal quantum efficiency. The Bellcore team further found that 23% of the lost quantum efficiency could be attributed to absorption by the Au reflector while only 5% derived from bulk parasitic effects. For purposes of solid-state photoluminescence cooling, the latter figure is encouragingly small.

These results motivated Gauck *et al.* (1995, 1997) to attempt bulk laser cooling of a direct-bandgap, III–V semiconductor heterostructure. The samples were grown by vapor-phase epitaxy at 1000 K and consisted of a nominally undoped GaAs active layer of thickness 0.5 to 2 μm embedded between two passivating layers of 2- to 3- μm -thick GaInP₂. The basic idea was to pump the material in the Urbach absorption tail, thus creating cold free carriers at the bottom of the conduction band and a complimentary population of holes at the top of the valence band. Subsequently, intraband thermalization of the free carriers followed by radiative recombination would extract heat from the semiconductor lattice. By virtue of the picosecond time scale for the thermalization steps and the nanosecond time scale for radiative relaxation, a high density of cooling power could in principle be sustained with this approach.

This simple picture, however, is complicated by the existence of two nonradiative relaxation mechanisms intrinsic to the sample. On the one hand, surface recombination, whose rate increases linearly with the carrier density, dominates the nonradiative loss at low densities. On the other hand, Auger recombination, which increases with the cube of the density, dominates the loss at high densities. Because of the quadratic dependence of the radiative recombination rate on carrier density a

density that optimizes the fluorescence quantum efficiency must therefore lie at some intermediate value.

The best experimental results were obtained for a 0.5- μm -thick GaAs layer within which the optimum carrier density was calculated to be of $8 \times 10^{17} \text{ cm}^{-3}$. In order to enhance the escape probability of the emitted photons, the 0.5-mm diameter heterostructure was mounted in optical contact with the flat surface of a ZnSe hemisphere 4 mm in radius. This material was chosen for its very low absorption over the GaAs emission band, despite its nonideal index match to the sample—ZnSe has an index of refraction of only 2.50. The hemisphere was anti-reflection-coated on its curved surface and the sample was pumped from its back side with a titanium-sapphire laser. Monte Carlo simulations were used to estimate that this output coupler reduced the number of photon reincarnations from 40 to 6, thus greatly increasing the external quantum efficiency η_Q^{ext} . The sample and output-coupler combination were suspended *in vacuo* and a thermistor used to measure their temperature. With the pump laser tuned to the mean emission wavelength of $\lambda_F = 866 \text{ nm}$, the observed heating rate gave a direct measure of η_Q^{ext} , namely 0.96. This value corresponded to an internal quantum efficiency of $(0.96)^{1/6} = 0.993$. While impressive, the longest wavelength at which the sample could be pumped with the intensity necessary to excite the optimum carrier density was 888 nm—a wavelength shifted from λ_F by only $1.4 k_B T$ —and therefore net cooling was not observed. On the other hand, the heating rate was found to decrease with the expected linear dependence on increasing wavelength all the way to the 888-nm limit, indicating that free-carrier absorption must be negligible. Under the assumption that this continues to hold true out to a pump detuning from λ_F of $2.2 k_B T$, thermal break even would be obtained with the existing external quantum efficiency. Conversely, break even would occur at the 888-nm pump wavelength by merely increasing the external quantum

efficiency to 0.972. Net laser cooling of GaAs thus appears achievable in the near future.

D. RUBY

An anti-Stokes fluorescence cooler is essentially a laser run in reverse: a coherent, directional beam of light illuminates an active medium yielding higher-frequency, broadband, more or less isotropic radiation as output. This viewpoint has motivated many of the choices of working materials for laser cooling in this section. In particular, within two years of the first successful demonstration of lasing in ruby ($\text{Al}_2\text{O}_3:\text{Cr}^{3+}$), Tsujikawa and Muraio (1963) proposed that optical cooling might be achieved in this material at temperatures near a few tens of kelvin. The cooling process would work by optical pumping from the Cr^{3+} electronic ground state to the lower member of the ion's two-fold 2E excited-state manifold, followed by thermalization across the 29 cm^{-1} energy gap between these two states. Subsequent emission from both levels (*i.e.*, on the well known R_1 and R_2 lines) would return the pumped ions to the ground state; the result of the cycle is thus extraction of heat from the host lattice. These researchers even suggested that cooling might be achievable in the millikelvin range by taking advantage of the 0.38 cm^{-1} splitting of the Cr^{3+} 4A_2 ground-state manifold.

Interestingly, Tucker (1961) at General Electric had previously observed the amplification of 9.3-GHz phonons resonant with this Zeeman-split pair of ground states when a population inversion was prepared by microwave pumping. In other words, stimulated phonon emission occurred as a result of a very strong spin-lattice coupling at this frequency. This concept has been recently extended to the amplification of 29-cm^{-1} phonons by selective excitation of the upper of the 2E levels with a pulsed excimer-pumped dye laser (Fokker *et al.*, 1997a, 1997b). The ultimate goal of

such experiments (Kittel, 1961) is to demonstrate “sound amplification by stimulated emission of phonons,” to paraphrase the usual acronym. By contrast, an anti-Stokes ruby cooler would consist of optically pumping the lower 2E level, rather than the upper one, and taking advantage of the strong spin-lattice coupling to absorb phonons rather than emit them.

Tsujikawa and Murao performed a detailed 4-level rate-equation analysis using the known R_1 lifetime and relative absorption cross sections for light polarized parallel or perpendicular to the trigonal axis of the host lattice. The dopant concentration was taken to be 500 ppm Cr_2O_3 by weight to give a peak absorption coefficient of 2 cm^{-1} . Further, Tsujikawa and Murao suggested silver plating the back side of the sample to enhance the pumping. The cooling rate was then computed in terms of the predicted cooling power as $\dot{T} = -\mathcal{Q}_c / C$, where C is the heat capacity of the sample, taken to be of the Debye T^3 form with $\theta_D = 800 \text{ K}$. The paper ends with some general remarks about limiting factors such as direct multiphonon or tunnel-assisted relaxation, de-excitation via Cr^{3+} aggregates, ion-lattice equilibration times, and self absorption of the fluorescence. However, by and large, not enough data were available at the time to characterize these processes in detail.

In fact, two years later Nelson and Sturge (1965) published a detailed analysis of the spectroscopy of ruby that clearly rules out the possibility of laser cooling of this system. The emission spectrum (see their Fig. 5) shows the existence of phonon sidebands on the Stokes side; although weak, they are so broad that their integrated area is comparable to that of the R lines! These sidebands peak at about 400 cm^{-1} below the $14,400 \text{ cm}^{-1}$ ${}^2E \rightarrow {}^4A_2$ transitions and extend down to almost $13,400 \text{ cm}^{-1}$. Hence, emission at the sideband frequencies with the combined emission of a photon and an average phonon will completely overwhelm the 29 cm^{-1} worth of cooling derived from the zero-phonon R_2 emission. More specifically, Nelson and Sturge defined the radiative efficiency of the R lines as the ratio of their integrated

fluorescence intensity to the total integrated fluorescence intensity. This quantity depends on temperature, polarization relative to the c -axis, and chromium ion concentration. For optically thin samples, the efficiency rises smoothly with decreasing temperature, leveling off at about 0.49 for polarization parallel to the c axis and at 0.83 for the perpendicular polarization. Given the magnitude of the Stokes shift in the sidebands, these results definitively rule out ruby as a cooling candidate.

E. RARE-EARTH IONS IN SOLIDS

As in the case of ruby, the death knell of many otherwise promising doped solid-state coolers is Stokes' deactivation of the excited active ions via the phonon sidebands. An important advantage of the rare-earth ions is that their optically active $4f$ levels are well-shielded from the lattice by the filled, outer $5s$ and $5p$ shells. This greatly reduces the strength of the vibronic sidebands, sharpens the homogeneous lines (leading to larger absorption coefficients and hence more efficient pumping), and suppresses multiphonon nonradiative relaxation.

Kastler (1950) was the first to propose fluorescence cooling of solids doped with rare-earth ions. For an appropriately doped salt crystal, he suggested pumping the weak anti-Stokes vibronic sidebands of rare-earth electronic transitions, which is necessarily accompanied by the absorption of lattice energy. Cooling would then result, assuming near-unit fluorescence quantum efficiency for the zero-phonon transitions back to the ground state. Kastler suggested that the cooling effect, though small, could be enhanced by the use of thermal shields that pass the fluorescence but block the blackbody radiation from the environment. In principle, this proposal is sound. However, the absorption strength of rare-earth vibronic sidebands has generally proved too small to encourage actual experiments.

Yatsiv (1961), at the Second International Conference on Quantum Electronics, was the first to clearly spell out the prototypical cooling cycle depicted in Fig. 1. He considered two groups of energy levels, one or both of which had intragroup level spacings on the order of $k_B T$ (adjustable at low temperatures by application of an external magnetic field), while the groups themselves were separated from one another by a large intergroup energy gap. Specifically, a gap of at least $10,000 \text{ cm}^{-1}$ was recommended, both for ease of optical pumping and to minimize the probability of nonradiative decay between the groups. A narrow-bandwidth source would be used to excite individual levels from the top of the ground-state group to the bottom of the excited group, so that no Stokes' emission would occur. Yatsiv suggested three pump sources for such an experiment: a high-intensity arc lamp from which a suitable frequency range is selected using a monochromator, a flash-lamp-pumped crystal identical to the cooling sample whose fluorescence spectrum is long-pass filtered, or, presciently, appropriate optical masers.

Under the assumption that the excited-state thermalization time is much shorter than the intergroup radiative relaxation times, Yatsiv performed a rate-equation analysis to derive the steady-state cooling rate. He specifically considered Gd^{3+} , whose large, $\sim 33,000 \text{ cm}^{-1}$ energy gap between the sharp $^8S_{7/2}$ ground-state and the $\{^6P_{7/2}, ^6P_{5/2}, ^6P_{3/2}\}$ excited states would guarantee negligible nonradiative relaxation. A Gd^{3+} concentration of 1 at% was recommended in order to balance the competing requirements of good pump absorption and minimal self absorption of the fluorescence. The radiative lifetime of Gd^{3+} out of the $^6P_{7/2}$ multiplet in stoichiometric, hydrated gadolinium chloride was known to be 7.8 ms, from which Yatsiv deduced values for the integrated absorption and emission cross sections. For a pump intensity of 1 mW/cm^2 , he thus estimated a cooling-power density of $3 \text{ } \mu\text{W/cm}^3$ at a sample working temperature of 10–40 K.

The first solid-state laser-cooling experiment of any kind was performed in 1968 by Kushida and Geusic (1968) at Bell Laboratories. They chose to work with YAG + 1 at% Nd³⁺ because this material could be used both as the refrigeration sample and to generate the pump laser radiation; in their experiment, both the lasing and cooling crystals were placed into the same optical cavity. The 0.1-inch-diameter by 2-inch-long cooling sample was supported by 3 needles inside an evacuable cell. The inner surfaces of this cell were gold coated, presumably to redirect scattered pump light back onto the sample, although this technique suffers the serious disadvantage of increasing the fluorescence self-absorption. When pumped at 1.064 μm , temperature changes of the sample were measured with an attached thermocouple and compared to those observed for an otherwise identical, undoped YAG rod.

For their experiment, Kushida and Geusic expected a volume cooling rate of $n_2 E_{cool} / \tau$, where n_2 is the excited-state population density, τ is the fluorescence decay time, and E_{cool} is the average absorbed phonon energy. Assuming thermal equilibrium among the emitting states and neglecting the small, intrinsic, nonradiative decay rates, an estimated value for E_{cool}/hc of 90 cm^{-1} was obtained by an appropriate sum of the net energy differences over all possible upper and lower levels. In vacuum, a sample temperature drop of 8.4 K below room temperature was thus predicted for a 100-W pump, while in air the predicted drop was 2.1 K. Under the latter conditions, the experiment yielded the expected time dependence of the sample's temperature but net cooling was not observed. Instead, only reduced heating was obtained: the final, steady-state temperature was found to be 0.6 K less than that of the undoped reference sample at a cavity power of 100 W. (Surprisingly, no cooling data is reported for the sample *in vacuo*.)

In search of an explanation for their results, Kushida and Geusic interpreted the $\sim 2\text{-K}$ temperature increase they observed for the reference sample as being due to direct absorption of the laser light by nonfluorescent impurities. For example, 50 ppb

of Dy^{3+} would account for the observed heating if this ion relaxed entirely by nonradiative processes. It was initially assumed that the doped sample would exhibit this same level of background heating. However, that a temperature difference of only 0.6 K was measured between the sample and the reference rather than the calculated 2.1 K implied that other parasitic heating effects must also have afflicted the doped sample. In particular, a reduction in the fluorescence quantum efficiency to 0.995 was enough to account for the discrepancy. In turn, this quantum efficiency could have resulted from a 30 s^{-1} multiphonon-decay rate across the 4700-cm^{-1} ${}^4F_{3/2} \rightarrow {}^4I_{15/2}$ energy gap of Nd^{3+} , a figure in good agreement with known nonradiative rates in other rare-earth ions. Kushida and Geusic mention that a similar nonradiative heating effect was seen when they attempted to laser cool the ${}^5I_7 \rightarrow {}^5I_8$ transition of YAG:Ho^{3+} . Unfortunately, no further details of this experiment are cited.

Chukova (1974), on the other hand, has argued that Kushida and Geusic's failure to obtain net cooling was due to an overly high intensity and an insufficiently narrow bandwidth of the pump source. She based these comments on purely thermodynamic calculations of the entropy fluxes of the laser and fluorescence radiation, obtaining a cooling efficiency of $\sim 30\%$ for a bandwidth of 10 MHz in the limit of zero pump intensity. This figure rises to over 60% as the laser line becomes infinitely sharp, but falls to zero for an intensity of about 10 W/mm^2 . In fact, she believed that a temperature drop of 37 K should have been obtained with a pump intensity of 1 W/cm^2 . However, this analysis appears to place too much weight upon idealized theoretical concepts. For example, it is clearly pointless to reduce the excitation bandwidth much below the absorption line's homogeneous width, which is certainly larger than 10 MHz at room temperature! All the more then, taking into consideration the strict, practical factors mentioned in the preceding paragraph, it is

surprising and encouraging that Kushida and Geusic managed to get as close to absolute cooling as they did.

Nevertheless, no further experimental attempts to laser cool rare-earth-doped solids were performed until 1995, when net cooling of a Yb^{3+} -doped glass was successfully demonstrated at Los Alamos National Laboratory. A detailed discussion of these results follows.

IV. Laser Cooling of Ytterbium-Doped ZBLANP Glass

The trivalent ytterbium ion is an ideal dopant for anti-Stokes fluorescence cooling of a solid host: within the energy gap of typical insulators, the ion's energy-level structure consists of only two Stark multiplets, namely, the ${}^2F_{7/2}$ ground-state multiplet and the ${}^2F_{5/2}$ excited-state multiplet located about 1.3 eV above the ground state. In all but the highest-symmetry hosts, the ground multiplet is split into a quartet of doubly degenerate states—the so-called Kramers' doublets—while the excited-state multiplet is split into a triplet of such states (cf. Fig. 4 for the detailed level structure in ZBLANP). Because the energy gap between the two multiplets is so large, multiphonon relaxation across the gap occurs at a rate orders of magnitude smaller than the radiative relaxation rate of 10^2 – 10^3 s $^{-1}$ (DeLoach *et al.*, 1993; Hasz *et al.*, 1993). Because of the sparse energy-level structure, pairs of proximate Yb^{3+} ions do not participate in energy-transfer reactions that open nonradiative relaxation pathways out of the ${}^2F_{5/2}$ multiplet, an effect that is otherwise common for excited states in rare-earth-doped solids. These factors combine to produce an emission quantum efficiency for ytterbium that approaches unity, even for high dopant concentrations. The overlap of the $\text{Yb}^{3+} {}^2F_{7/2} \rightarrow {}^2F_{5/2}$ absorption band with the broad tuning range of the Ti:sapphire laser is of great advantage in performing experiments with this electronic species.

Figure 5 shows the absorption and emission spectra of Yb^{3+} -doped $\text{ZrF}_4\text{-BaF}_2\text{-LaF}_3\text{-AlF}_3\text{-NaF-PbF}_2$ (ZBLANP) glass. The choice of this host material, a variation of the more common ZBLAN glass composition, is motivated by three considerations. The most important is that much effort has been devoted to producing high-purity ZBLAN-based glasses because of their potential applications in ultra-low-loss optical communications (Aggarwal and Lu, 1991). However, compared with silica—indeed compared with many other glass hosts (Zou and Toratini, 1995)— Yb^{3+} in ZBLAN glasses exhibits a greater anti-Stokes frequency shift for a given value of the absorption coefficient. Hence, this material holds the promise of greater cooling power than other glass hosts. Finally, as a heavy-metal glass, the material's maximum phonon frequency of only 580 cm^{-1} (Deol *et al.*, 1993) helps inhibit nonradiative multiphonon relaxation in both the Yb^{3+} ion itself and, perhaps more importantly, in other impurities that might quench the Yb^{3+} emission.

Another important property of this impurity system is that the emission spectrum at room temperature is independent of the pump wavelength and pump intensity. This implies that the 7-level Yb^{3+} system can be treated as homogeneously broadened and that it is therefore reducible to an effective two-level system. Within this two-level model, a single population density is attached to each of the ground- and excited-state manifolds. In turn, the absorption cross sections for individual transitions between various members of the ground- and excited-state multiplets are collapsed into a single wavelength-dependent equivalent that is applicable across the entire ${}^2F_{7/2} \rightarrow {}^2F_{5/2}$ band. An analogous stimulated-emission cross section is similarly defined. Figure 6 shows our measurements of these quantities at room temperature.

A. PHOTOTHERMAL DEFLECTION SPECTROSCOPY

An important technique for assessing the potential of condensed-matter systems to exhibit laser cooling and for diagnosing parasitic heating processes is photothermal deflection spectroscopy (Jackson *et al.*, 1981). Aside from the ease with which such measurements can be performed, photothermal deflection spectroscopy specifically addresses only microscopic aspects of the cooling mechanism since solely the interior of the sample is probed.

A schematic of our spectrometer is shown in Fig. 7; the experiment works in the following way. A cw Ti:sapphire laser is optically chopped and focused through the sample, which has been well polished on the entrance and exit faces. A counter-propagating HeNe laser beam is focused through the same region of the sample as the pump beam but is slightly displaced from it in order to probe the region where the pump-induced thermal gradient is largest. The thermal gradient, in turn, gives rise to a refractive-index gradient that can be viewed as comprising a weak prism in the sample. Heating or cooling of the host lattice arising from nonradiative interactions between the host and the impurity ions will therefore deflect the HeNe probe beam when the pump beam is turned on. This deflection is detected with a position-sensitive detector optically isolated from the infrared pump beam; for the small magnitudes of deflection in our experiments, a dual split photodiode gives a linear response directly proportional to the magnitude of the index gradient generated in the sample. The deflection signal is then averaged with a digital oscilloscope or demodulated with a vector lock-in amplifier referenced to the optical chopper. A chopping frequency of between 0.5 and 1 Hz is used to insure that thermal steady state is nearly attained within the sample.

With this configuration, a definitive signature of anti-Stokes fluorescence cooling is the 180° signal-phase shift expected when the pump wavelength is tuned

from the Stokes to the anti-Stokes region of the absorption spectrum. Figure 8 shows such a transition when the pump wavelength is tuned from 980 to 1010 nm in a 300-K ZBLANP sample doped with 1 wt% Yb³⁺.

More information about the cooling process can be obtained by measuring the amplitude of the deflection signal as a function of pump wavelength. Such a spectrum, normalized at each wavelength by the pump power, is shown in Fig. 9 by the solid circles. An interpretation of this spectrum is possible by considering the flow of energy into and out of the pumped volume. Excluding thermal conduction, the rate of energy accumulation per unit volume in the sample for a pump wavelength of λ is

$$\rho(\lambda) = n_{7/2}\sigma_{abs}(\lambda)I - n_{5/2}\sigma_{se}(\lambda)I - \frac{hc}{\lambda_F}\gamma_{rad}n_{5/2} + \alpha_b I + \kappa n_{5/2}, \quad (1)$$

where I is the pump intensity, $\sigma_{abs}(\lambda)$ and $\sigma_{se}(\lambda)$ are the absorption and stimulated-emission cross sections at the pump wavelength, respectively (cf. Fig. 6), α_b quantifies a broadband, nonsaturable absorption resulting from parasitic impurities such as transition metals, and κ is a heating rate resulting from nonradiative energy transfer from excited-state Yb³⁺ ions to quenching centers that subsequently relax exothermically. The quantity λ_F is of special significance in this expression; it is the wavelength of an emitted photon of average energy and is given by²

$$\frac{hc}{\lambda_F} = \langle h\nu \rangle = \frac{\int h\nu\Phi_\nu d\nu}{\int \Phi_\nu d\nu} = \frac{\int F_\nu d\nu}{\int \frac{F_\nu}{h\nu} d\nu} = hc \frac{\int F_\lambda d\lambda}{\int \lambda F_\lambda d\lambda}, \quad (2)$$

²This corrects the erroneous definition used in our previous work (Mungan *et al.*, 1997c), although only a 0.5-nm increase in λ_F is obtained in applying the correct expression.

where Φ_ν is the emitted photon flux density (units of number per unit time per unit frequency interval), $F_\nu = h\nu\Phi_\nu$ is the Yb^{3+} emission spectral density (units of power per unit frequency interval), and $F_\lambda = \nu^2 F_\nu / c$ is the corresponding quantity in wavelength units. It is F_λ that is plotted in Fig. 5(b), as measured with a grating spectrometer. Finally, the factors $n_{7/2}$ and $n_{5/2}$ are the steady-state ground- and excited-state population densities, respectively; they are pump-intensity dependent and must satisfy the equations

$$0 = \dot{n}_{5/2} = \frac{I\lambda}{hc} [n_{7/2}\sigma_{abs}(\lambda) - n_{5/2}\sigma_{se}(\lambda)] - \gamma_{rad}n_{5/2} \quad (3)$$

and

$$n_{7/2} + n_{5/2} = N, \quad (4)$$

where N is the total number density of ions.

Combining Eqs. (1), (3), and (4) finally yields for the rate of laser-induced heat accumulation per unit pump intensity

$$\frac{\dot{\rho}}{I} = \frac{N\sigma_{abs}(I_s/I)(1 - \lambda/\lambda_{F^*})}{1 + \sigma_{se}/\sigma_{abs} + I_s/I} + \alpha_b, \quad (5)$$

where I_s is a characteristic wavelength-dependent saturation intensity given by $I_s = hc\gamma_{rad}/(\lambda\sigma_{abs})$ and $\lambda_{F^*} = [1/\lambda_F - \kappa/(hc\gamma_{rad})]^{-1}$ is the effective mean emission wavelength. If the pump intensity is small ($I \ll I_s$), Eq. (5) simplifies to

$$\frac{\dot{\rho}_{I \ll I_s}}{I} = N\sigma_{abs}(1 - \lambda/\lambda_{F^*}) + \alpha_b. \quad (6)$$

Since the steady-state refractive-index gradient created by the pump beam is proportional to the rate of heat deposition (note that thermal conduction out of the pumped volume establishes an equilibrium index distribution), so is the deflection angle and hence the above expressions can be applied as theoretical fits to the data of Fig. 9 with λ_{F^*} , α_b , and an overall scaling factor taken as adjustable parameters. Also required is an adjustable parameter a , the area of the pump spot within the probed volume; $P_{laser} = aI$ is therefore the measured pump power.

The solid line shown in Fig. 9 is a fit of Eq. (5) to the data. The excellent agreement between the model and the data validates our assertion that the Yb^{3+} system is effectively homogeneously broadened at room temperature. Also shown in the figure as the dotted line is the photothermal response that would have been obtained had no optical saturation occurred during the measurement. Although the fit determines values of all of the free parameters, a better determination of the most interesting parameters, λ_{F^*} and α_b , is obtained by restricting attention to the spectral region between 990 and 1050 nm where the zero-crossing occurs and where the data are most sensitive to the value of α_b . Over this limited wavelength range, the data and their accompanying fit are shown in Fig. 10. The fitting parameters are $\lambda_{F^*} = 995.3 \pm 0.3$ nm and $\alpha_b = (1.5 \pm 4) \times 10^{-5}$ cm⁻¹. Since the former quantity is in excellent agreement with the independently measured value of $\lambda_{F^*} = 995.5 \pm 2$ nm, we conclude that the heating rate due to energy transfer to quenching centers, κ , is indistinguishable from zero for a doping level of 1 wt%. Since the error bar on the otherwise small value of α_b is several times larger than the value itself, we also conclude that no evidence is found for nonradiative transitions of background parasitic impurities. In short, the measurements show that for a ZBLANP sample doped with 1 wt% Yb^{3+} , the photothermal deflection amplitudes are indistinguishable from their ideal values and therefore the emission quantum efficiency as measured *internal to the sample* must be very nearly unity.

An interesting question to ask with respect to these room-temperature measurements is whether comparable results can be obtained at lower temperatures. Figure 11 shows the absorption cross section of ZBLANP:Yb³⁺ at 300, 150, 100, and 50 K; emission spectra obtained at these same temperatures are shown in Fig. 12. The minimal shift in λ_{F^*} with temperature that is evident by inspection of the emission spectra, in combination with the persistent, albeit weakening, Yb³⁺ absorption beyond 1000 nm, indicate that anti-Stokes fluorescence cooling of ZBLANP:Yb³⁺ should be observable at temperatures at least as low as 100 K.

Figure 13 verifies this expectation by showing photothermal deflection measurements obtained for three different sample temperatures. In this case, the data are acquired in the unsaturated mode [Eq. (6)] and further are normalized with respect to both pump intensity and linear absorption coefficient; the expected signals are thus proportional to

$$\frac{\dot{\rho}_{I \ll I_s}}{N\sigma_{abs}I} = (1 - \lambda / \lambda_{F^*}) + \alpha_b / N\sigma_{abs}. \quad (7)$$

This expression predicts an essentially linear dependence of the normalized deflection signal on the pump wavelength when the background absorption is small; the straight solid line drawn in the figure thus shows the expected photothermal deflection signal in the limit $\alpha_b \rightarrow 0$, with λ_{F^*} set for convenience to its 300-K value of 995.5 nm. The data demonstrate the potential for laser cooling of the ZBLANP:Yb³⁺ system at cryogenic temperatures.

B. BULK COOLING EXPERIMENTS

The photothermal deflection results do not strictly allow one to claim that laser cooling of a bulk solid is guaranteed, since the technique does not reveal heating effects arising from interactions of either the pump beam or the emitted fluorescence with the surface of the sample. On the contrary, a net temperature reduction must be measured for the sample as a whole. For this purpose, a mutually compatible sample geometry and thermometric technique must be chosen to minimize extraneous heating. We developed two approaches to the measurement of net cooling of a solid.

In our initial investigations (Epstein *et al.*, 1995a), a $2.5 \times 2.5 \times 6.9\text{-mm}^3$ sample was supported in a vacuum chamber on a pair of thin glass sides. This configuration reduced the sample heating due to thermal conduction from the chamber walls to the point where the total load was dominated by the net absorption of room-temperature blackbody radiation. A thermometer in this experiment was constructed by attaching a 1-mm^2 piece of gold foil to the sample and painting the exposed surface with black paint. Measurement of the thermal emission from the foil with a liquid-nitrogen-cooled InSb camera gave the temperature change when a reference image captured at room temperature was compared with a second image collected after the sample had been exposed to the pump laser. To monitor and compensate for temperature drifts of the chamber during the experiment, a second, similarly prepared sample not exposed to the pump beam served as a standard. Calibration of the camera signal was accomplished by simultaneous measurement of a heated sample with both the camera and a thermocouple. We obtained a temperature drop of 0.3 K with this apparatus for a pump power of ~ 1 W at a laser wavelength of 1015 nm, thus demonstrating for the first time net cooling of a condensed material.

A significant disadvantage of the latter experiment, however, was that the maximum temperature change was limited by the small net value of the fluorescence cooling power compared with the radiative heat load from the environment. More quantitatively, the equilibrium temperature reached by the sample, T_S , satisfies the equation

$$P_{cool} = A \int \varepsilon_\nu \pi [B_\nu(T_R) - B_\nu(T_S)] d\nu, \quad (8)$$

where A is the surface area of the sample, $\pi B_\nu(T)$ is the radiative hemispherical energy emission rate per unit area at frequency ν from a blackbody at temperature T , ε_ν is the frequency-dependent emissivity of the sample (which for simplicity is taken to be temperature independent), and T_R is the temperature of the sample environment. If the temperature difference $\Delta T = T_S - T_R$ between the sample and the environment is small, the above expression is approximated by

$$P_{cool} \approx -A \int \varepsilon_\nu \pi \left. \frac{\partial B_\nu(T)}{\partial T} \right|_{T_R} \Delta T d\nu = -4A \varepsilon_{eff} \sigma_B T_R^3 \Delta T, \quad (9)$$

where σ_B is the Stefan-Boltzmann constant and ε_{eff} is an effective emissivity defined such that $\varepsilon_{eff} \rightarrow 1$ in the limit $\varepsilon_\nu \rightarrow 1$.

Equation (9) shows that a reduction in the sample's surface area will increase the observed temperature drop for a given value of the cooling power. Motivated by this observation, a new experiment was designed using Yb³⁺-doped ZBLANP optical fibers. The sample consisted of a 175- μm -diameter doped inner core surrounded by a lower-index undoped cladding that brought the total diameter to 250 μm ; the length of the sample was ~ 1 cm. The numerical aperture of this multimode waveguide was 0.2. In order to avoid extraneous absorption of the emitted fluorescence, no protec-

tive polymer coating was applied to the fiber. Pump radiation from the Ti:sapphire laser was focused into the fiber core by a microscope objective mounted inside the vacuum space. Because the earlier thermometric technique is impractical for samples of such small size, we developed a non-contact approach that exploited the temperature dependence of the Yb^{3+} emission spectrum. The method improves upon the analogous technique employed by Clark and Rumbles (1996) in that it is the *shape* of the entire emission spectrum that is measured rather than its absolute magnitude at a select wavelength; in this way, use of a separate fluorescence excitation source is avoided and the sensitivity of the alignment is reduced. To measure the spectrum, a second microscope objective was also mounted within the vacuum space. Outside the chamber, the collected fluorescence was imaged onto a silica-fiber bundle that fed a CCD optical multichannel analyzer. With this detection scheme, broadband emission spectra could be captured in a time span of between 30 and 300 s. Independent calibration of the temperature dependence of the emission spectrum was accomplished by back-filling the vacuum chamber with helium gas and measuring the spectrum at four separate calibration points in the vicinity of room temperature.

Figure 14 shows the best result we have obtained to date: in panel (a) are plotted two calibration spectra measured at temperatures of 303 K and 290 K; for emphasis, the inset shows the arithmetic difference between these two spectra when the amplitudes of the $0' \rightarrow 0$ peaks at 975 nm are normalized to unity. For a pump wavelength of 1015 nm, panel (b) shows the spectra obtained for two different values of the pump power incident on the fiber. The magnitude of the difference spectrum in the latter measurements, when compared with the reference, indicates a temperature drop of 21 K. This is an improvement on earlier work employing the fiber geometry (Mungan *et al.*, 1997b), for which a temperature drop of 16 K was obtained, and is

currently the largest temperature decrease ever reported for a condensed-phase laser-cooling experiment.

As with photothermal deflection spectroscopy, measurement of the temperature change as a function of the pump wavelength exposes interesting details of the cooling process. The solid circles plotted in Fig. 15 show such a spectrum, where the temperature changes have been normalized by the pump power. In order to understand the spectrum, we apply an optical-pumping model derived from Eq. (5). Combining this equation with Eq. (9), the expected temperature drop of the fiber per unit pump power is given by

$$\Delta T / P_{laser} = \frac{\dot{\rho} / I}{4\pi D \epsilon_{eff} \sigma_B T_R^3} = \frac{N \sigma_{abs} (a_{eff} I_s / P) (1 - \lambda / \lambda_{F^*})}{1 + \sigma_{se} / \sigma_{abs} + a_{eff} I_s / P} + \alpha_b}{4\pi D \epsilon_{eff} \sigma_B T_R^3}, \quad (10)$$

where P_{laser} is the pump power, D is the diameter of the fiber, and a_{eff} is an effective pump-spot area within the fiber core. Four unknowns appear in this expression: the effective mean emission-photon wavelength λ_{F^*} , the background absorption coefficient α_b , the effective pump area a_{eff} , and the effective emissivity ϵ_{eff} .

For the purposes of fitting the data of Fig. 15, we take $\alpha_b \equiv 0$, a choice well justified by the results of the photothermal deflection measurements. Rather than adopting ϵ_{eff} as a fitting parameter, however, an independent measurement of this quantity is possible by measuring the *time dependence* of the fluorescence spectrum after the fiber is suddenly exposed to the pump beam. The fluorescence signal at a chosen wavelength is monitored, with an exponential relaxation towards equilibrium expected for small departures from the ambient temperature. In terms of the exponen-

tial time constant τ_c , the ZBLAN mass density $\rho_m = 4.31 \text{ g cm}^{-3}$, and the specific heat $c_m = 0.596 \text{ J g}^{-1} \text{ K}^{-1}$ (Hasz *et al.*, 1993), the effective emissivity is given by³

$$\epsilon_{eff} = \frac{c_m \rho_m D}{16 \tau_c \sigma_B T_R^3}. \quad (11)$$

Following multiple runs, the average value of the relaxation time constant for a 250- μm fiber was found to be $29.3 \pm 0.6 \text{ s}$. This corresponds through Eq. (11) to an effective emissivity⁴ of 0.90 ± 0.02 .

With α_b and ϵ_{eff} now fixed, the solid line in Fig. 15 shows a fit of Eq. (10) to the temperature changes, with only λ_{F^*} and a_{eff} taken as adjustable parameters. The fitted values are 997.6 nm and $7.92 \times 10^{-5} \text{ cm}^2$, respectively, indicating that the *external* fluorescence quantum efficiency is 99.8% and that the pump-spot diameter is only $\sim 100 \mu\text{m}$, somewhat smaller than the actual core diameter of $175 \mu\text{m}$. The latter result implies that only lower-order modes of the fiber are occupied by the pump radiation. The dashed curve in Fig. 15 shows the expected cooling spectrum in the unsaturated regime ($P_{laser} \rightarrow 0$); optical saturation due to the small spot size in the fiber has evidently limited the maximum observable temperature change in this experiment.

As a final check on the issue of optical saturation, Fig. 16 shows the power-normalized temperature changes measured in a 250- μm fiber as a function of pump power for two different pump wavelengths. Also shown are fits of Eq. (10) to the two data sets, with λ_{F^*} taken to be 997.6 nm, so that the only adjustable parameter is the effective area a_{eff} . The larger power-normalized temperature changes observed for the lower pump powers further confirm the effect of optical saturation in this exper-

³Owing to the small amount of PbF_2 (2-3%) in the ZBLANP composition, values of the mass density and specific heat for ZBLAN are used as approximations to the corresponding values for ZBLANP.

⁴A value of 1.0 was assumed in our previous work (Mungan *et al.*, 1997b).

iment; mode scrambling of the input radiation might therefore improve the pump's filling of the fiber core and thereby yield larger temperature drops for a given laser power.

V. Fundamental Limits

In this section we examine from three different perspectives the issues that affect the fundamental limits of laser-cooled condensed matter. In the first, we focus attention on *microscopic* aspects of the problem by developing a thermodynamic picture of the cooling process. This analysis is partly motivated by its academic interest but it will also offer a few insights into how microscopic parameters of the impurity-host system might be manipulated to optimize thermodynamic efficiencies. In the second perspective, we identify physical mechanisms that limit the minimum temperature that might be obtained in a condensed-matter laser-cooling experiment. Quantitative estimates of the minimum temperature will be derived. Finally, the last perspective focuses on more macroscopic aspects of the cooling problem and addresses the possibility of constructing a useful optically pumped cryogenic refrigerator based on the ZBLANP:Yb³⁺ system.

A. THERMODYNAMICS

In general, a collection of impurity ions arrayed within a solid host can be viewed as an energy-conversion device capable of performing some useful function at the necessary expense of generating waste heat. As such, condensed-phase cooling experiments are open to conventional thermodynamic analysis. Energy and entropy are accepted by the device as inputs, then transformed in accord with the device's working details—thereby yielding work or refrigeration—and finally rejected as outputs

in quantities constrained by the first law of thermodynamics and in forms constrained by the second law. In our development below of a thermodynamic description of laser-cooled solids, we will first offer a picture of energy and entropy flow in an energy-conversion device that is sufficiently general to include the roles of input and output radiation fields. We will then argue that a simpler and more familiar description is possible, with one caveat, that will display two advantages. The first of these is that the analysis will not require the explicit introduction of terms for the energy and entropy of propagating light fields; the second advantage is that the simpler description will help focus attention on those aspects of laser cooling that are most relevant to optimizing the physics of the cooling process.

1. *General Refrigerator*

We begin with Fig. 17, which shows a refrigeration process for which a flow of pump energy at the rate \dot{E}_p , with an affiliated rate of entropy flow \dot{S}_p , into a converter of temperature T leads to the extraction of heat at the rate \dot{Q}_c from a low-temperature reservoir at temperature T_c . The refrigerator is also presumed to deposit exhaust energy and entropy at rates of \dot{E}_h and \dot{S}_h , respectively, into an output reservoir. In analogy with the presentation of Landsberg and Tonge (1980), we have here adopted a broader picture of refrigeration than that found in elementary texts by allowing for the possibility that the pump source could be more general than a supplier of pure work while the output reservoir might be more general than a receiver of pure heat. Hence, insofar as the pump and output reservoir are concerned, entropy flows are taken as fundamental quantities instead of the thermodynamic temperatures. It is this generalization that specifically enables a thermodynamic analysis that includes the possibility of a pump source and an exhaust in the form of electromagnetic radiation. Returning to Fig. 17, note that we have allowed for the

possibility that energy and entropy might accumulate in the converter at the rates \dot{E} and \dot{S} and that unspecified irreversible processes internal to the converter generate entropy at the rate of \dot{S}_g .

With these definitions, and for a converter temperature of T , the energy and entropy flows into the converter must therefore satisfy

$$\dot{E} = \dot{E}_p + \dot{Q}_c - \dot{E}_h \quad (12)$$

and

$$\dot{S} = \dot{S}_p + \dot{Q}_c / T - \dot{S}_h + \dot{S}_g. \quad (13)$$

In the latter equation, \dot{S}_g simply expresses the rate of entropy generation that occurs irreversibly anywhere in the system. In the optical context, possible phenomena contributing to \dot{S}_g are nonradiative relaxation within the converter (in other words, irreversible absorption of the pump laser light), and line-broadened or multidirectional radiative emission to the environment. Therefore, in the case of a completely reversible refrigerator, $\dot{S}_g = 0$. Assuming the converter to be in steady-state operation ($\dot{E} = \dot{S} = 0$), Eqs. (12) and (13) can be manipulated to yield the first-law efficiency, or coefficient of performance (COP), of the refrigerator:

$$\eta_1 \equiv \frac{\dot{Q}_c}{\dot{E}_p} = \frac{T(1/T_{F_h} - 1/T_{F_p}) - T\dot{S}_g / \dot{E}_p}{1 - T/T_{F_h}}, \quad (14)$$

where $T_{F_p} = \dot{E}_p / \dot{S}_p$ and $T_{F_h} = \dot{E}_h / \dot{S}_h$ are purely algebraic substitutions known as *flux temperatures* whose introduction is motivated by a desire to derive Carnot-like expressions for thermodynamic efficiencies in this more general context (Landsberg

and Tonge, 1980). Maximum first-law efficiency is obtained for a reversible refrigerator and is given by

$$\eta_1^{rev} = \frac{T(1 - T_{F_h} / T_{F_p})}{T_{F_h} - T}. \quad (15)$$

2. A Three-Level Optical Refrigerator

In order to proceed further, a more specific model is now needed for the converter, pump, and output reservoir. Figure 18 shows a generic optically pumped refrigerator comprised of a three-level system with states labeled 0, 1, and 2 plus couplings to the pump source, low-temperature reservoir, and output reservoir. The pump can be taken to be any source of narrow-band electromagnetic radiation resonant with the $0 \rightarrow 1$ transition (of transition energy E) while the output reservoir, which serves only as a receiver of fluorescence from the $2 \rightarrow 0$ transition (of energy $\varepsilon + E$), can be taken as free space. The low-temperature reservoir is simply the host lattice within which the three-level impurity atoms are embedded; it couples levels 1 and 2, which are spaced by energy ε , but is otherwise idealized to be decoupled from level 0. By virtue of the 1–2 coupling, and since the populations in levels 1 and 2 are taken to be rapidly equilibrated with respect to each other, heat is subsumed by the converter at temperature T_c , and thus $T \equiv T_c$.

All that remains in order to apply Eqs. (14) or (15) to the computation of the coefficient of performance for this optical refrigerator is to find explicit expressions for the rates of pump and output energy and entropy flow when the applicable radiation fields are not necessarily in equilibrium. This statement means that for the purposes of deriving thermodynamic quantities for the refrigerator, individual pho-

ton-mode occupation numbers for either the pump radiation or the output radiation are not required to be Bose-Einstein distributed with a unique thermodynamic temperature; instead, individual radiation modes can be taken as independent, decoupled oscillators with which any one is affiliated well defined energy and entropy fluxes. In this way, a sum of the energy and entropy fluxes over all of the occupied modes yields well defined totals for these quantities, in much the same way that the total energy and entropy are well defined for nuclear spins and a solid lattice even when the spin and lattice temperatures are unequal. With this understanding, the fluxes (for unpolarized fields) are formally given by

$$\dot{E}_i = \int I_v^i(\hat{n}, \mathbf{r}) \cos \theta d\nu d\Omega da; \quad (16)$$

$$I_v^i(\hat{n}, \mathbf{r}) = \frac{c}{4\pi} u_v^i; \quad u_v^i = \frac{8\pi h \nu^3}{c^3} n_v^i$$

and

$$\dot{S}_i = \int \Xi_v^i(\hat{n}, \mathbf{r}) \cos \theta d\nu d\Omega da; \quad (17)$$

$$\Xi_v^i(\hat{n}, \mathbf{r}) = \frac{c}{4\pi} s_v^i; \quad s_v^i = \frac{2k_B \nu^2}{c^3} [(1 + n_v^i) \ln(1 + n_v^i) - n_v^i \ln(n_v^i)],$$

where $i = p$ or h for the pump and output radiation fields, respectively, and $I_v^i(\hat{n}, \mathbf{r})$ is a quantity known as the specific intensity (Mihalas, 1978); at the frequency ν , it is the rate of radiation energy flow at the position \mathbf{r} in the direction \hat{n} through a unit area within unit frequency interval into unit solid angle. The factor u_v^i is the radiation energy density at frequency ν that would be found in a blackbody cavity exhibiting the specific intensity $I_v^i(\hat{n}, \mathbf{r})$, an identification that allows the assignment of a brightness temperature for the radiation at all values of ν , \hat{n} , and \mathbf{r} . The factor n_v^i is

the photon occupation number corresponding to this energy density; it is related to the brightness temperature, $T_{B_i}(v, \mathbf{n}, \mathbf{r})$, according to $n_v^i = 1 / [\exp(hv / k_B T_{B_i}) - 1]$. Finally, the entropy terms $\Xi_v^i(\hat{\mathbf{n}}, \mathbf{r})$ and s_v^i are defined in analogous fashion to the energy terms $I_v^i(\hat{\mathbf{n}}, \mathbf{r})$ and u_v^i . Hence, Eq. (16) provides a means for finding n_v^i as a function of v , $\hat{\mathbf{n}}$, and \mathbf{r} , while with this knowledge Eq. (17) provides a means for computing \mathcal{S}_i . The integrals are taken over any surface that bounds the refrigerator, with da being the element of surface area, $d\Omega$ the element of solid angle, and θ the angle between $\hat{\mathbf{n}}$ and the local surface normal.

3. A Simpler Approach to the Three-Level Optical Refrigerator

While Eqs. (16) and (17) provide a complete prescription for computing the needed thermodynamic quantities, their use requires detailed spectroscopic knowledge of the pump and especially the output radiation fields. Although a laser (with $\mathcal{S}_p \rightarrow 0$ in the limit of infinite intensity, zero linewidth, or perfect beam quality) can be taken as an idealized pump source, the degree of line broadening assumed for the $2 \rightarrow 0$ output transition will have a significant effect on the fluorescence flux temperature. Moreover, since for condensed phases line broadening and luminescence emission into multiple directions in space necessarily involve irreversible processes, calculation of the COP of the refrigerator will be complicated by the requisite use of Eq. (14).

We therefore adopt for the remainder of this discussion—at a small expense to be described below—a simpler approach with the advantages that direct consideration of radiation fields is unnecessary and that intrinsically irreversible processes affiliated with these fields will be removed. By insisting that the refrigerator only interact reversibly with the pump and output reservoirs, emphasis remains placed on the microscopic aspects of the refrigerator's internal operation. Equation (15) will

therefore prove adequate to the task of calculating a coefficient of performance with which to compare the COP derived from a specific physical model of the refrigerator. Such a comparison will reveal the best strategies for thermodynamic optimization. This new picture will also prove more familiar as heat alone will be exchanged between the refrigerator and the pump, the low-temperature reservoir, and the high-temperature reservoir.

The new picture, the essence of which was apparently first discussed by Scovil and co-workers (Scovil and Schulz-DuBois, 1959; Geusic *et al.*, 1967) and by Weinstein (1960), is shown in Fig. 19: the optical pump source is replaced by a heat bath that exchanges energy with the refrigerator only through the 0–1 transitions; it may be idealized as an ensemble of harmonic oscillators with resonant frequencies closely bunched around the 0→1 transition frequency. Since only levels 0 and 1 are involved in this interaction, the populations in these levels, n_0 and n_1 , determine a well-defined thermodynamic temperature,

$$T_{01} = \frac{E / k_B}{-\ln(n_1 / n_0)}. \quad (18)$$

If the temperature of the pump bath, T_p , is set equal to T_{01} , a reversible exchange of energy is assured between the pump and the two-level system comprised of the 0 and 1 states. The output reservoir is constructed in a similar way with a second well defined thermodynamic temperature given by

$$T_{02} = \frac{(\varepsilon + E) / k_B}{\varepsilon / k_B T_c - \ln(n_1 / n_0)}. \quad (19)$$

As with the pump reservoir, reversible exchange is assured for $T_h = T_{02}$.

With these definitions for the nature and temperature of the pump and output heat baths under reversible operation of the refrigerator, Eq. (15) for the COP becomes

$$\eta_1^{rev} = \frac{T_c(1 - T_h / T_p)}{T_h - T_c}. \quad (20)$$

Note that in this expression, absolute thermodynamic temperatures have replaced the flux temperatures called for in Eq. (15) precisely because these quantities are identical when the pump and output reservoir are comprised of conventional heat baths. Substitution for T_p and T_h with the help of Eqs. (18) and (19) gives

$$\eta_1^{rev} = \frac{\varepsilon}{E}, \quad (21)$$

a result we could have foreseen by noting that for reversible operation heat ε is removed from the low-temperature reservoir only through a net investment of heat E from the pump.

The simple result of Eq. (21) has been obtained with one sacrifice in generality: by eliminating the consideration of entropy and possible heat removal produced by line broadening, we have explicitly eliminated the possibility that broadening due to phonon collisions or to spectral diffusion within an inhomogeneously broadened line can contribute to the cooling effect. Most simply, an example of this exception is a two-level impurity system with a homogeneously broadened upper state. Optical pumping with a narrow-band source *below* the center frequency of the transition will cool the host lattice as a consequence of phonon collision broadening. Although this represents in principle a viable mechanism for optical refrigeration, one that might best be analyzed in terms of Eq. (14) and the required entropy calculations of

one or both of the pump and output radiation fields, we continue to assume that line broadening makes little contribution to refrigeration in the three-level system of interest here.

4. A Model Three-Level Optical Refrigerator

Figure 20(a) now shows an explicit physical model for pumping and relaxation processes in a three-level system used as a refrigerator. We assume that the pump source is a laser of photon energy $E = h\nu$, while radiative relaxation out of the two excited states occurs at rates of γ_1 and γ_2 , respectively, nonradiative relaxation (as a consequence of impurity quenching or pure multiphonon relaxation to the ground state) occurs at the rate Γ for both excited states, and g_0 , g_1 , and g_2 are the level degeneracies. The double-headed arrow between levels 1 and 2 denotes the nonradiative thermalization of these two states, which we assume to occur at a rate much larger than all other rates in the model. Hence, levels 1 and 2 are always thermally equilibrated with respect to each other. With these assumptions and definitions, the equations that the populations in the three levels must satisfy are

$$\dot{n}_1 + \dot{n}_2 = \frac{I\sigma_{abs}}{E}(n_0 - \frac{g_0}{g_1}n_1) - (\Gamma + \gamma_1)n_1 - (\Gamma + \gamma_2)n_2, \quad (22a)$$

$$n_2 = \frac{g_2}{g_1}n_1 e^{-\varepsilon/k_B T_c}, \quad (22b)$$

and

$$n_0 + n_1 + n_2 = N, \quad (22c)$$

where \dot{n}_1 and \dot{n}_2 denote the time rates of change of the level 1 and level 2 population densities, respectively, I is the intensity of the pump laser, and σ_{abs} is the absorption cross section for the $0 \rightarrow 1$ transition. Note that the second equation expresses our assumption of fast thermal equilibration of the two excited states (with a host lattice of temperature T_c), while the third expresses the conservation of the total number density of atoms, N .

Expressions for the rate of heat extraction per unit volume by this model refrigerator, \dot{Q}' , and the corresponding required rate at which work must be supplied, \dot{W}' , in terms of the level population densities are

$$\dot{Q}' = \varepsilon \gamma_2 n_2 - \Gamma E n_1 - \Gamma(E + \varepsilon) n_2 \quad (23)$$

and

$$\dot{W}' = E \gamma_1 (I / I_s) (n_0 - \frac{g_0}{g_1} n_1), \quad (24)$$

where $I_s = \gamma_1 E / \sigma_{abs}$ is the saturation intensity of the $0 \rightarrow 1$ transition. In the latter equation the rate of supplied work is taken to be that portion of the laser power that is actually *absorbed* by the three-level impurities; in this way, emphasis remains placed on the purely microscopic aspects of the refrigerator's operation.

Assuming cw laser excitation of the system, steady-state population densities are achieved and Eqs. (22) can be easily solved for the quantities n_0 , n_1 , and n_2 . Substitution of these steady-state solutions into Eqs. (23) and (24) yields for the model coefficient of performance of the refrigerator

$$\eta'_1 = \frac{\dot{Q}'}{\dot{W}'} = \frac{\varepsilon}{E} \frac{\gamma_2 (g_2 / g_1) e^{-\varepsilon / k_B T_c} - \Gamma (E / \varepsilon) [1 + (g_2 / g_1) e^{-\varepsilon / k_B T_c}]}{\gamma_1 + \gamma_2 (g_2 / g_1) e^{-\varepsilon / k_B T_c} + \Gamma [1 + (g_2 / g_1) e^{-\varepsilon / k_B T_c}]} \quad (25)$$

and therefore for the second-law efficiency

$$\eta_2 = \frac{\eta'_1}{\eta_1} = \frac{\gamma_2(g_2 / g_1)e^{-\varepsilon/k_B T_c} - \Gamma(E / \varepsilon)[1 + (g_2 / g_1)e^{-\varepsilon/k_B T_c}]}{\gamma_1 + \gamma_2(g_2 / g_1)e^{-\varepsilon/k_B T_c} + \Gamma[1 + (g_2 / g_1)e^{-\varepsilon/k_B T_c}]} \quad (26)$$

Note that the latter result recalls Eq. (21) for the coefficient of performance under reversible operation. If nonradiative transitions to the ground state are negligible, $\Gamma \rightarrow 0$, the above equations become

$$\eta'_1 = \frac{\varepsilon}{E} \frac{(\gamma_2 g_2 / \gamma_1 g_1)e^{-\varepsilon/k_B T_c}}{1 + (\gamma_2 g_2 / \gamma_1 g_1)e^{-\varepsilon/k_B T_c}} \quad (27)$$

and

$$\eta_2 = \frac{(\gamma_2 g_2 / \gamma_1 g_1)e^{-\varepsilon/k_B T_c}}{1 + (\gamma_2 g_2 / \gamma_1 g_1)e^{-\varepsilon/k_B T_c}} \quad (28)$$

Inspection of Eqs. (25) through (28) lead to the following conclusions on the optimization of the refrigerator:

1. In the presence of nonradiative transitions to the ground state, both increased first- and second-law efficiencies are obtained by decreasing E , the ground-state to excited-state energy gap. This amounts to decreasing the temperature of the output reservoir. In the absence of nonradiative transitions to the ground state, only the first-law efficiency is improved by decreasing E .

2. Increased first- and second-law efficiencies are obtained by increasing the ratio $\gamma_2 g_2 / \gamma_1 g_1$. This is illustrated in Fig. 21, which plots both efficiencies as functions of the level splitting ε for various values of this ratio. Note in the figure that for $\gamma_2 g_2 / \gamma_1 g_1 = 10$, second-law efficiencies greater than 50% are obtainable in the range of splittings that optimizes the first-law efficiency.

3. In the presence of nonradiative transitions to the ground state, the minimum obtainable temperature depends on the value of Γ , as determined by Eq. (25).

It is interesting to compare these results with a different three-level model for the refrigerator, as shown in Fig. 20(b). In analogy with Eqs. (22), the population densities must satisfy

$$\dot{n}_0 + \dot{n}_1 = -\frac{I\sigma_{abs}}{E} \left(n_1 - \frac{g_1}{g_2} n_2 \right) + (2\Gamma + \gamma_0 + \gamma_1) n_2, \quad (29a)$$

$$n_1 = \frac{g_1}{g_0} n_0 e^{-\varepsilon / k_B T_c}, \quad (29b)$$

and as before

$$n_0 + n_1 + n_2 = N. \quad (29c)$$

The corresponding rates of heat extraction and supplied work are

$$\dot{Q}' = \varepsilon \gamma_0 n_2 - \Gamma(2E + \varepsilon) n_2 \quad (30)$$

and

$$\dot{W}' = E\gamma_1(I/I_s)(n_1 - \frac{g_1}{g_2}n_2), \quad (31)$$

while in the steady state the coefficient of performance reduces to

$$\eta'_1 = \frac{\varepsilon}{E} \frac{\gamma_0 - \Gamma(2E/\varepsilon + 1)}{\gamma_0 + \gamma_1 + 2\Gamma}. \quad (32)$$

Because $\eta_1^{rev} = \varepsilon/E$ is still the coefficient of performance under reversible operation for this new model, the second-law efficiency becomes

$$\eta_2 = \frac{\gamma_0 - \Gamma(2E/\varepsilon + 1)}{\gamma_0 + \gamma_1 + 2\Gamma}. \quad (33)$$

These results differ strikingly from those obtained with the model of Fig. 20(a). While the effective reduction in temperature of the output reservoir that is commensurate with a decrease in E still yields the expected improvements in first- and second-law efficiencies, these efficiencies are no longer temperature dependent and moreover no longer exhibit a fundamental limiting temperature when Γ is nonzero, at least as long as \dot{Q}' is initially positive. Gone, however, is the advantage of large relative degeneracies, g_1/g_0 , in the narrowly spaced levels—second-law efficiency near unity requires larger values of the ratio γ_0/γ_1 than is necessary for the corresponding ratio in the first model. All of these differences are a consequence of the temperature-dependent population that resides in level 1 of the second model: since the absorption of pump light decreases as the temperature is lowered, no power is absorbed that cannot be exploited in extracting heat from the host lattice. In short, the refrigerator becomes transparent as it cools, thus offering no opportunity for nonradiative transitions to heat the lattice.

The thermodynamic analysis of the two simple models just described illustrates essential features of laser-cooled solids when interlevel thermalization is responsible for heat removal from the host lattice. While beyond the scope of this review, a combination of the two models, with perhaps the addition of more realistic incorporation of parasitic nonradiative processes, should prove useful in the analysis of Yb^{3+} -based systems as well as of general impurity-doped insulators and even semiconductors.

B. MINIMUM TEMPERATURE

An initial estimate of the minimum temperature to which a solid may be laser cooled can be obtained by equating the rate of heat generation by nonradiative mechanisms to the temperature-dependent cooling power predicted by a chosen model of the cooling process. For this purpose, we will suppose that the three-level model presented in detail above can be applied at all temperatures and further that no nonradiative transitions contribute to heating of the host lattice ($\Gamma = 0$). Instead, unavoidable inelastic optical processes intrinsic to the undoped solid host will determine the heat load that the refrigerator must support at low temperatures.

The primary mechanisms (Lines, 1991) that we will consider are (1) multiphonon absorption, which dominates optical loss in the host lattice on the low-frequency side of the transmission window, (2) indirect electronic interband absorption, which dominates the loss on the high-frequency side and is known as the Urbach edge, and (3) lattice Raman scattering, which dominates all other inelastic light scattering phenomena (such as Brillouin scattering). Exciton transitions, impurity-induced effects on the intrinsic electronic or multiphonon absorption, and free-carrier absorption will be presumed to be too weak or too limited in frequency range to make a significant contribution to the head load.

Figure 22 shows in graphical form estimates of the heat load contributed by the three mechanisms just listed for three types of solids: silica glass, heavy-metal fluoride glass, and crystalline KCl. The meaning of the units nW/cmW on the ordinate axis is that for 1 W of incident pump power driving the cooling process, absorption or inelastic scattering will contribute the indicated heat load per centimeter of path length traveled by the driving beam. For multiphonon absorption, the heat load is given by $P_{load}[\text{nW/cmW}] \approx 10^9 \alpha_{MP}(\nu, T)$, where

$$\alpha_{MP}(\nu, T) = A_0 \frac{[n(\nu_0) + 1]^N}{n(\nu) + 1} \exp(-b\nu / \nu_0) \quad (34)$$

is the N -phonon absorption coefficient (in cm^{-1}) with $N \equiv \nu / \nu_0$, ν_0 is a typical phonon frequency, and $n(\nu) = 1 / [\exp(h\nu / k_B T) - 1]$ is the Bose-Einstein occupation number for a phonon of frequency ν at temperature T (Bendow, 1991). The parameters A_0 and b are purely material-dependent constants. Note that this form was derived for multiphonon absorption in crystals, although analogous frequency and temperature dependences are commonly observed in disordered materials as well (Bendow, 1991). The Urbach edge in crystals likewise shows an exponential frequency dependence:

$$\alpha_{Ur}(\nu, T) = A'_0 \exp[b'(\nu - \nu_0) / k_B T], \quad (35)$$

with the indicated temperature dependence being only approximately obeyed (Lines, 1991). For glasses, the frequency dependence of indirect interband absorption is more complicated but still tends to exhibit overall an approximately exponential form. In contrast to multiphonon absorption, only a weak temperature dependence is observed for the electronic edge in glasses (Lines, 1991).

Referring again to Fig. 22, the “V”-shaped curves show the sum of the multiphonon and Urbach absorption spectra for both silica and heavy-metal fluoride glasses at room temperature, while for crystalline KCl, the electronic absorption is so weak in the region below 20,000 cm^{-1} that only the multiphonon absorption is shown.

The curves representing the heat load due to Raman scattering are given by

$$P_{load}[\text{nW/cmW}] \approx 10^9 \cdot 4\pi \left. \frac{d\sigma}{d\Omega} \right|_{\nu_0} \left(\frac{\nu}{\nu_0} \right)^4 \left(\frac{\nu_{Stokes}}{\nu} \right), \quad (36)$$

where $(d\sigma/d\Omega)_{\nu_0}$ is the Stokes Raman cross section (with units of $\text{cm}^{-1} \text{sr}^{-1}$) integrated over polarization and Stokes frequency; the average Raman Stokes shift is ν_{Stokes} . The scattering direction is taken to be perpendicular to the pump laser beam (of frequency ν_0) with the factor of 4π introduced under the simplifying approximation that the scattering is isotropic.

Figure 22 immediately reveals that greater heat loads are expected for disordered host materials; at room temperature they are limited by multiphonon and Urbach-edge absorption, depending on the pump frequency. In the zero-temperature limit, extrapolation by eye of the electronic edge absorption (which is only weakly temperature dependent) to low frequencies shows that this mechanism dominates the heat load at most frequencies of interest. For crystals, Raman scattering limits the heat load at all but the lowest frequencies.

An estimate of the minimum attainable temperature is given by

$$T_{\min} \approx P_{load} h\nu / k_B \alpha_{ions}, \quad (37)$$

where ν is the frequency of the pump laser and α_{ions} is the absorption coefficient of the dopant three-level systems with an energy splitting $\varepsilon \approx k_B T_{min}$ optimized for operation at the minimum temperature. Thus for $\nu = 10,000 \text{ cm}^{-1}$, $\alpha_{ions} = 1 \text{ cm}^{-1}$, and $P_{load} = 0.02 \text{ nW/cmW}$ (the Raman limit for KCl), $T_{min} \approx 1 \text{ mK}$. In strongly absorbing samples T_{min} may fall into the microkelvin range. These figures are lower bounds on the temperature to which a solid material might be optically cooled, at least for mechanisms providing $\sim k_B T_{min}$ of heat extraction per cycled pump photon. Note that for the three-level model, however, the energy splitting ε corresponding to 1 mK is only a few tens of MHz; therefore, absorption and emission broadening effects and the interlevel thermalization rate must be compatible with cooling across such a small energy gap in order for such low temperatures to be obtainable in practice.

C. MAXIMUM COOLING POWER AND OPTICAL REFRIGERATORS

A natural application of laser-cooled solids is in the construction of optically pumped cryogenic refrigerators. In this context, the most important performance characteristics are the absolute efficiency of the cooling process (defined as the ratio of the cooling power to the *incident* laser power) and the volume density of cooling power that might be obtained in the refrigerator's working substance. We will specifically discuss the performance of an optical refrigerator based on the ZBLANP:Yb³⁺ system.

Equation (5) for the rate of energy accumulation per unit volume in the sample can be recast in the following way:

$$\dot{\rho}_{cool}(I, \nu, T) = \frac{N\gamma_{rad}(T)h\nu[v_F(T)/\nu - 1]}{1 + \sigma_{se}(\nu, T)/\sigma_{abs}(\nu, T) + I_s(\nu, T)/I'} \quad (38)$$

where a sign change has been introduced so that positive values of $\dot{\rho}_{cool}$ indicate cooling of the material, the loss terms κ and α_b have been set to zero, ν is the pump frequency, and $h\nu_F$ is the average energy of an emitted photon. All functional dependences of the various factors are shown explicitly; in particular, the stimulated-emission and absorption cross sections are strongly temperature dependent, owing to the exponential dependence of the populations found in the individual members of the Yb^{3+} upper and lower Stark-split multiplets. Temperature-dependent line broadening will also affect these factors.

It is useful at this point to take advantage of a relationship first derived by McCumber (1964) for the ratio of the stimulated-emission and absorption cross sections in broadband systems:

$$\frac{\sigma_{se}(\nu, T)}{\sigma_{abs}(\nu, T)} = \frac{Z_{7/2}(T)}{Z_{5/2}(T)} \exp[h(\nu_{00\ominus} - \nu) / k_B T], \quad (39)$$

where $Z_i(T)$ is the partition function for the multiplet 2F_i , with the zero of energy defined at the lowest lying member of the multiplet, and $\nu_{00\ominus} = 10,261 \text{ cm}^{-1}$ is the frequency corresponding to transitions between these two zero levels.

Substitution of this relation into Eq. (38) yields

$$\dot{\rho}_{cool} = \frac{N\gamma_{rad}h\nu[\nu_F / \nu - 1]}{1 + \frac{Z_{7/2}}{Z_{5/2}} \exp[h(\nu_{00\ominus} - \nu) / k_B T] + I_s / I}. \quad (40)$$

This last result allows us to calculate the expected cooling-power density for any pump intensity and any temperature as a function of the pump frequency. In the limit $I \rightarrow \infty$, and choosing the pump frequency to maximize the cooling power, the maximum cooling-power density can be obtained as a function of temperature.

Figure 23 shows this quantity for a concentration of 1 wt% Yb^{3+} or equivalently $N = 2.42 \times 10^{20}$ ions/cm³. The maximum power density of ~ 50 W/cm³ at 300 K falls to ~ 1 W/cm³ at 100 K and to ~ 0.1 W/cm³ at 77 K.

While these values of the cooling density are revealing, they overestimate what is obtainable in practice since they derive from infinite pump intensity. Equation (40) can be used to plot the expected cooling-power density as a function of pump intensity for a given temperature of the cooling element. Figure 24 shows this result, where for each temperature and laser intensity the pump wavelength has been chosen so as to maximize the cooling power. (The data of Fig. 11 were used in these calculations.)

One can obtain a better feeling for the meaning of these cooling-density curves by considering a cubic cooling element of volume 1 cm³. If this element is illuminated with a 100-W laser whose beam is in the shape of a square 1 cm on a side, then for a 1-wt%-doped sample the expected cooling power will be ~ 200 mW at 300 K, ~ 10 mW at 100 K, and ~ 2 mW at 77 K. If we now take advantage of the fact that ZBLANP can support a maximum Yb^{3+} concentration of 3 wt%, and also design the cooling element into an optical cavity with a Q of 10 for the pump radiation (this increases the circulating intensity in the cooling element from 100 W to ~ 1000 W), the cooling powers increase to ~ 6 W at 300 K, ~ 240 mW at 100 K, and to ~ 60 mW at 77 K. The latter values correspond to efficiencies of 6.0%, 0.24%, and 0.060%, respectively. These figures may be compared with those of a typical Stirling-cycle refrigerator, which produces ~ 1 W of cooling power at 77 K with an efficiency of $\sim 1\%$.

Another perspective on the cooling efficiency is given in Fig. 25, which plots the quantity $\dot{\rho}_{cool} / I$ as a function of the pump intensity I . The curves clearly indicate the values of the intensity at which the efficiency begins to fall off as a consequence of optical saturation. Finally, Fig. 26 plots the cooling efficiency $\dot{\rho}_{cool} / I$ as a function of the cooling-power density obtained at the pump intensity I . This figure reveals

the range of cooling-power densities available before optical saturation begins to compromise the efficiency.

The preceding, general analysis indicates the potential of optical cryogenic refrigeration, but it also makes clear that great challenges remain in developing a practical and competitive device. Efficient refrigerators most likely will require the preparation of new host materials that support higher concentrations of Yb^{3+} . They also may require a cooling cycle based on other active dopants and the corresponding development of new high-power, compact, and rugged laser sources.

VI. Conclusions and Prospects

Despite its 70-year history, the concept of anti-Stokes photoluminescence cooling of matter has only recently become practical, as a consequence of the laser pump sources and ultra-high-purity materials developed in the past 10 years. Further advances will continue to depend heavily on these factors. As far as the Yb^{3+} species is concerned, of particular interest will be the development of host materials that allow higher concentrations of the active ion; in this way, greater cooling densities can be achieved and hence lower temperatures for a given heat load from the surroundings. Crystalline hosts are the best prospects in this regard: they offer not only the possibility of continuously adjustable concentrations all the way up to the stoichiometric limit but also sharper absorption lines than in glasses and therefore increased absorption of the pump radiation.

Indeed, with an eye towards developing optically pumped cryogenic refrigerators, simple scaling of the ZBLANP: Yb^{3+} results up to 100% concentration yields at a working temperature of 100 K an upper limit on the cooling power of about 1 W in a 1 cm^3 sample pumped with 100 W. This estimate ignores the effects of radiation trapping by reabsorption, which becomes serious at high concentrations and requires

that special sample geometries be used. The practical problem of managing 100 W of fluorescence radiating into all directions around a small cooling element should not be underestimated. Nevertheless, newly developed high-power semiconductor diode lasers (Razeghi, 1995) operating at wavelengths near 1015 nm with reasonably high electrical-to-optical conversion efficiencies increase the prospects of developing a practical device. Furthermore, recent spectroscopic studies of Yb³⁺-doped crystals (DeLoach *et al.*, 1993) help identify several host materials (e.g. LiYF₄) favorable to anti-Stokes fluorescence cooling.

The greatest challenge, however, to the advance of Yb³⁺-based laser cooling is the reduction of parasitic quenching centers that provide nonradiative de-excitation pathways for the excited state. It is informative to consider more closely how such heat-generating processes work (Kaplyanski and MacFarlane, 1987). An Yb³⁺ ion in the excited $^2F_{5/2}$ state can interact through electric-multipole coupling with neighboring ions. If a near resonance exists between the Yb³⁺ $^2F_{5/2} \rightarrow ^2F_{7/2}$ transition and a comparable transition in the neighbor (be it a second Yb³⁺ ion or a quenching impurity), radiationless exchange of energy from one ion to the other is possible. In the event of dipole-dipole coupling, this exchange occurs at the rate $W \propto R^{-6}$, where R is the distance between the donor and acceptor ions. Even for a very low concentration of quenching centers, the Yb³⁺ excitation can hop from site to site until a quenching center is encountered. As the Yb³⁺ concentration N goes up, the hopping rate will increase as N^2 —as will the quenching rate—even if the concentration of quenching centers remains fixed. The problem is aggravated if the multipole coupling is of higher order than dipole-dipole. Indeed, strong evidence for Yb³⁺ quadrupole-quadrupole coupling—with a hopping rate $W \propto R^{-10}$ and hence an accompanying $N^{3.3}$ increase in the quenching rate with concentration—has already been reported for a silicate-glass host (Brundage and Yen, 1986). For ZBLANP, the multipole order of the energy-transfer coupling is unknown. These considerations underscore the

difficulties ahead: both new standards or methods of purification—an especially challenging task for rare-earth species owing to their similar chemistry—and new diagnostics capable of detecting impurity concentrations below the parts-per-million level will be needed as the concentration of the active ion is increased. Materials scientists must make a lie of the old saw, “To a chemist, nothing is clean.”

Beyond laser cooling of Yb^{3+} ions, the level structure of Tm^{3+} (Sanghera and Aggarwal, 1993) shows promise of yielding net cooling by optical pumping of the ${}^3H_6 \rightarrow {}^3F_4$ transition near $1.9 \mu\text{m}$. The excited state is expected to exhibit high fluorescence quantum efficiency in low-phonon hosts, despite the smaller energy gap than that of Yb^{3+} , while the ion’s higher-lying states appear to have energies for which upconversion effects between pairs of $\text{Tm}^{3+}({}^3F_4)$ ions are inhibited, especially at low temperatures. Indeed, the ion may be more suited to operation at cryogenic temperatures than Yb^{3+} . The absence, however, of high-power, tunable, cw lasers in the $2\text{-}\mu\text{m}$ spectral region presents an obstacle to experiments with this species, although the Co:MgF_2 laser at least makes possible pulsed photothermal deflection measurements.

Outside the realm of impurity-doped insulators, recent experiments with semiconductors make net anti-Stokes fluorescence cooling of these materials appear achievable (Gauck *et al.*, 1997). Owing to the nanosecond time scale for radiative recombination in direct-gap semiconductors, cooling densities exceeding those of rare-earth-doped insulators are likely, provided that the problem of fluorescence escape from these high-refractive-index materials can be solved. Other new ideas for laser cooling of solids include the cooling of a magnetic spin system (Kalachev *et al.*, 1996; Kalachev and Samartsev, 1997), a phonon mode (Andrianov and Samartsev, 1996b), or Frenkel excitons (Andrianov and Samartsev, 1996a). Andrianov and Samartsev’s (1997b) suggestions for exploiting superradiant phenomena offer further food for thought.

Finally, another long-term idea for improving laser cooling of solids takes advantage of photonic band gap materials (Joannopoulos *et al.*, 1995). The idea is to fabricate a refractive-index structure within the cooling element that would establish a three-dimensional photonic gap immediately below the pump frequency. In this way, emission at Stokes frequencies falling within the gap would be inhibited, thereby enhancing the cooling power derived from the anti-Stokes emission. Continuing in this speculative vein, Garret *et al.* (1997) have recently demonstrated the creation of squeezed phonon states in crystalline KTaO_3 . Inspired by these results, Burin *et al.* (1997) have identified a new approach to laser cooling of vibrating atoms arrayed within an optical lattice. Although the degree of squeezing observed in the KTaO_3 experiment was too small to be practical as a cooling technique, future advances may make these ideas applicable to conventional solids. A condensed-phase realization of the ideas of Lloyd (1997a, 1997b) on coherent pumping and on the quantum-mechanical Maxwell's demon (cf. Sec. II.C) are at the limit of at least our experimental sobriety. Nevertheless, these imaginative ideas offer plenty of inspiration for continued research.

Acknowledgments

One of us (TRG) thanks with great pleasure T.W. Darling, A. Migliori, G.W. Swift, and W.H. Zurek for helpful discussions on thermodynamics, and especially X. Luo and M.D. Eisaman for their outstanding experimental contributions to this work. CEM acknowledges enlightening interactions with M.I. Buchwald, B.C. Edwards, and R.I. Epstein and the support of the College of Science and Technology at UWF. This work was performed in part under the auspices of the United States Department of Energy.

References

1. Aggarwal, I.D. and Lu, G. (1991). "Fluoride Glass Fiber Optics." Academic Press, San Diego.
2. Anderson, M.H., Ensher, J.R., Matthews, M.R., Weiman, C.E., and Cornell, E.A. (1995). Observation of Bose-Einstein condensation in a dilute atomic vapor. Science 269, 198.
3. Andrianov, S.N. and Samartsev, V.V. (1996a). Exciton mechanism of laser cooling in solid-state systems. Laser Physics 6 (5), 949.
4. Andrianov, S.N. and Samartsev, V.V. (1996b). Laser cooling of the phonon mode in a molecular crystal. Laser Physics 6 (4), 759.
5. Andrianov, S.N. and Samartsev, V.V. (1997a). Laser cooling of matter in condensed phase. Laser Physics 7 (4), 1.
6. Andrianov, S.N. and Samartsev, V.V. (1997b). Optical superradiation and laser cooling. Laser Physics 7 (1), 1.
7. Bartana, A., Kosloff, R., and Tannor, D.J. (1997). Laser cooling of internal degrees of freedom II. J. Chem. Phys. 106, 1435.
8. Bendow, B. (1991). Transparency of Bulk Halide Glasses. In "Fluoride Glass Fiber Optics" (I.D. Aggarwal and G. Lu, ed.), p. 85. Academic Press, San Diego.
9. Berdahl, P. (1985). Radiant refrigeration by semiconductor diodes. J. Appl. Phys. 58, 1369.
10. Boyer, L.L., Harrington, J.A., Hass, M., and Rosenstock, H.B. (1975). Optical Absorption by Alkali Halides: Possible Structure in the Multiphonon Region. In "Optical Properties of Highly Transparent Solids" (S.S. Mitra and B. Bendow, ed.), Optical Physics and Engineering, p. 59. Plenum Press, New York.
11. Bradley, W.E. (1959). Electronic cooling device and method for the fabrication thereof. U.S. Patent. No. 2,898,743 (Philco Corporation).
12. Brundage, R.T. and Yen, W.M. (1986). Energy transfer among Yb^{3+} ions in silicate glass. Phys. Rev. B 34, 8810.
13. Burin, A.L., Birman, J.L., Bulatov, A., and Rabitz, H. (1997). Squeezing atomic vibrations in an optical lattice. Phys. Rev. Lett. (submitted).
14. Chang, M.S., Elliott, S.S., Gustafson, T.K., Hu, C., and Jain, R.K. (1972). Observation of anti-Stokes fluorescence in organic dye solutions. IEEE J. Quantum Electronics 8, 527.
15. Chu, S. (1991). Laser manipulation of atoms and particles. Science 253, 861.
16. Chukova, Yu. P. (1969a). Maximum light yield of luminescent light sources. Opt. Spectrosc. 26, 251.
17. Chukova, Yu. P. (1969b). Thermodynamic limit of the luminescence efficiency. JETP Lett. 10, 294.
18. Chukova, Yu. P. (1971). Thermodynamic limit to the efficiency of broadband photoluminescence. Bull. Acad. Sci. USSR Phys. Ser. 35, 1349.
19. Chukova, Yu. P. (1974). Influence of excitation-line characteristics on efficiency of spectral conversion of energy by ions of trivalent neodymium in yttrium-aluminum garnet. Bull. Acad. Sci. USSR Phys. Ser. 38, 57.
20. Chukova, Yu. P. (1976). The region of thermodynamic admissibility of light efficiencies larger than unity. Sov. Phys. JETP 41, 613.
21. Clark, J.L. and Rumbles, G. (1996). Laser cooling in the condensed phase by frequency up-conversion. Phys. Rev. Lett. 76, 2037.
22. Cohen-Tannoudji, C.N. and Phillips, W.D. (1990). New mechanisms for laser cooling. Phys. Today 43 (10), 33.
23. DeLoach, L.D., Payne, S.A., Chase, L.L., Smith, L.K., Kway, W.L., and Krupke, W.F. (1993). Evaluation of absorption and emission properties of Yb^{3+} doped crystals for laser applications. IEEE J. Quantum Electron. 29, 1179.
24. Deol, R.S., Hewak, D.W., Jordery, S., Jha, A., Poulain, M., Baró, M.D., and Payne, D.N. (1993). Improved fluoride glasses for 1.3 μm optical amplifiers. J. Non-Cryst. Solids 161, 257.
25. Djeu, N. (1978). Laser cooling of gases by reradiation at higher frequency transitions. Opt. Commun. 26, 354.

26. Djeu, N. and Whitney, W.T. (1981). Laser cooling by spontaneous anti-Stokes scattering. Phys. Rev. Lett. 46, 236.
27. Dousmanis, G.C., Mueller, C.W., and Nelson, H. (1963). Effect of doping on frequency of stimulated and incoherent emission in GaAs diodes. Appl. Phys. Lett. 3, 133.
28. Dousmanis, G.C., Mueller, C.W., Nelson, H., and Petzinger, K.G. (1964). Evidence of refrigerating action by means of photon emission in semiconductor diodes. Phys. Rev. 133, A316.
29. Epstein, R.I., Buchwald, M.I., Edwards, B.C., Gosnell, T.R., and Mungan, C.E. (1995a). Observation of laser-induced fluorescent cooling of a solid. Nature (London) 377, 500.
30. Epstein, R.I., Edwards, B.C., Buchwald, M.I., and Gosnell, T.R. (1995b). Fluorescent Refrigeration. U.S. Patent. No. 5,447,032 (University of California).
31. Erickson, L.E. (1972). On anti-Stokes luminescence from Rhodamine 6G in ethanol solutions. J. Lumin. 5, 1.
32. Fokker, P.A., Dijkhuis, J.I., and Wijn, H.W. de (1997a). Stimulated emission of phonons in an acoustical cavity. Phys. Rev. B 55, 2925.
33. Fokker, P.A., Koster, W.D., Dijkhuis, J.I., Wijn, H.W. de, Lu, L., Meltzer, R.S., and Yen, W.M. (1997b). Stimulated emission of phonons in a ruby fiber. Phys. Rev. B 56, 2306.
34. Gallo, P., Massacurai, V., Ruocco, G., and Signorelli, G. (1991). Absolute two-phonon Raman cross section in potassium chloride. Phys. Rev. B 43, 14268.
35. Garrett, G.A., Rojo, A.G., Sood, A.K., Whittaker, J.D., and Merlin, R. (1997). Vacuum squeezing of solids: Macroscopic quantum states driven by light pulses. Science 275, 1638.
36. Gauck, H., Gfroerer, T.H., Renn, M.J., Cornell, E.A., and Bertness, K.A. (1997). External radiative quantum efficiency of 96% from a GaAs/GaInP heterostructure. Appl. Phys. A 64, 143.
37. Gauck, H.G., Renn, M.J., Cornell, E.A., and Bertness, K.A. (1995). Laser refrigeration in the solid state. Postdeadline Papers of the Quantum Electronics and Laser Science Conference, Baltimore, MD, #QPD16.
38. Gerthsen, P. and Kauer, E. (1965). The luminescence diode acting as a heat pump. Phys. Lett. 17, 255.
39. Geusic, J.E., Schulz-DuBois, E.O., and Scovil, H.E.D. (1967). Quantum equivalent of the Carnot cycle. Phys. Rev. 156, 343.
40. Geva, E. and Kosloff, R. (1996). The quantum heat engine and heat pump: An irreversible thermodynamic analysis of the three-level amplifier. J. Chem. Phys. 104, 7681.
41. Hänsch, T.W. and Schawlow, A.L. (1975). Cooling of gases by laser radiation. Opt. Commun. 13, 68.
42. Hasz, W.C., Whang, J.H., and Moynihan, C.T. (1993). Comparison of physical properties of ZrF₄- and HfF₄-based melts and glasses. J. Non-Cryst. Solids 161, 127.
43. Haynes, J.R. and Briggs, H.B. (1952). Radiation produced in germanium and silicon by electron-hole recombination. Phys. Rev. 86, 647.
44. Heiman, D., Hellwarth, R.W., and Hamilton, D.S. (1979). Raman scattering and nonlinear refractive index measurements of optical glasses. J. Noncryst. Solids 34, 63.
45. Jablonski, A. (1933). Efficiency of anti-Stokes fluorescence in dyes. Nature (London) 131, 839.
46. Jackson, W.B., Amer, N.M., Boccara, A.C., and Fournier, D. (1981). Photothermal deflection spectroscopy and detection. Appl. Opt. 20, 1333.
47. Joannopoulos, J.D., Meade, R.D., and Winn, J.N. (1995). "Photonic Crystals." Princeton University Press, Princeton.
48. Kafri, O. and Levine, R.D. (1974). Thermodynamics of adiabatic laser processes: Optical heaters and refrigerators. Opt. Commun. 12, 118.
49. Kalachev, A.A., Karamyshev, S.B., and Samartsev, V.V. (1996). Laser cooling of the spin system in Van Vleck paramagnetics. Laser Physics 6 (1), 27.
50. Kalachev, A.A. and Samartsev, V.V. (1997). Specific features of local data erasure and laser cooling in Van Vleck paramagnetics. Laser Physics 7 (2), 1.
51. Kaplyanski, A.A. and MacFarlane, R.M. (1987). "Spectroscopy of Solids Containing Rare Earth Ions." North Holland, Amsterdam.

52. Kastler, A. (1950). Quelques suggestions concernant la production optique et la détection optique d'une inégalité de population des niveaux de quantification spatiale des atomes: Application à l'expérience de Stern et Gerlach et à la résonance magnétique. *J. Phys. Radium* 11, 255.
53. Ketskeméty, I. and Farkas, É. (1970). Neuere Überlegungen bezüglich der oberen Schranke der Fluoreszenzausbeute. *Acta Phys. Chem. Szeged (Hungary)* 16, 77.
54. Keyes, R.J. and Quist, T.M. (1962). Recombination radiation emitted by gallium arsenide. *Proc. I.R.E.* 50, 1822.
55. Kittel, C. (1961). Phonon masers and the phonon bottleneck. *Phys. Rev. Lett.* 6, 449.
56. Kushida, T. and Geusic, J.E. (1968). Optical refrigeration in Nd-doped yttrium aluminum garnet. *Phys. Rev. Lett.* 21, 1172.
57. Landau, L. (1946). On the thermodynamics of photoluminescence. *J. Phys. (Moscow)* 10, 503.
58. Landsberg, P.T. and Evans, D.A. (1968). Thermodynamic limits for some light-producing devices. *Phys. Rev.* 166, 242.
59. Landsberg, P.T. and Tonge, G. (1980). Thermodynamic energy conversion efficiencies. *J. Appl. Phys.* 51, R1.
60. Lehovec, K., Accardo, C.A., and Jamgochian, E. (1951). Injected light emission of silicon carbide crystals. *Phys. Rev.* 83, 603.
61. Lehovec, K., Accardo, C.A., and Jamgochian, E. (1953). Light emission produced by current injected into a green silicon-carbide crystal. *Phys. Rev.* 89, 20.
62. Lines, M.E. (1991). Interaction of Light with Matter: Theoretical Overview. In "Handbook of Infrared Optical Materials" (P. Klocek, ed.), Optical Engineering, p. 71. Marcel Dekker, New York.
63. Lloyd, S. (1997a). Quantum optical refrigeration. *Phys. Rev. A* (submitted).
64. Lloyd, S. (1997b). A quantum-mechanical Maxwell's demon. *Phys. Rev. A* (accepted for publication).
65. Mazurenko, Yu. T. (1965a). Some properties of lasers from the point of view of thermodynamics. *Opt. Spectrosc.* 19, 85.
66. Mazurenko, Yu. T. (1965b). A thermodynamic treatment of the process of photoluminescence. *Opt. Spectrosc.* 18, 24.
67. McCumber, D.E. (1964). Einstein relations connecting broadband emission and absorption spectra. *Phys. Rev.* 136, A954.
68. Mihalas, D. (1978). "Stellar Atmospheres." W.H. Freeman, San Francisco. Chap. 1.
69. Miniscalco, W.J. (1993). Optical and Electronic Properties of Rare Earth Ions in Glasses. In "Rare Earth Doped Fiber Lasers and Amplifiers" (M.J.F. Digonnet, ed.), p. 19. Marcel Dekker, New York.
70. Mungan, C.E., Buchwald, M.I., Edwards, B.C., Epstein, R.I., and Gosnell, T.R. (1997a). Internal laser cooling of Yb³⁺-doped glass measured between 100 and 300 K. *Appl. Phys. Lett.* 71, 1458.
71. Mungan, C.E., Buchwald, M.I., Edwards, B.C., Epstein, R.I., and Gosnell, T.R. (1997b). Laser cooling of a solid by 16 K starting from room temperature. *Phys. Rev. Lett.* 78, 1030.
72. Mungan, C.E., Buchwald, M.I., Edwards, B.C., Epstein, R.I., and Gosnell, T.R. (1997c). Spectroscopic determination of the expected optical cooling of ytterbium-doped glass. *Mat. Sci. Forum* 239-241, 501.
73. Mungan, C.E. and Gosnell, T.R. (1996). Comment on "Laser cooling in the condensed phase by frequency up-conversion". *Phys. Rev. Lett.* 77, 2840.
74. Nelson, D.F. and Sturge, M.D. (1965). Relation between absorption and emission in the region of the R lines of ruby. *Phys. Rev.* 137, A1117.
75. Newman, R. (1953). Optical studies of injected carriers. II: Recombination radiation in germanium. *Phys. Rev.* 91, 1313.
76. Oraevsky, A.N. (1996). Cooling of semiconductors by laser radiation. *J. Russ. Laser Research* 17, 471.
77. Pankove, J.I. (1975). "Optical Processes in Semiconductors." Dover, New York. p. 193.
78. Prigogine, I. (1954). "Introduction to Thermodynamics of Irreversible Processes." 3rd ed., Wiley, New York. p. 17.

79. Pringsheim, P. (1929). Zwei Bemerkungen über den Unterschied von Lumineszenz- und Temperaturstrahlung. Z. Physik 57, 739.
80. Pringsheim, P. (1946). Some remarks concerning the difference between luminescence and temperature radiation: Anti-Stokes fluorescence. J. Phys. (Moscow) 10, 495.
81. Raman, C.V. (1928). A change of wavelength in light scattering. Nature (London) 121, 619.
82. Razeghi, M. (1995). InGaAsP-based high power laser diodes. Optics & Photonics News 6 (8), 16.
83. Rivlin, L.A. and Zadernovsky, A.A. (1997). Laser cooling of semiconductors. Opt. Commun. 139, 219.
84. Rumbles, G. and Clark, J.L. (1996). Rumbles and Clark Reply. Phys. Rev. Lett. 77, 2841.
85. Sanghera, J.S. and Aggarwal, I.D. (1993). Rare Earth Doped Heavy-Metal Fluoride Glass Fibers. In "Rare Earth Doped Fiber Lasers and Amplifiers" (M.J.F. Digonnet, ed.), p. 423. Marcel Dekker, New York.
86. Schnitzer, I., Yablonovitch, E., Caneau, C., and Gmitter, T.J. (1993). Ultrahigh spontaneous emission quantum efficiency, 99.7% internally and 72% externally, from AlGaAs/GaAs/AlGaAs double heterostructures. Appl. Phys. Lett. 62, 131.
87. Scovil, H.E.D. and Schulz-DuBois, E.O. (1959). Three-level masers as heat engines. Phys. Rev. Lett. 2, 262.
88. Stepanov, B.I. and Gribkovskii, V.P. (1968). "Theory of Luminescence." Iliffe Books, London. p. 322.
89. Stokes, G.G. (1852). On the change of refrangibility of light. Phil. Trans. 143, 463.
90. Tauc, J. (1957). The share of thermal energy taken from the surroundings in the electroluminescent energy radiated from a $p-n$ junction. Czech. J. Phys. 7, 275.
91. Treanor, C.E., Rich, J.W., and Rehm, R.G. (1967). Vibrational relaxation of anharmonic oscillators with exchange-dominated collisions. J. Chem. Phys. 48, 1798.
92. Tsujikawa, I. and Murao, T. (1963). Possibility of optical cooling of ruby. J. Phys. Soc. Jpn. 18, 503.
93. Tucker, E.B. (1961). Amplification of 9.3-kMc/sec ultrasonic pulses by maser action in ruby. Phys. Rev. Lett. 6, 547.
94. Vavilov, S. (1945). Some remarks on the Stokes law. J. Phys. (Moscow) 9, 68.
95. Vavilov, S. (1946). Photoluminescence and thermodynamics. J. Phys. (Moscow) 10, 499.
96. Weinstein, M.A. (1960). Thermodynamic limitation on the conversion of heat into light. J. Opt. Soc. Am. 50, 597.
97. Wineland, D.J. and Itano, W.M. (1987). Laser cooling. Phys. Today 40 (6), 34.
98. Wood, R.W. (1928). Anti-Stokes radiation of fluorescent liquids. Phil. Mag. 6, 310.
99. Yardley, J.T. (1971). Population inversion and energy transfer in CO Lasers. Appl. Opt. 10, 1760.
100. Yatsiv, S. (1961). Anti-Stokes Fluorescence as a Cooling Process. In "Advances in Quantum Electronics" (J.R. Singer, ed.), p. 200. Columbia University Press, New York.
101. Zadernovskii, A.A. and Rivlin, L.A. (1996). Laser cooling of a semiconductor (optical heat engine). Quantum Electronics 26, 1100.
102. Zander, C. (1991). Abkühlung einer Farbstofflösung durch Anti-Stokes-Fluoreszenz. Ph.D. thesis, Universität Siegen.
103. Zander, C. and Drexhage, K.H. (1995). Cooling of a dye solution by anti-Stokes fluorescence. In "Advances in Photochemistry" (D.C. Neckers, D.H. Volman, and G. von Bünau, ed.), Vol. 20, p. 59. Wiley, New York.
104. Zou, X. and Toratini, H. (1995). Evaluation of the spectroscopic properties of Yb^{3+} -doped glasses. Phys. Rev. B 52, 15889.

Figure Captions

FIG. 1. Generic energy-level diagram for an impurity ion in a solid host. The arrows indicate pump and relaxation processes leading to anti-Stokes fluorescence cooling of the system.

FIG. 2. A three-level maser viewed as a heat engine. Reversing the direction of operation yields a microwave-pumped refrigerator.

FIG. 3. Double-heat-engine picture for analyzing the efficiency of laser operation. The optical pump is taken to be a flash lamp, for the sake of specificity. The input and output radiation fields in this model are taken to constitute heat exchanges with thermal reservoirs having the indicated temperatures. Note that $T_{FL} \rightarrow \infty$ if the laser radiation is ideal, as indicated in the figure by the higher level for the output reservoir.

FIG. 4. Energy-level diagram for Yb^{3+} in a $\text{ZrF}_4\text{-BaF}_2\text{-LaF}_3\text{-AlF}_3\text{-NaF-PbF}_2$ (ZBLANP) glass host. The assigned energies are determined from our emission and absorption spectra measured at a sample temperature of 2 K.

FIG. 5. (a) Absorption coefficient at 300 K for a ZBLANP host doped with 1 wt% Yb^{3+} or 2.42×10^{20} ions/cm³. (b) Fluorescence spectrum of ZBLANP: Yb^{3+} at 300 K.

FIG. 6. Absorption and stimulated-emission cross sections of Yb^{3+} in a ZBLANP host. The stimulated-emission cross section is calculated from the fluorescence spec-

trum of Fig. 5(b) using the Füchtbauer-Ladenburg equation as quoted by DeLoach *et al.* (1993).

FIG. 7. Schematic of the photothermal deflection spectrometer. The pump beam (thin dark line) induces a refractive-index gradient in the sample that in turn deflects the HeNe probe beam (thick gray line). Detection of the deflected probe beam is accomplished with a dual split photodiode.

FIG. 8. Averaged signals obtained with the photothermal deflection apparatus of Fig. 7 for pump wavelengths of 980 and 1010 nm. The sample is ZBLANP + 1 wt% Yb³⁺. The 180°-phase difference between the signals indicates that a transition from laser heating to cooling has occurred.

FIG. 9. Photothermal deflection spectrum of ZBLANP + 1 wt% Yb³⁺ at 300 K (solid circles), where the raw deflection amplitudes have been normalized by the pump power at each wavelength. The solid curve shows a fit of Eq. (5) to the data and indicates that optical saturation of Yb³⁺ occurs during the measurement. The dashed line shows the expected response in the unsaturated limit, as determined by Eq. (6), with the values of the needed parameters set to those found in the fit of Eq. (5).

FIG. 10. Photothermal deflection spectrum of ZBLANP + 1 wt% Yb³⁺ at 300 K (solid circles) in the 990-1050 nm range. The data are normalized by the pump power. The solid curve shows a fit of Eq. (5) to the data with $\lambda_{F^*} = 995.3 \pm 0.3$ nm and $\alpha_b = (1.5 \pm 4) \times 10^{-5}$ cm⁻¹.

FIG. 11. Absorption cross sections for Yb^{3+} in a ZBLANP host at the indicated temperatures. Individual transitions between specific states are indicated using the labeling scheme of Fig. 4.

FIG. 12. ZBLANP: Yb^{3+} fluorescence spectra at the same temperatures as shown in Fig. 11. Individual transitions between specific states are indicated using the labeling scheme of Fig. 4.

FIG. 13. Photothermal deflection measurements for ZBLANP + 1 wt% Yb^{3+} at 300, 150, and 100 K. The data are normalized with respect to the laser power and the absorption coefficient at the pump wavelength. The solid line shows a plot of Eq. (7) for $\lambda_{F^*} = 995.5$ nm in the limit $\alpha_b \rightarrow 0$.

FIG. 14. Emission spectra for a ZBLANP + 1 wt% Yb^{3+} fiber of 250- μm total diameter that demonstrate laser cooling of the fiber. All spectra are normalized to unit amplitude at the 975-nm emission peak. (a) Temperature-calibration spectra, with their arithmetic difference plotted in the inset. The temperature difference between the two spectra is 13 K. (b) Spectra obtained for two values of the pump power at 1015 nm, with their difference plotted in the inset. Based on the calibration data in (a), the laser-induced temperature drop from room temperature is 21 K.

FIG. 15. Temperature changes, normalized by the pump power, measured as a function of pump wavelength (solid circles). The sample is a 250- μm diameter ZBLANP fiber doped with 1 wt% Yb^{3+} . The solid curve shows a fit of Eq. (10) to the data with fitting parameters of $\lambda_{F^*} = 997.6$ nm and $a_{eff} = 7.92 \times 10^{-5}$ cm².

FIG. 16. Power-normalized temperature changes as a function of pump power at laser wavelengths of 1010 nm (solid circles) and 1015 nm (open circles). The solid and dashed curves show fits of Eq. (10) to the data. The measurements further support the optical saturation model developed in the text.

FIG. 17. A generalized refrigerator. Both energy and entropy are accepted by the device as inputs and ejected as outputs. The refrigerator operates at temperature T , and accumulates energy and entropy at the rates \dot{E} and \dot{S} , respectively. Due to irreversible processes, excess entropy is produced at the rate \dot{S}_g .

FIG. 18. Generic laser-pumped refrigeration scheme based on a three-level model. Pairs of levels are identified with the components of the generalized refrigerator of Fig. 17; the pump and output reservoir may exchange radiation resonant with the two-level systems to which they are coupled.

FIG. 19. Simplification of the three-level laser-pumped refrigerator, as depicted in Fig. 18, where the pump and output reservoir have been replaced with heat baths that interact only with the indicated two-level systems.

FIG. 20. Explicit models for pump and relaxation processes in the optically pumped three-level refrigerator for two different arrangements of the energy levels. Purely radiative transitions are shown as solid lines while nonradiative transitions are shown as dashed lines.

FIG. 21. (a) Coefficients of performance (or first-law efficiencies)—in units of $k_B T_c / E$ —for the three-level refrigerator of Fig. 20(a). The curves are plotted as a function of the upper-manifold level splitting ε at fixed operating temperature T_c

and fixed intermanifold energy gap E . (b) Second-law efficiencies for the same model. Curves are derived from Eqs. (27) and (28) and given for three different ratios of the product of the level degeneracy and radiative relaxation rate in the two excited states.

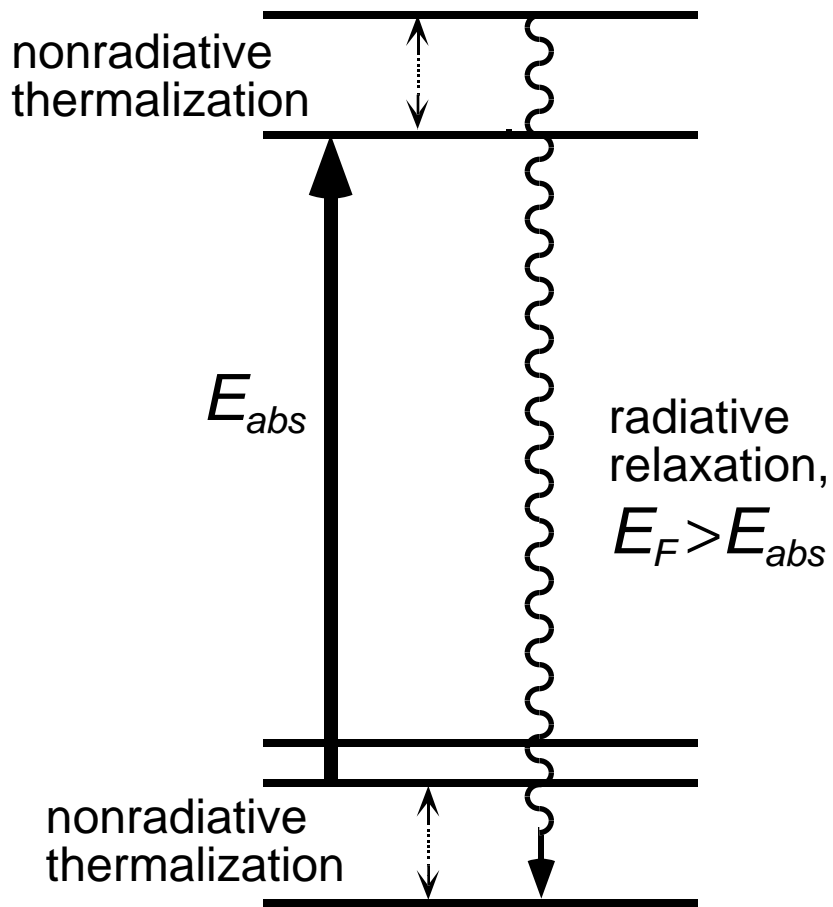
FIG. 22. Intrinsic optical loss expressed in terms of the heat generated per unit path length per unit pump power as a function of the laser frequency for three typical optical materials. Solid “V”-shaped curves are the sum of the multiphonon optical absorption and the Urbach-edge absorption except for the KCl curve, where the Urbach edge is too weak to be shown. Dashed lines show the heat load due to Raman scattering. All curves are for materials at 300 K. References: silica-glass multiphonon and Urbach edge absorption (Lines, 1991); heavy-metal-fluoride-glass multiphonon and Urbach-edge absorption (Bendow, 1991); KCl multiphonon absorption (Boyer *et al.*, 1975); silica Raman scattering (Heiman *et al.*, 1979); KCl Raman scattering (Gallo *et al.*, 1991).

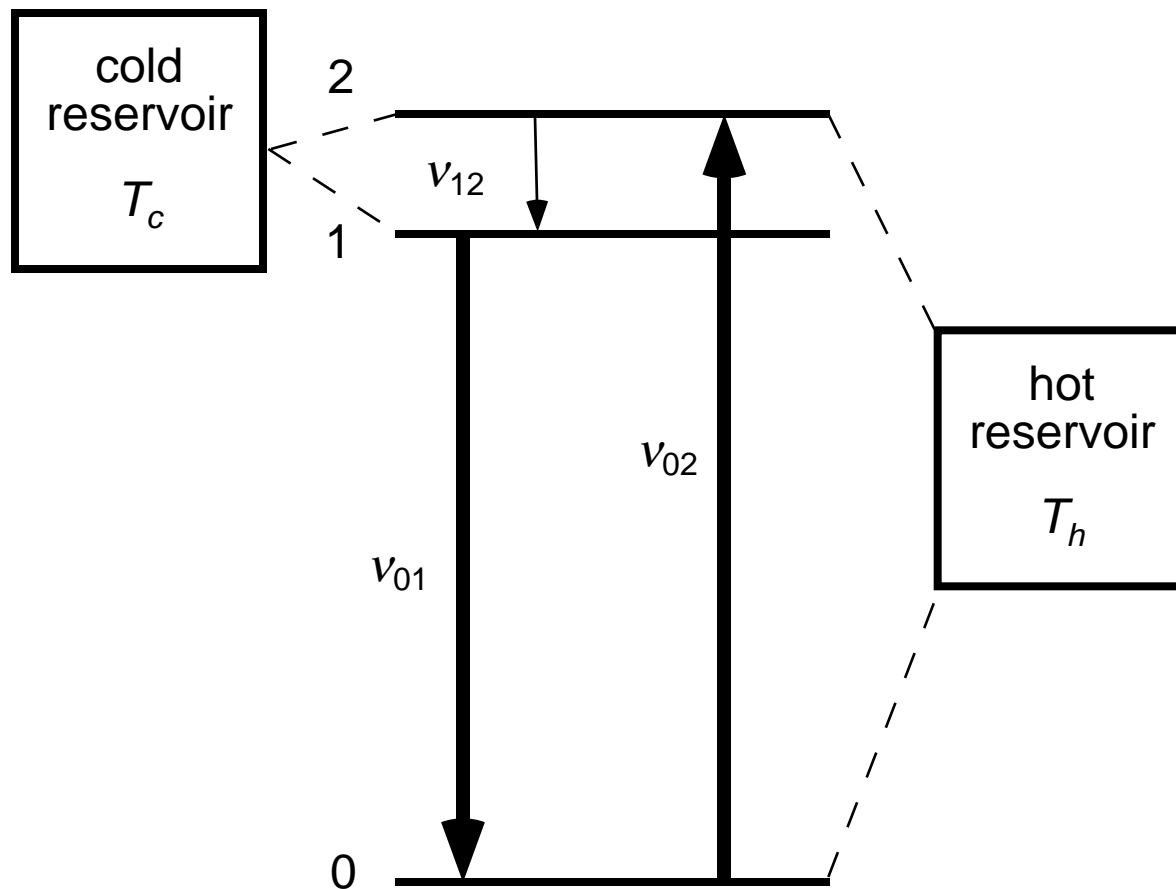
FIG. 23. Theoretical maximum cooling-power density expected for a ZBLANP host doped with 1 wt% Yb^{3+} . The curve is derived from Eq. (40) in the limit $I \rightarrow \infty$.

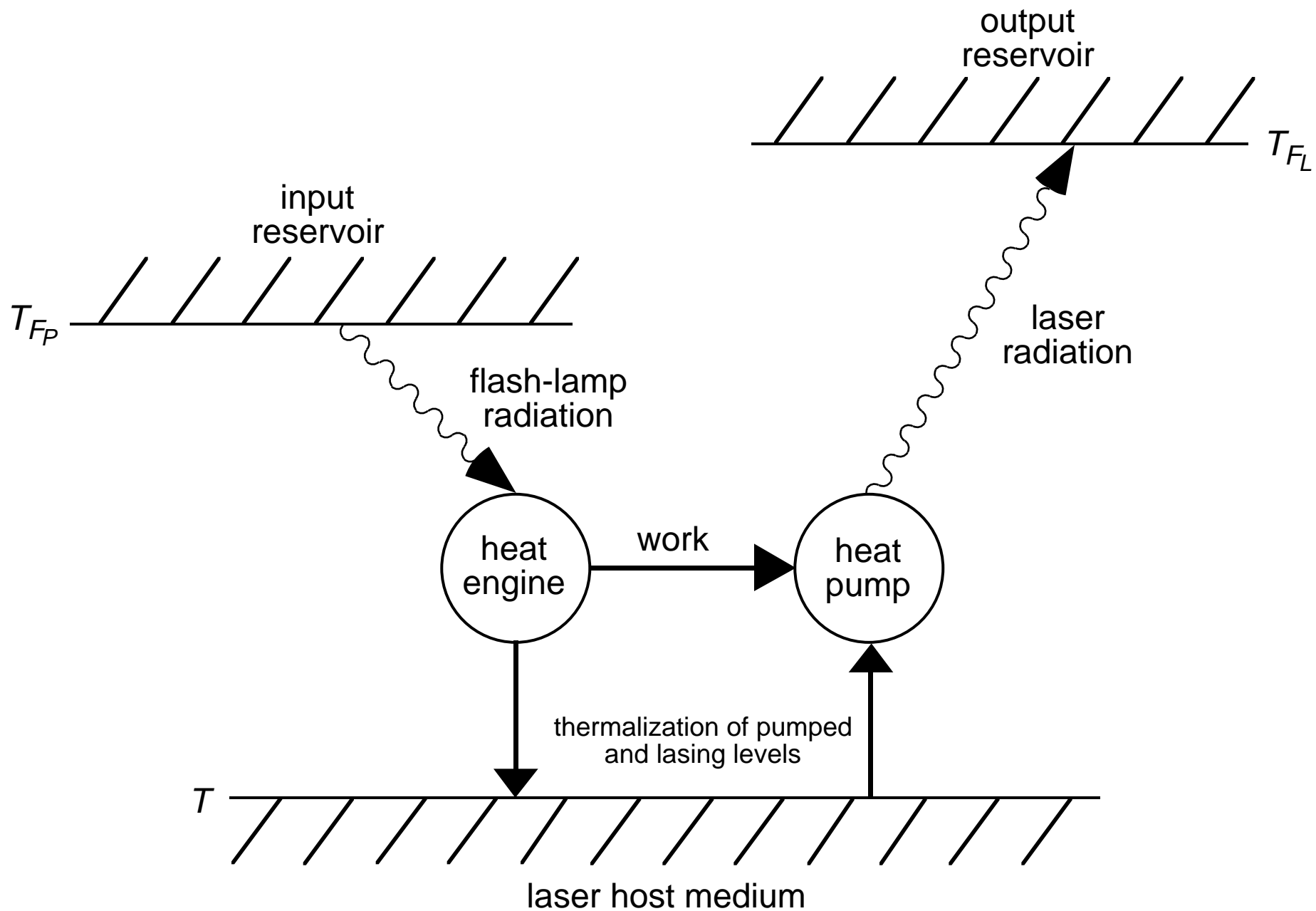
FIG. 24. Theoretical cooling-power density for ZBLANP + 1 wt% Yb^{3+} as a function of pump intensity for four different temperatures. The curves are derived from Eq. (40) and measurements of the Yb^{3+} absorption cross section (cf. Fig. 11).

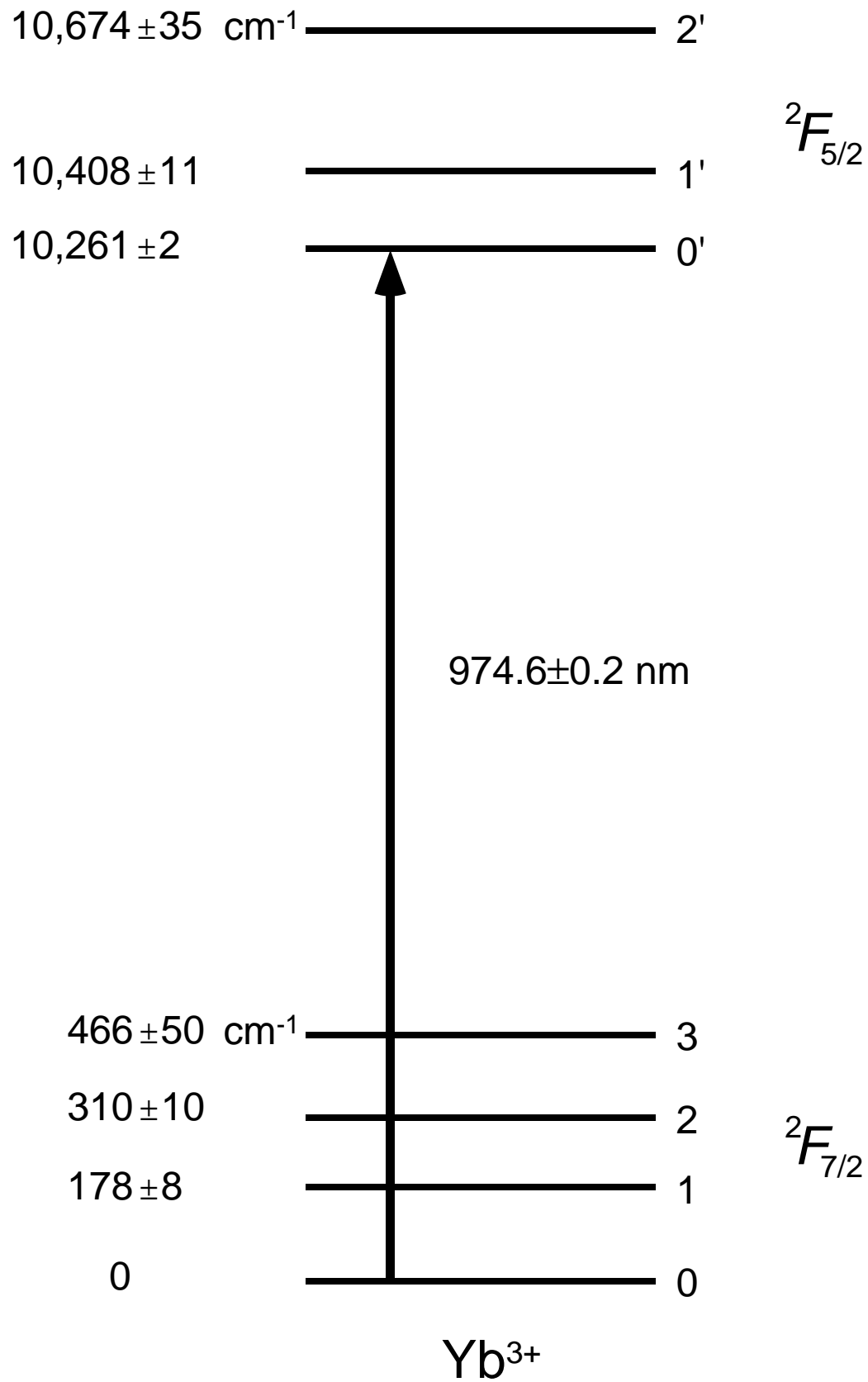
FIG. 25. Theoretical cooling efficiencies for ZBLANP + 1 wt% Yb^{3+} as a function of pump intensity for four different temperatures. The curves are derived from Eq. (40) and measurements of the Yb^{3+} absorption cross section (cf. Fig. 11); they show the decline in efficiency that results from optical saturation.

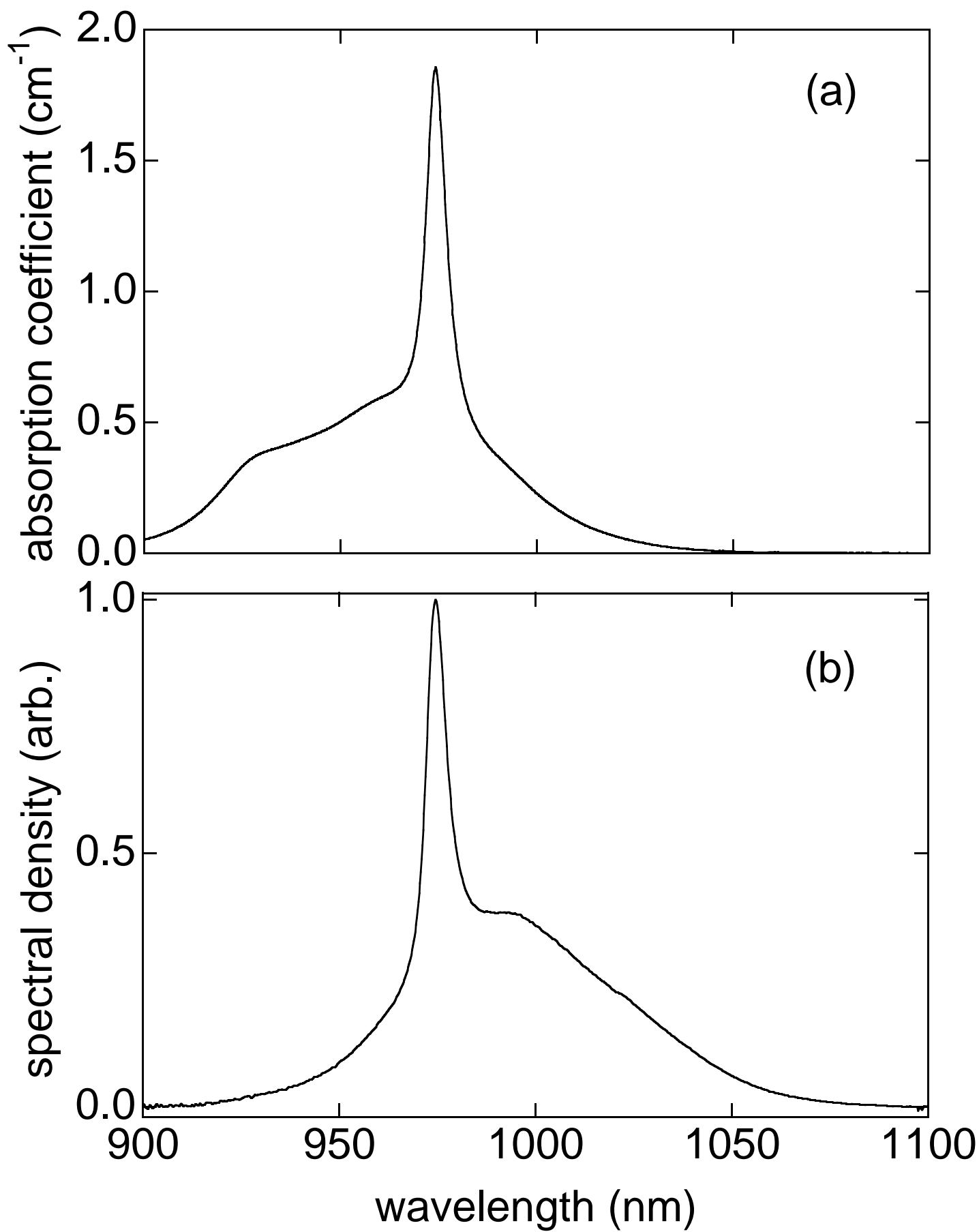
FIG. 26. Theoretical cooling efficiencies for ZBLANP + 1 wt% Yb³⁺ as a function of cooling-power density for four different temperatures. The curves are derived from Eq. (40) and measurements of the Yb³⁺ absorption cross section (cf. Fig. 11); they show the range of cooling-power densities over which the cooling efficiency is uncompromised by optical saturation.

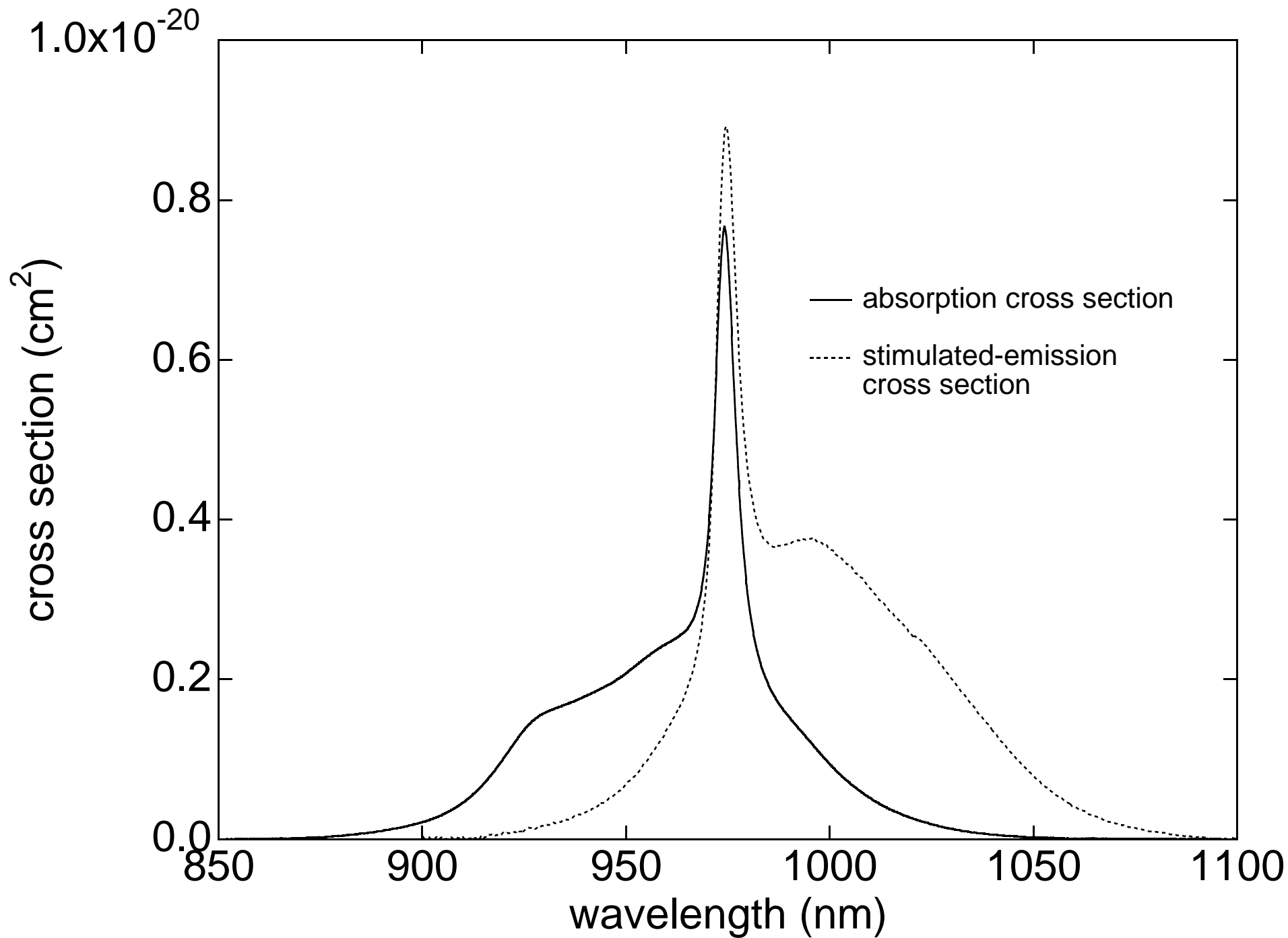


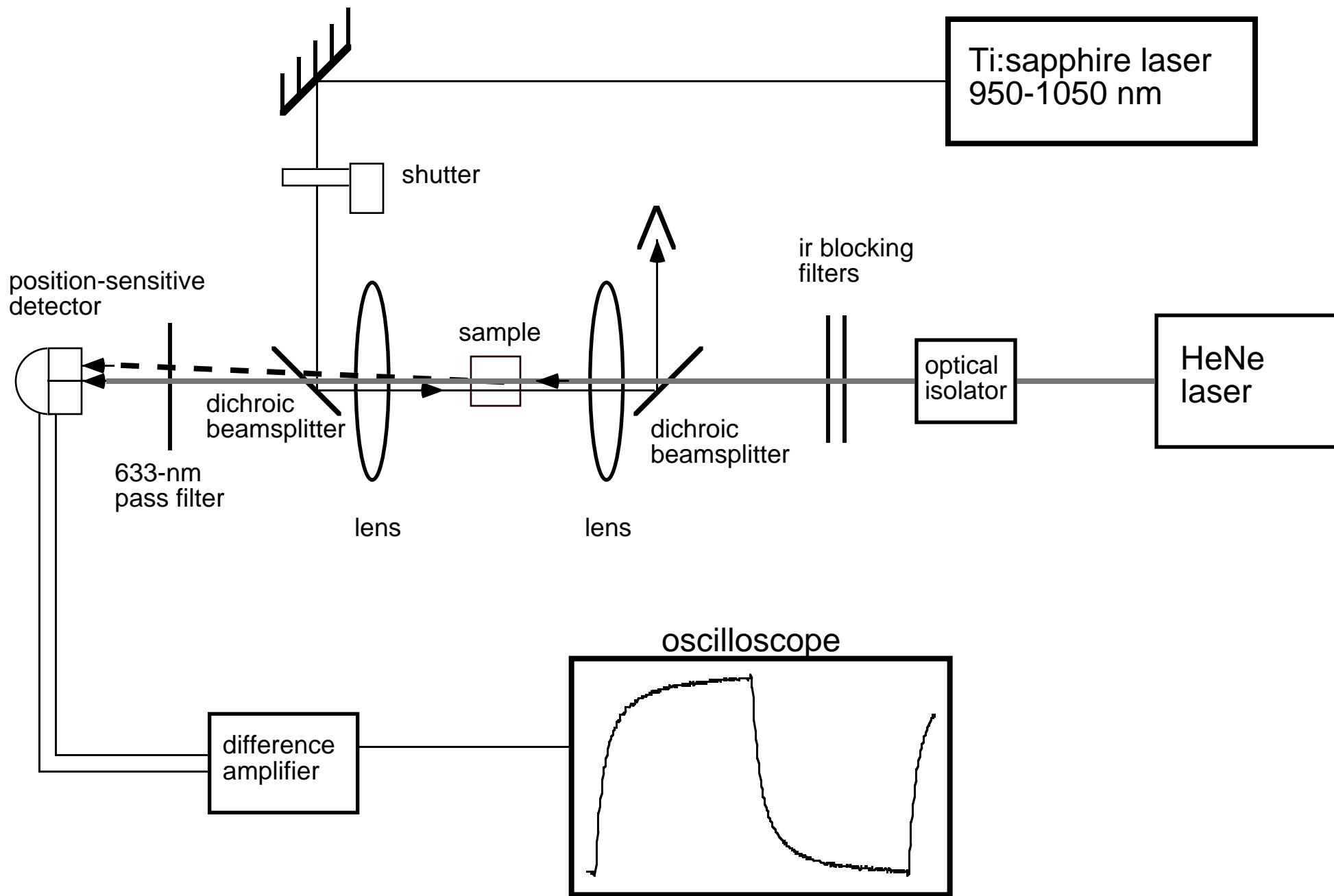


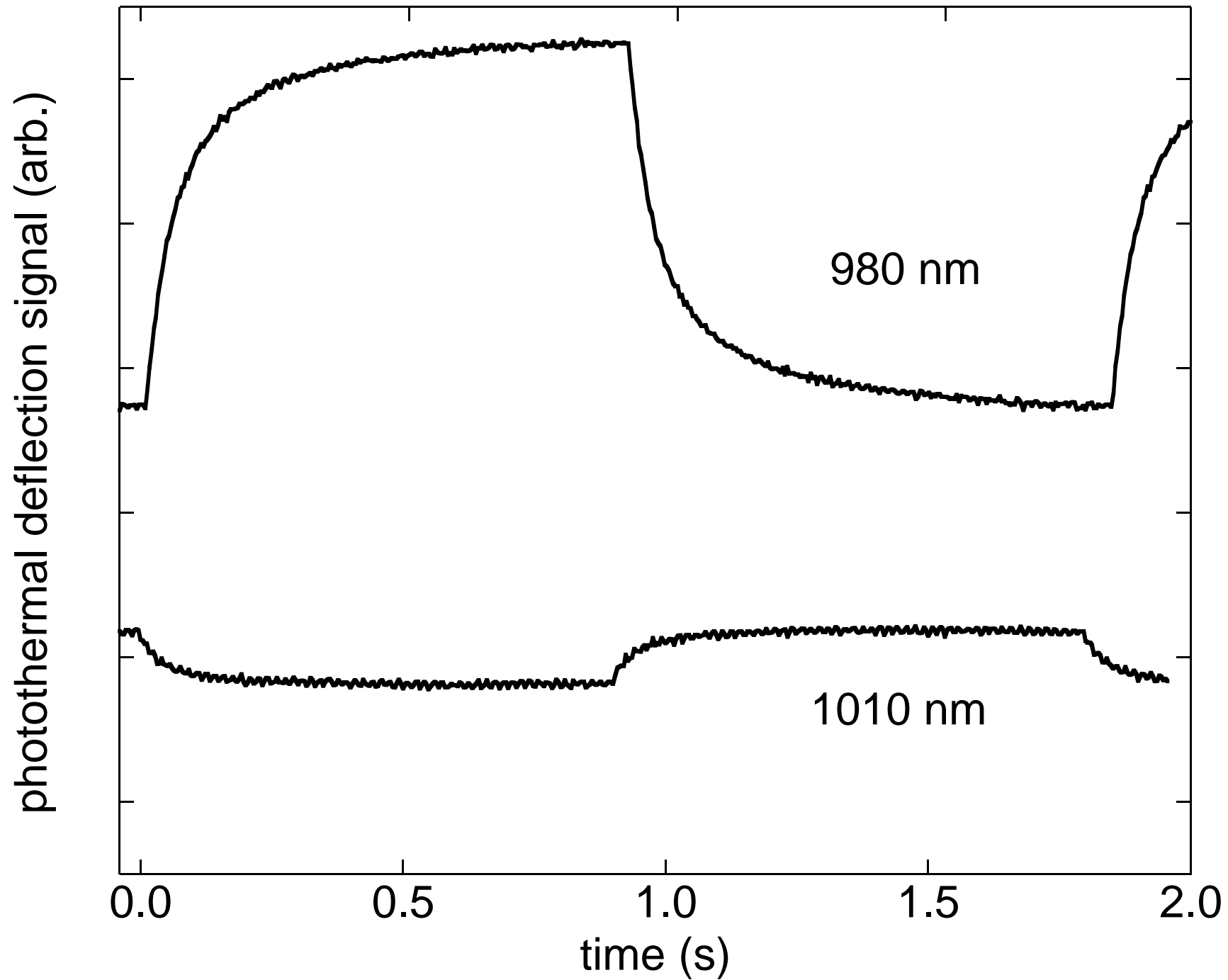


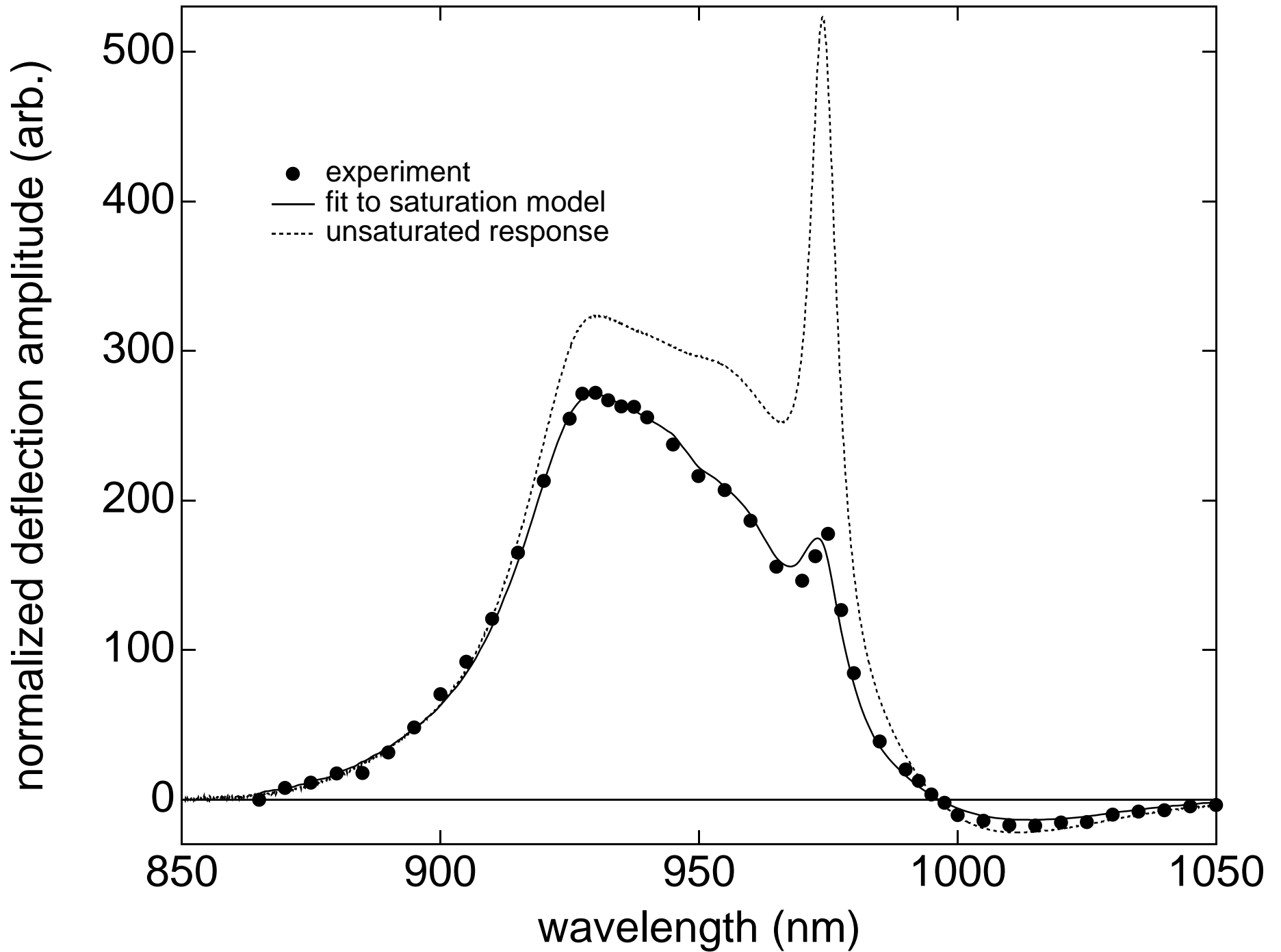


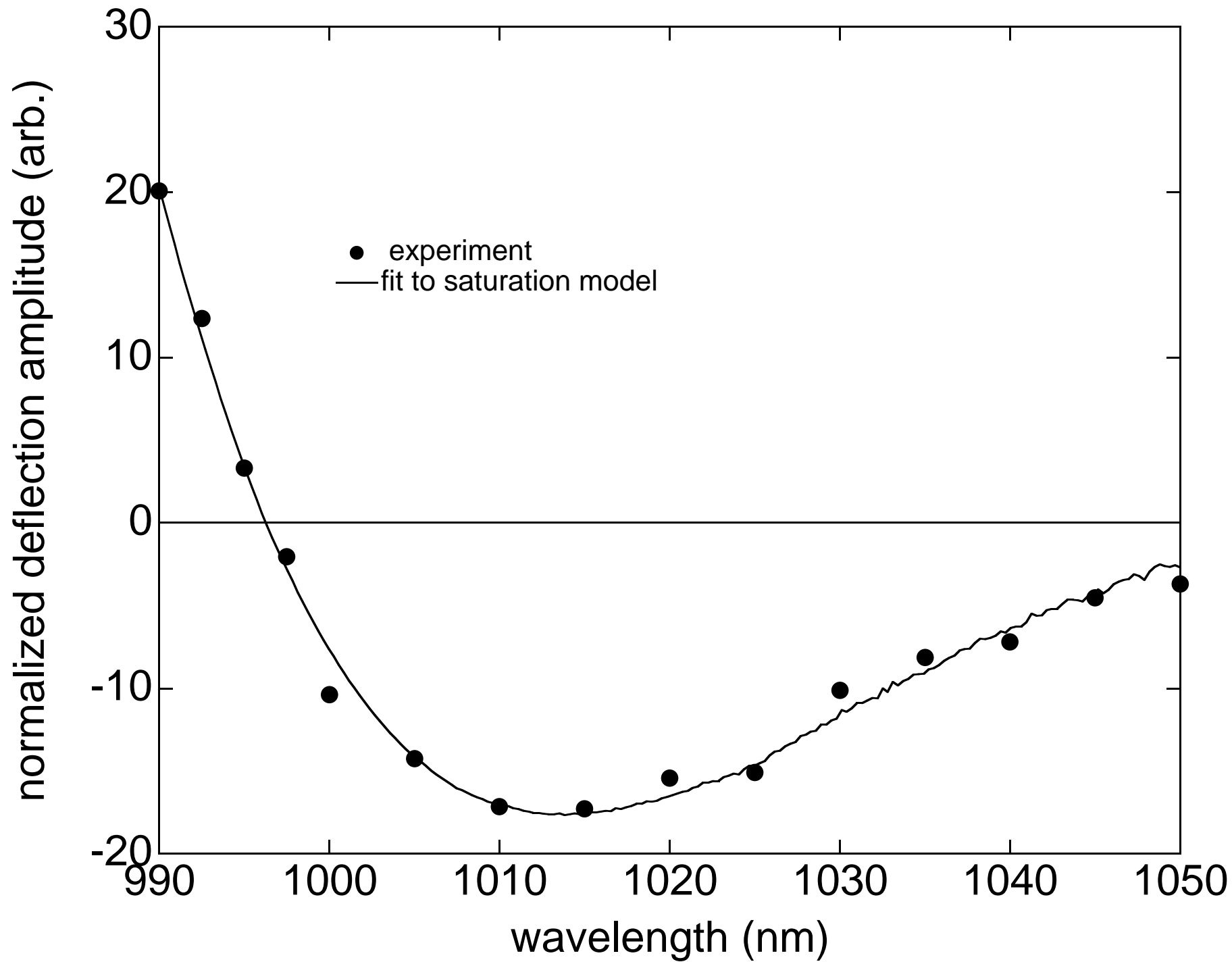


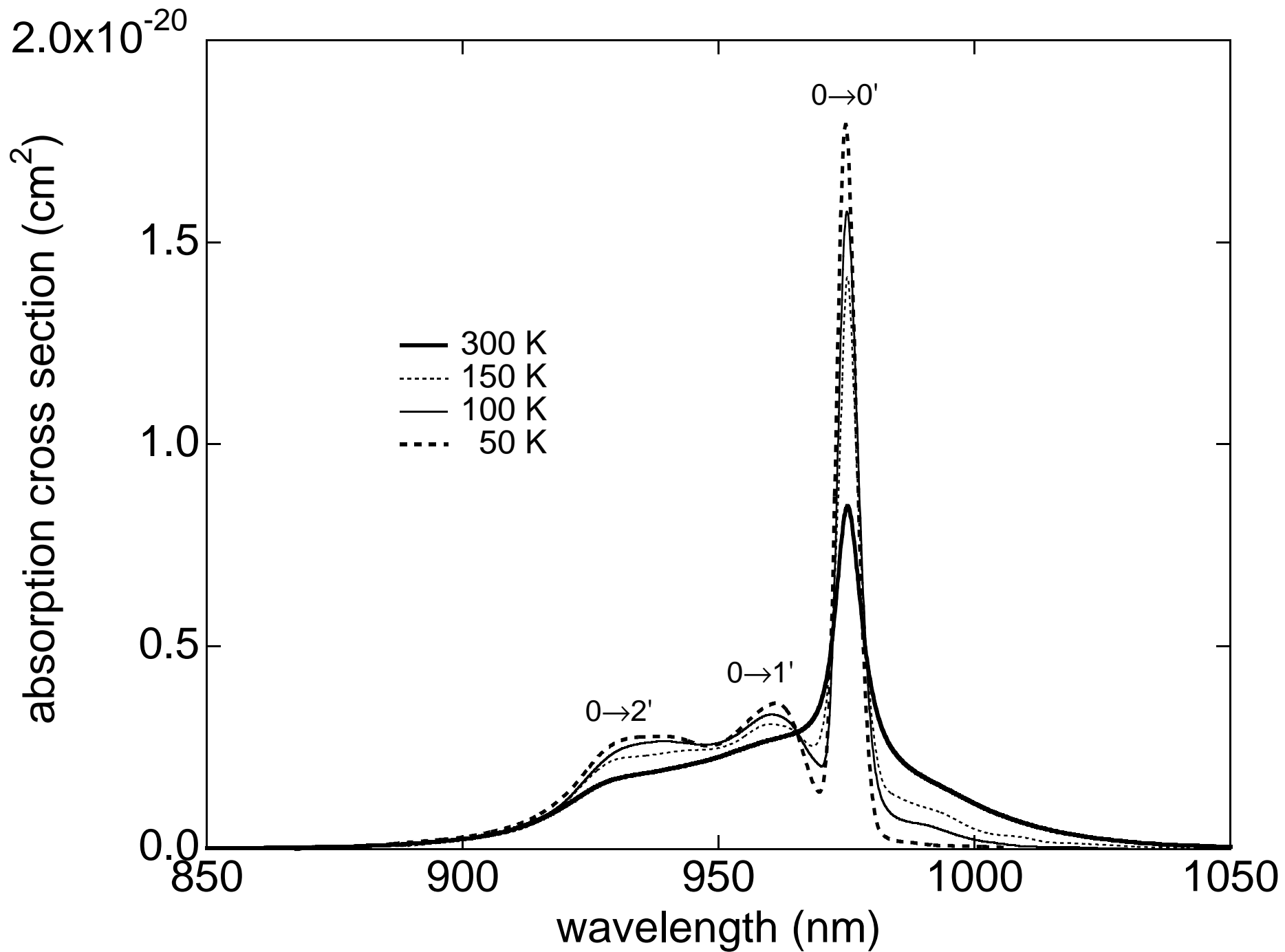


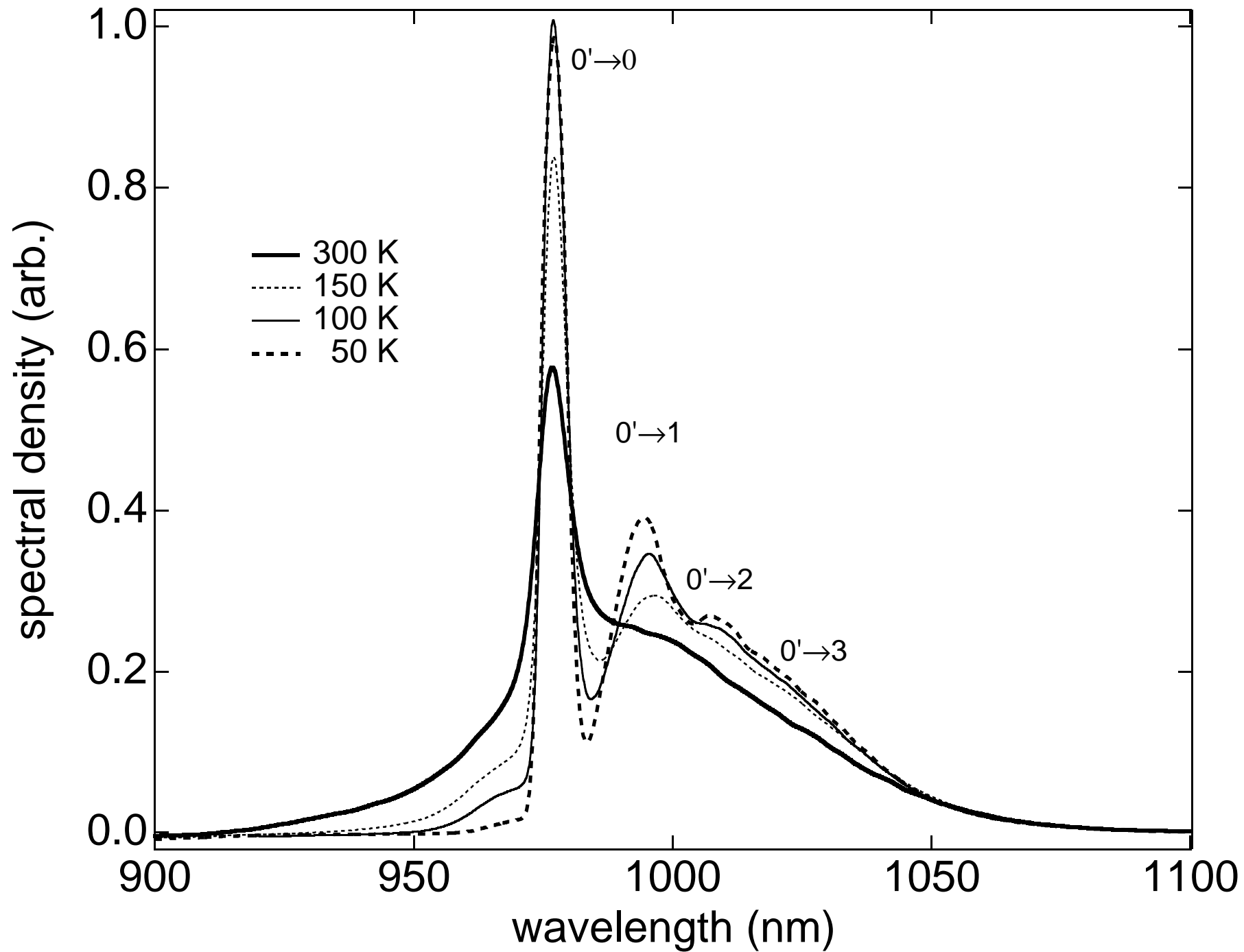


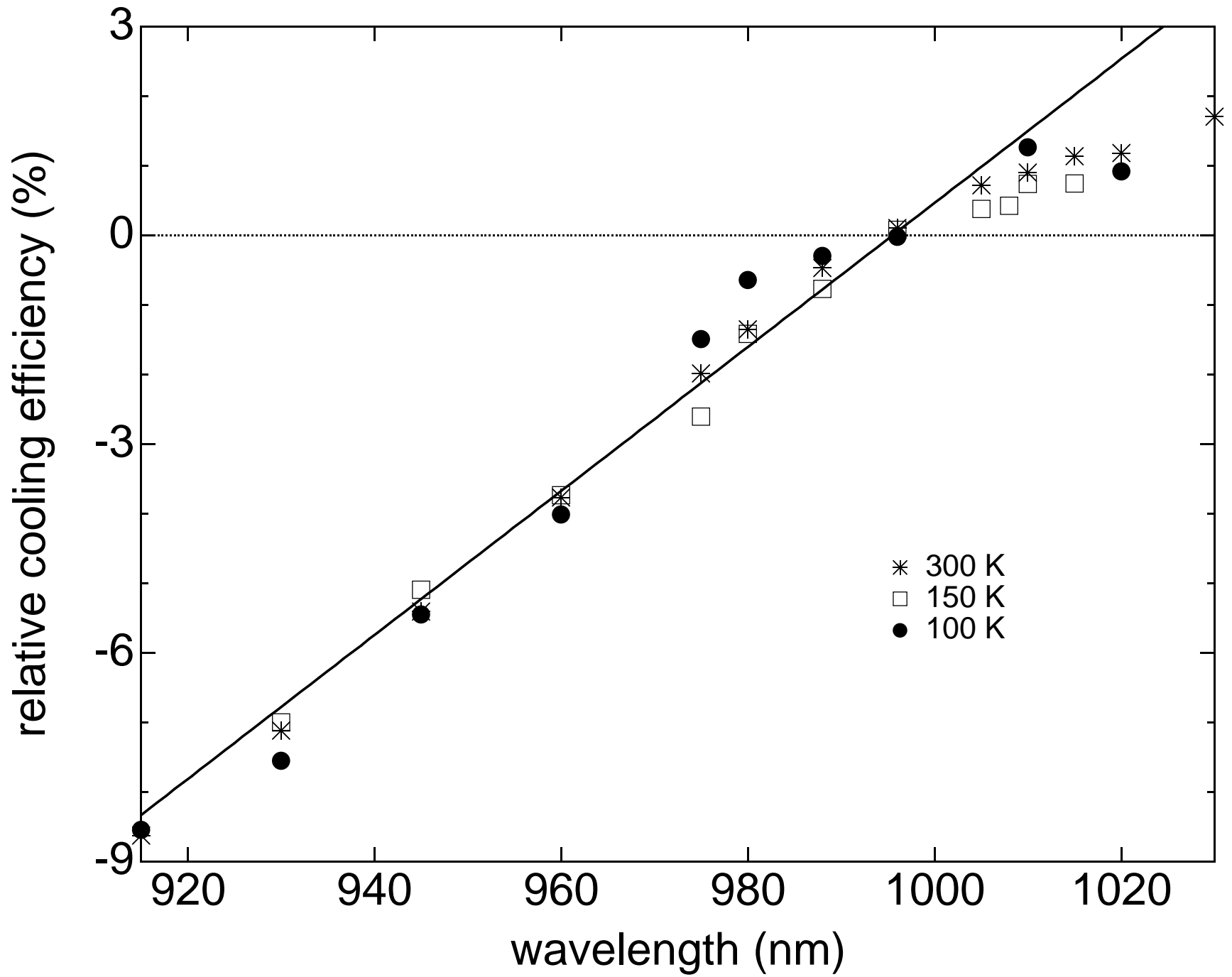


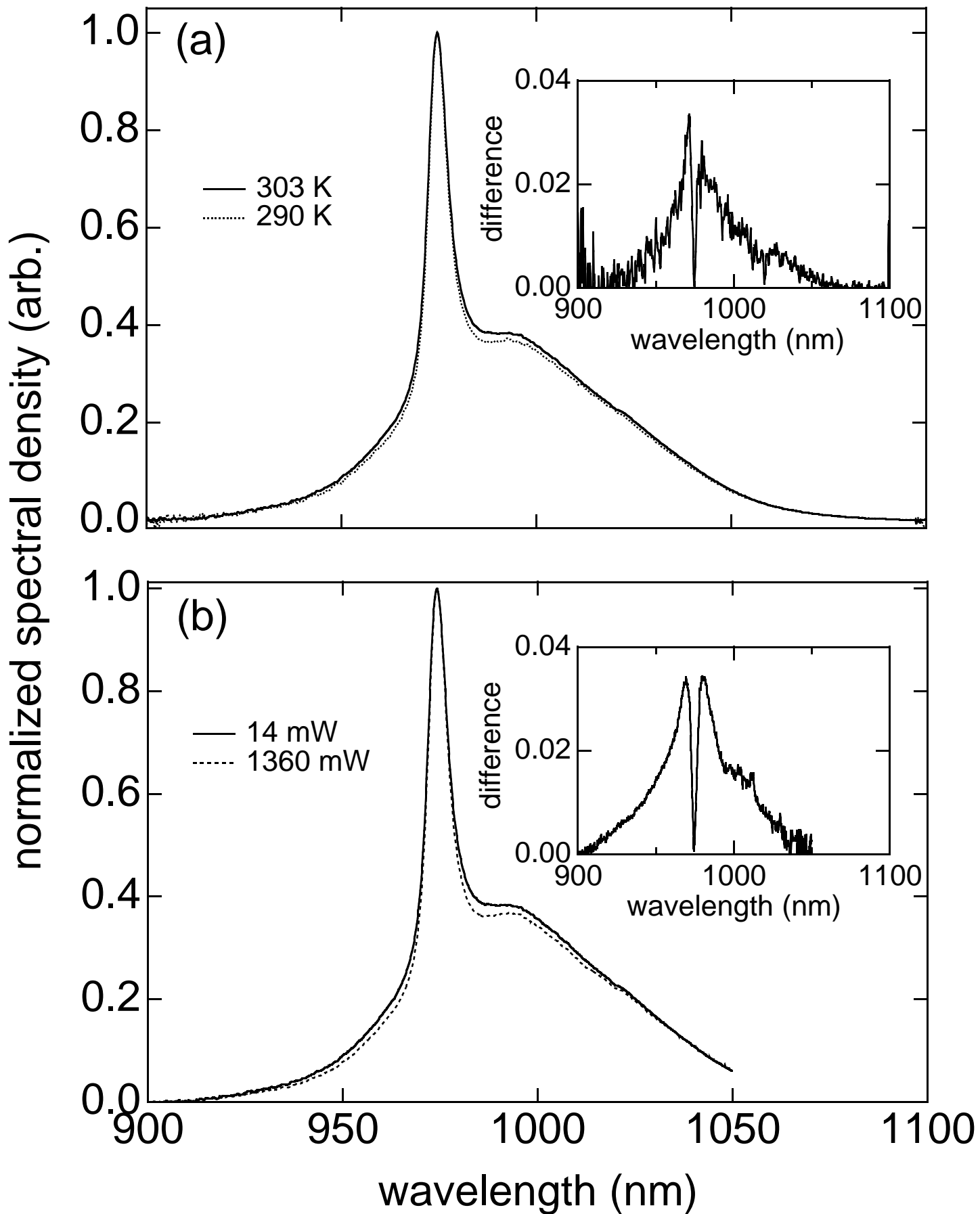


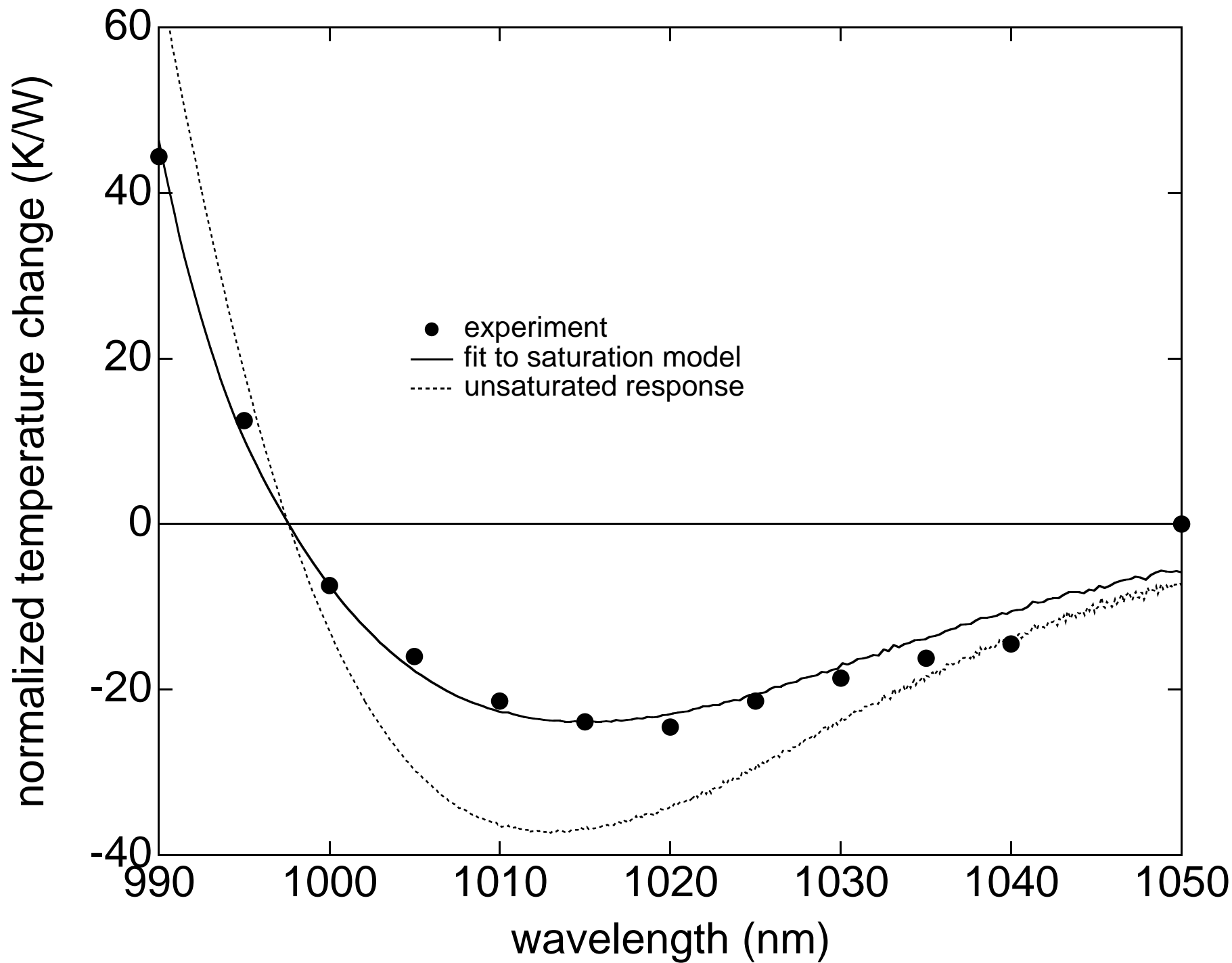


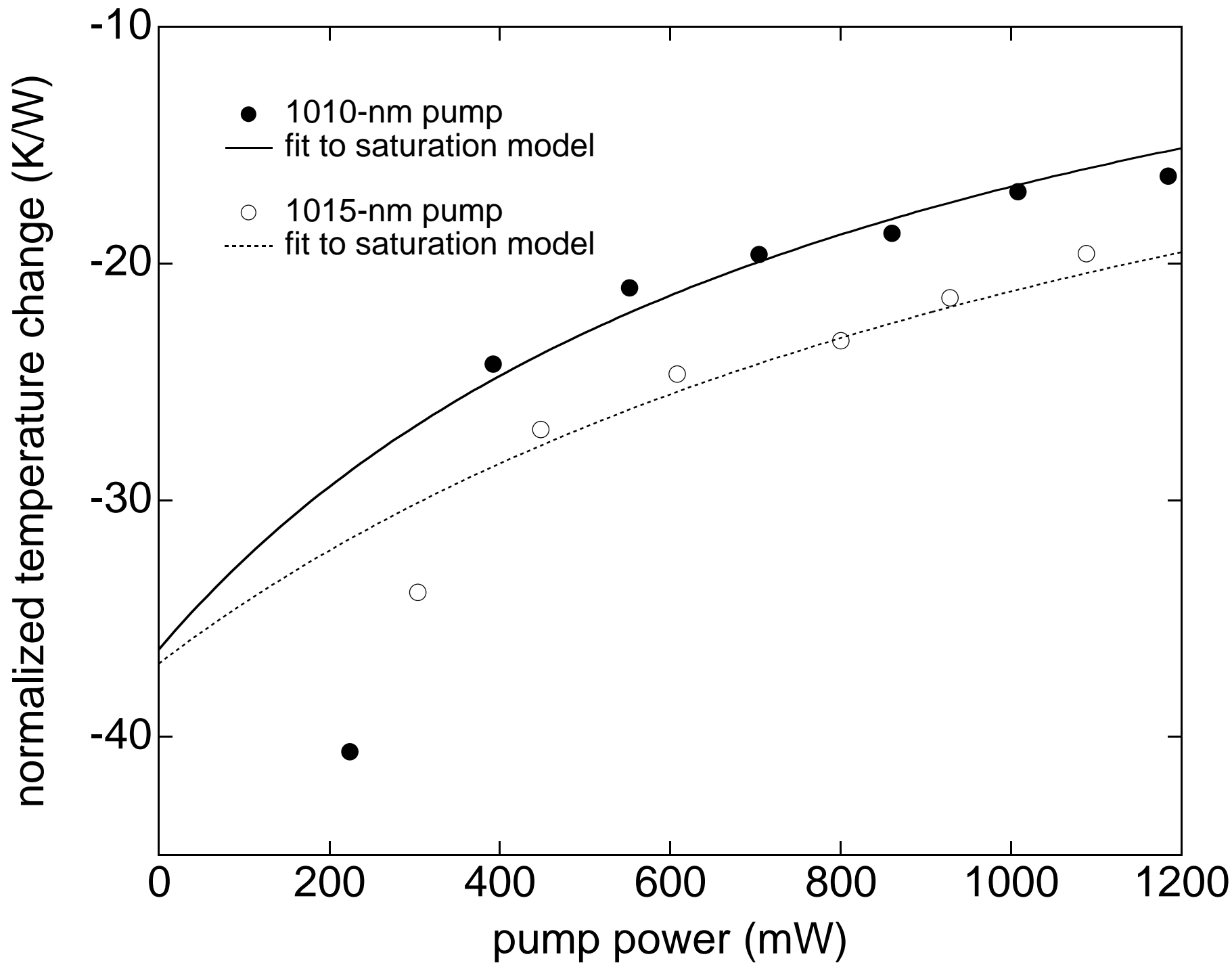


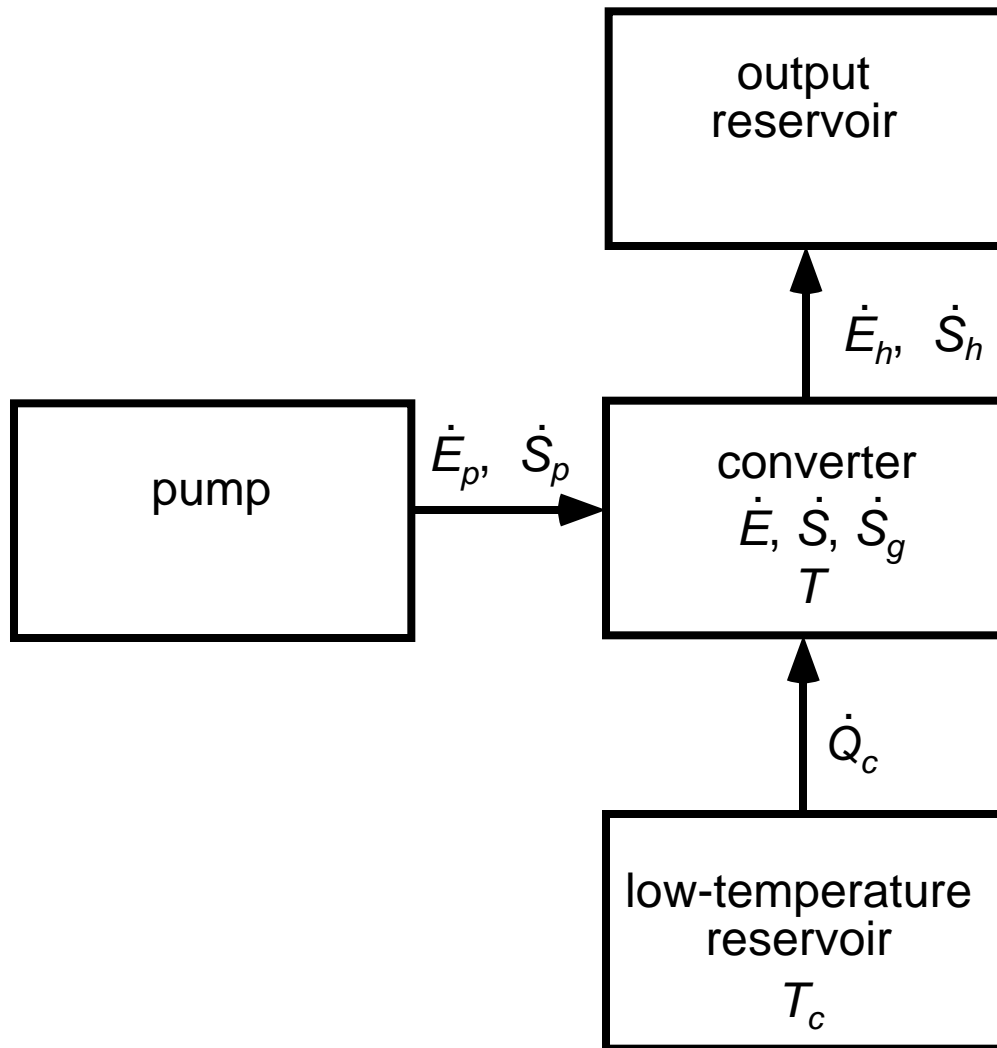


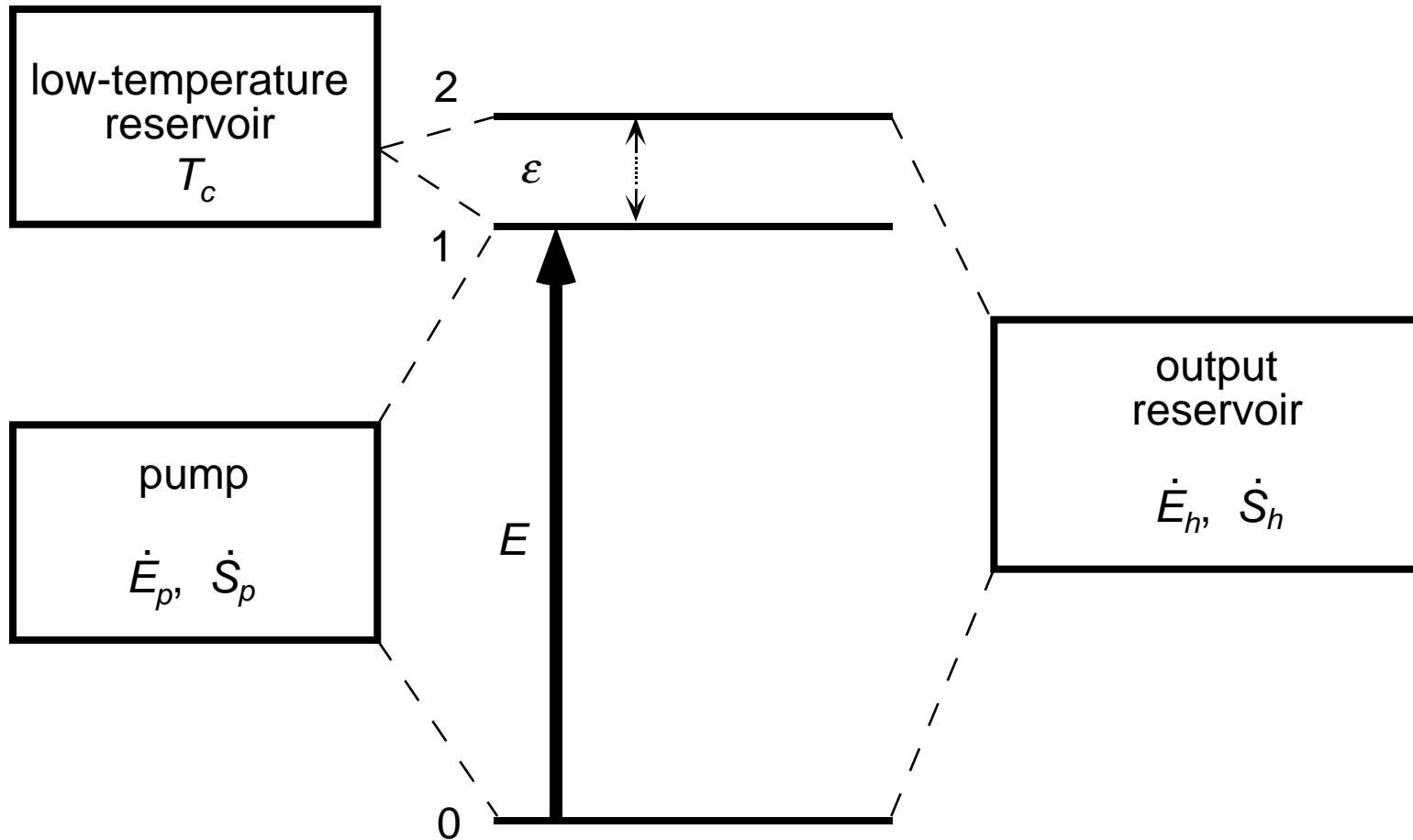


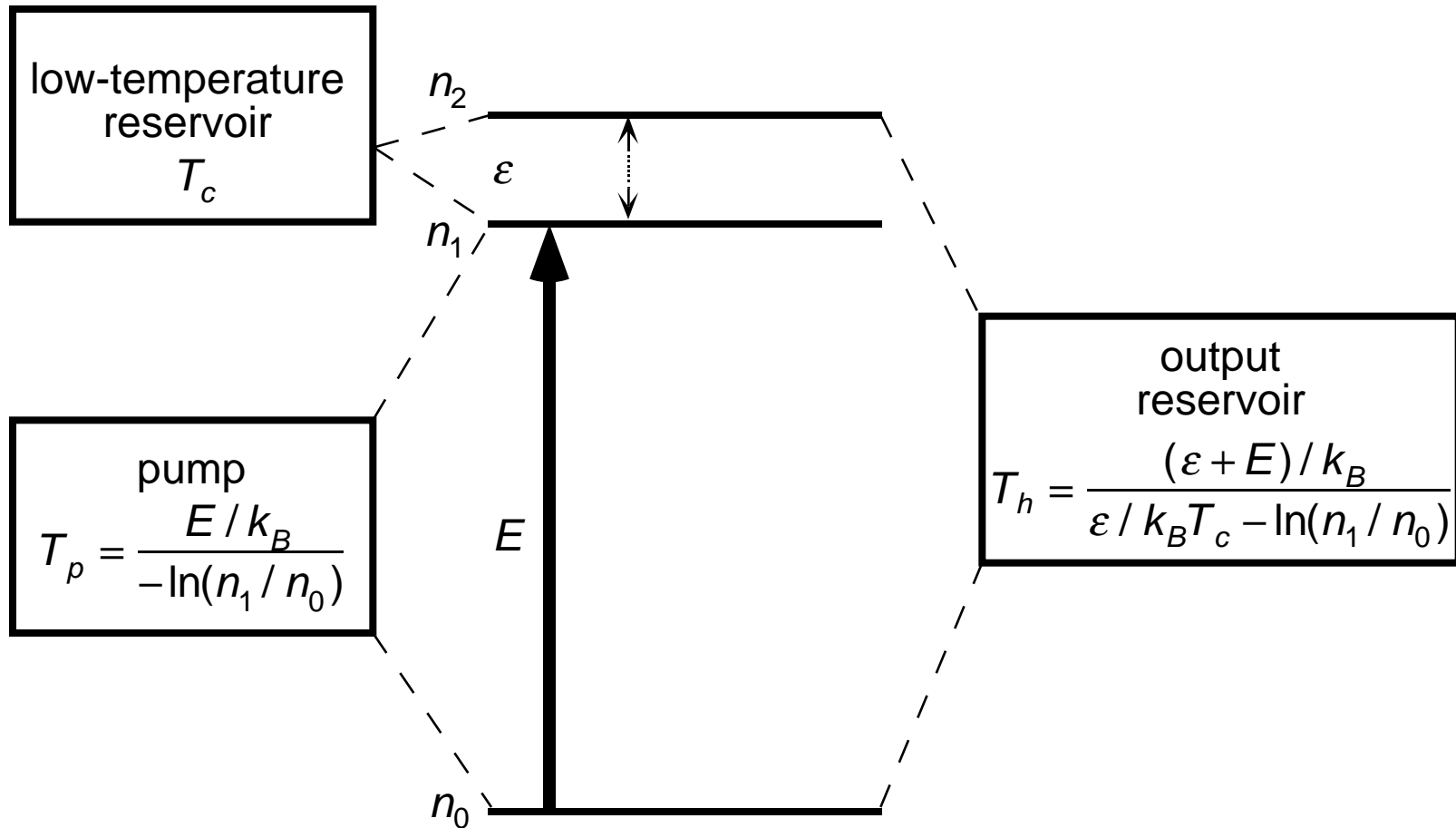


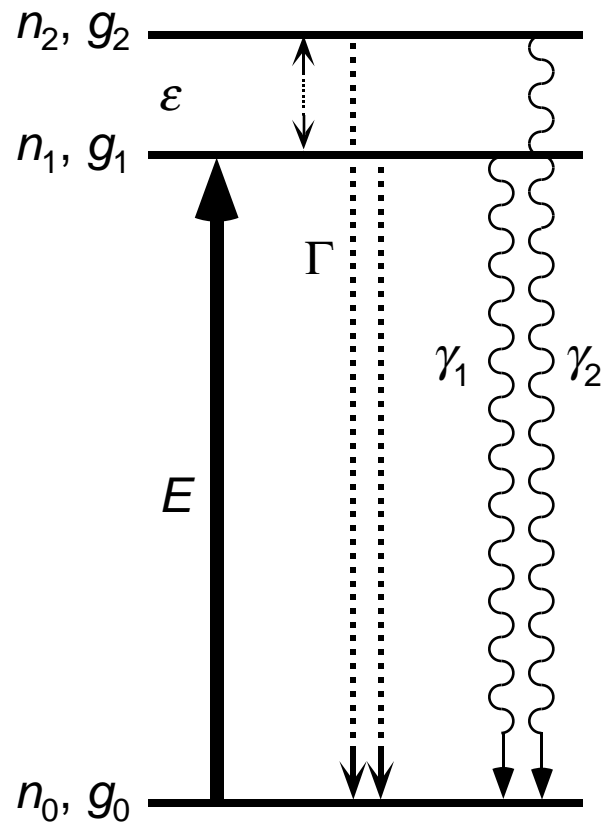




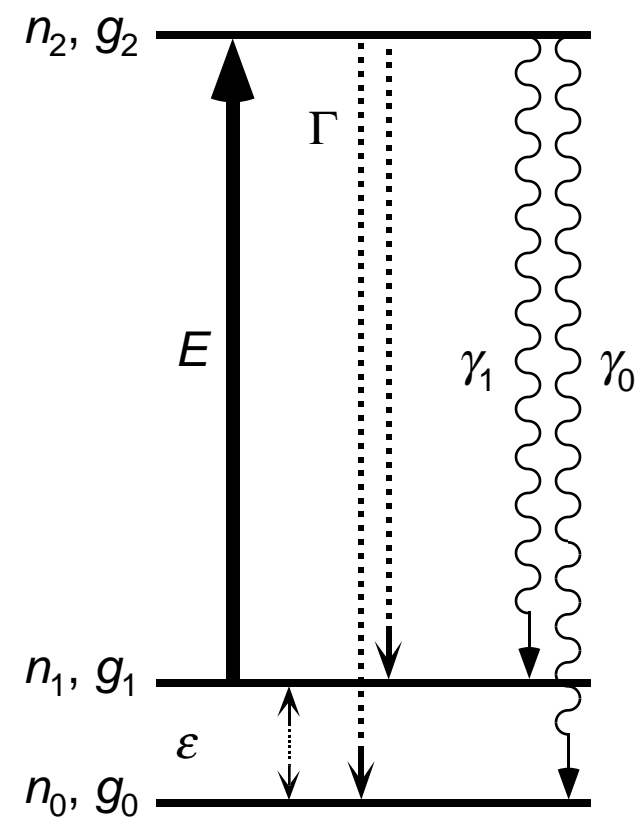








(a)



(b)

